UNIVERSITA' DEGLI STUDI DI PADOVA

Facoltà di Scienze MM. FF. NN.

Dipartimento di Scienze Chimiche

Tesi di Laurea Magistrale in Chimica

FULLERENES, PEPTIDES AND RADICALS

Relatore: Prof. Flavio Maran

Controrelatore: Dott. Alberto Gasparotto

Laureando: Luca Garbuio

Anno Accademico 2010-2011

Acknowledgements

Ringrazio la mia famiglia, Giuliano, Amelia, Veronica e Elena e Sarah-Jane, mio zio Gino e zia Anna, per il loro supporto totale.

I thank Professor Flavio Maran for having taught me his reliable *modus operandi* toward research, and for his fundamental support throughout my thesis. I thank all the wonderful people of the Electrochemistry Group of Professor Flavio Maran at the University of Padua. In particular, I thank Dr. Sabrina Antonello for her assistance in carrying out the electrochemistry measurements and Dr. Ivan Guryanov for countless discussions on synthetic issues and for his priceless help and assistance throughout the peptide synthesis work, without which I would still be under in the lab trying to obtain the peptides. I also thank Professor Fernando Formaggio for helpful discussions on peptides and Dr. Marco Ruzzi for helpful discussions on EPR but not exclusively.

I thank both Professor Flavio Maran and Professor Nicholas J. Turro of Columbia University for having made my dream real!

I thank all stimulating people I met during my experience at Columbia University in New York City. In particular, I thank Dr. Yongjun Li for having supervised my experimental work while at Columbia and for helpful discussions.

Riassunto

Questa tesi riguarda la sintesi, caratterizzazione e l'investigazione di una serie di composti nei quali il fullerene C_{60}, peptidi e radicali liberi sono accoppiati. In particolare, due serie di composti sono stati sintetizzati, caratterizzati dalla presenza del fullerene e / o da una funzione nitrossido covalentemente legati alle estremità di un piccolo peptide rigido. Le caratteristiche di questo peptide sono tali per cui un forte momento di dipolo molecolare sorge orientato lungo l'asse molecolare principale. Poiché il verso del dipolo è invertito nelle due serie di composti, chiamati 2- e 2+, si prevede che l'effetto generato dal dipolo, per esempio sulle proprietà redox dei gruppi localizzati alle sue estremità (la funzione nitrossido e il fullerene), sia opposto. L'analisi conformazionale in soluzione ha fornito utili informazioni riguardo la struttura secondaria dei peptidi. Dalle misure elettrochimiche (*cyclic voltammetry* e *differential pulse voltammetry*) sono stati ottenuti i potenziali standard dei composti sotto esame. In fine, è stata effettuata la sintesi di due fullerene-peptidi impiegando l'endofullerene $H_2@C_{60}$.

Abbreviations used

Symbols and abbreviations for amino acids and peptides are in accord with the recommendations of the IUPAC-IUB Commission on Nomenclature (J. *Biol. Chem.* **1972**, 247, 977). The optically active α-amino acid is of L-chirality. Other abbreviations used are as follow:

Z, benzyloxycarbonyl
Boc, *tert*-butyloxycarbonyl
O*t*Bu, *tert*-butylester
Me, methyl
Aib, α-aminoisobutyric acid
NMM, N-methylmorpholine
HOAt, 7-aza-1-hydroxybenzotriazole
EDC.HCl, N-ethyl-N'(3-dimethylaminopropyl)carbodiimide hydrochloride
Piv, *tert*-butyl-carbonyl or pivaloyl
DIEA, N,N-diisopropyl-ethyl-amine
DEA, diethylamine
Fp, fulleropyrrolidine
Fpr, fulleroproline
EtOAc, ethyl acetate
MeOH, methanol
AcOH, acetic acid
TEA, triethylamine
TFA, trifluoroacetic acid
DCM, dichloromethane
EtOH, ethanol
n-BuOH, n-butanol
TOAC, 2,2,6,6-tetramethylpiperidine-1-oxyl-4-amino-4-carboxylic acid
Cyanuric fluoride, 2,4,6-trifluoro-1,3,5-triazine
py, pyridine
TMS, tetramethylsilane
ACN, acetonitrile
EP, light petroleum
Fmoc-OSu, N-(9-Fluorenylmethoxycarbonyloxy)succinimide
Fmoc, N-9-Fluorenylmethoxycarbonyloxy
R_f, TLC retention factor
Mp, melting point
FT-IR, Fourier transformation Infrared spectroscopy
NMR, nuclear magnetic resonance
MALDI, matrix-assisted laser desorption ionization
ESI, electron spray ionization
CD, circular dichroism
TR-EPR, time resolved-electronic paramagnetic resonance
DMF, dimethylformamide

DMSO, dimtheylsulphoxide
CV, cyclic voltammetry
DPV, differential pulse voltammetry
TBAH, tetrabutylammonium hexafluorophosphate
Fc, ferrocene
Trt, triphenylmethyl or trityl
ROESY, rotating-frame Overhauser effect spectroscopy
SCE, standard calomel electrode
DCTB, trans-2-[3-(4-*tert*-Butylphenyl)-2-methyl-2-propenylidene]malonitrile
DCE, 1,2-dichloroethane
PH, diphenylhydrazine
t-, tert-
r.t., room temperature

Index

Chapter 1. Introduction……13

1.1 Introduction on Fullerene……13
1.1.1 Properties of Fullerene C_{60}……14
1.1.2 About the chemistry of Fullerene C_{60}……17
1.1.3 The endofullerene $H_2@C_{60}$……19
1.2 Nitroxide radicals in solution……19
1.2.2 About TOAC amino acid……21
1.3 α-aminoisobutyric acid (Aib) and the 3_{10}-helix……22
1.4 Characteristics of the investigated systems 2+ and 2-……24
1.5 Purpose of the thesis……27

Chapter 2. Experimental……29

2.1 Chemicals……29
2.2 Instrumentations……29
2.2.1 Electrochemistry……30
2.3 Synthesis of fullerene-peptide 2-……31
2.4 Synthesis of fullerene-peptide 2+……34
2.5 Synthesis of fullerene-peptide 2- reference……38
2.6 Synthesis of fullerene-peptide 2+ reference……40
2.7 Synthesis of peptide-reference 2-……41
2.8 Synthesis of peptide-reference 2+……42
2.9 Synthesis of Boc-TOAC-NH*t*Bu……43

Chapter 3. Results and discussion……45

3.1 Synthetic approach……45
3.1.1 Protection of the amino group……45
3.1.2 Protection of the carboxylic function……46
3.1.3 Carboxyl activation……46
3.1.4 N-substituted-3,4-fulleropyrrolidines……47
3.2 The fullerene-Aib-peptide and the attempts for its synthesis……48
3.2.1 Nucleophilic attack to the saturated carbon of α-bromoamides……49
3.2.2 Use of activated ester……52
3.2.3 Use of acyl chloride / bromide……53
3.2.4 Novel strategy through fulleroproline……54
3.3 Investigation and Characterization in solution……59
3.3.1 FT-IR characterization of the 2+ and 2- systems……60
3.3.2 ^{1}H NMR characterization of fullerene-peptides-reference 2+

and 2-……63
3.3.3 Quenching of systems bearing the nitroxide monitored by cw-EPR……70
3.3.4 ^{1}H NMR characterization of systems bearing the nitroxide……74
3.3.5 UV-vis characterization of fullerene-peptides……80
3.3.6 Electrochemical investigation of systems 2+ and 2-……81

Chapter 4. Conclusion……89

Chapter 5. References……93

1. Introduction

1.1 Introduction on Fullerene

Buckimsterfullerenes are a family of organic molecules that constitute one of the allotrope forms of carbon. The name comes from the architect Buckimster Fuller whose constructing philosophy seems inspired by the spherical shape built up of fused pentagons and hexagons of fullerenes[1]. C_{60} is the smallest stable fullerene containing 20 hexagons and 12 pentagons[6a], followed then by the higher fullerenes such as C_{70}[1]. C_{60} is also known as (C_{60}-I_h)[5,6]fullerene because it has 60 carbon atoms that form a sphere belonging to the icosahedral symmetry group I_h and the numbers in brackets [5,6] indicate the presence of only pentagons and hexagons[1]. Since its discovery in the 1985 and its first large scale production in the 1990 by resistive heating of graphite[2], C_{60} has been subjected to several investigations for its unique properties and potential applications as a superconductor[3], as a ferromagnet[4], in electro-optic devices[5] and medicinal chemistry[6].

Figure 1.1 *The Montreal Biosphere by Buckimster Fuller, Montreal, 1967.*

1.1.1 Properties of Fullerene C_{60}

C_{60} has an outer diameter estimated as 7.10 Å. If you also take into account the thickness of the π-electron cloud, the diameter becomes 10.34 Å[7].

For the icosahedral symmetry I_h, the state, corresponding to the quantum number 5 for the angular momentum l, splits into the $h_u + t_{1u} + t_{2u}$ irreducible representations [8]. The lowest occupied energy level HOMO (highest occupied molecular orbital) , h_u, in the neutral C_{60} is 5-fold degenerated and completely filled with 10 electrons[9]. The symmetry of orbitals h_u is such that antibonding interactions with [5,6]-bonds, linking a pentagon with a hexagon, take place whereas bonding interactions are promoted for [6,6]-bonds, shared between two hexagons[1,6a,8,10]. These alternate interactions bring about two different length bonds: the former is called "long bond" (1.45 Å long) or 5,6 junction. The latter is the "short bond" (1.38 Å long) also termed 6,6 junction which possesses more electron density[1,6a,8,10]. In the lowest energy Kekulè structure, the double bonds are located only at the 6,6 junction[6a].

C_{60} strongly absorbs in UV region and weaker but significant bands in the visible region (410-620nm) make C_{60} solutions purple, due to orbital forbidden singlet-singlet transitions[1,6a,11,18]. Absorptions in the range 190-410 nm are due to allowed $^1T_{1u}$-^1A_g transitions instead[1,11,18]. When functionalized, it retains the same basic characteristics but, in addition, the absorption of the derivatives extends further into the near-IR region[12]. Its photophysical properties are very interesting. When it is photoexcited, the singlet state decays very efficiently via Inter System Crossing to the triplet excited state with triplet quantum yields very high ($\Phi_T \approx 0.96$) and relative long triplet lifetime (135 μs)[1,12,13,14,15]. The triplet state can give off phosphorescence[12] or can be deactivated in several ways such as ground state quenching[2], triplet-triplet annihilation[12], electron transfer to acceptor molecules[17], quenching by molecular oxygen leading to singlet oxygen[13], quenched by free radicals[16].

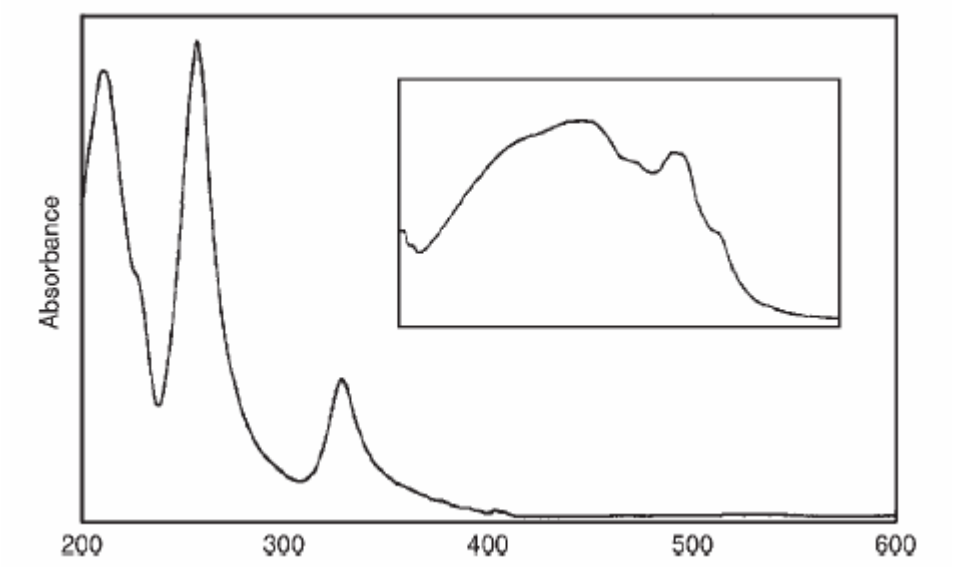

Figure 1.2 *Optical absorption spectrum of C_{60} in hexane. Inset: 420-470 nm region*[1].

Because of its high symmetry, C_{60} shows a single peak in the ^{13}C NMR at 143.2 ppm[1] in benzene-d_6. It was calculated that it has a longitudinal time relaxation fairly long, higher than 20 seconds[11].

In electron transfer reactions, C_{60} plays an important role owe to its low reorganization energy[1,12]. The buckybull is able to promote long-lived charge separated states[1,17]. Whereas its HOMO is 5-fold degenerate and fully occupied with 10 electrons, its LUMO (lowest unoccupied molecular orbital) and LUMO+1 are triple degenerated[35] and characterized by a relative low energy[1,19] so that C_{60} can reversibly receive up to 6 electrons in one-electron transfer processes[20]. Due to the extensive delocalization of the negative charge over many carbon atoms, the mono-anion is quite stable in the absence of oxygen[14]. The voltammetric experiments were carried out, for example using the mixed solvent system ACN / toluene 1:5 and at -10° C. The potentials measured ($E_{1/2}$) were -0.98, -1.37, -1.87, -2.35, -2.85 and -3.26 V vs Fc/Fc^+ [19]. It is important to emphasize that the penta- and the hexa-anions are stable and exhibit reversible behavior on the voltammetric time scale[19]. In the anionic species, Jahn-Teller instability is expected to decrease the symmetry of C_{60}[28,30]. Lower symmetry is also produced in solvents of low dielectric constant by the presence of the counterion[29,30].

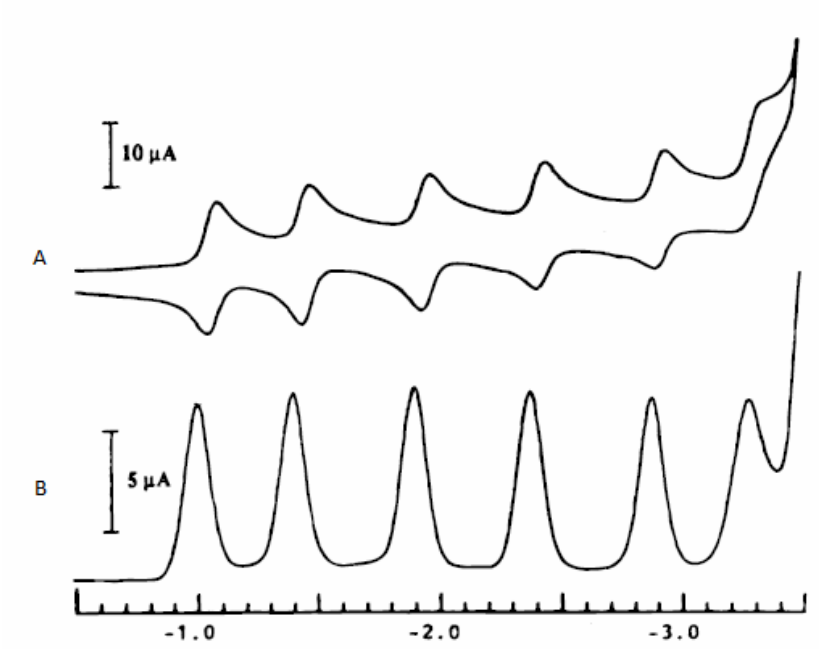

***Figure 1.3**. Reduction of C_{60} vs Fc/Fc^+ in ACN/toluene 1:5 with TBAH as supporting electrolyte at -10° C. A) CV, scan rate = 100 mV s^{-1}; B) DPV, scan rate = 25 mV s^{-1}, pulse with = 50 mV, period = 300 ms [19].*

Chemical reduction can be carried out employing electropositive metals such as alkali metals[9a,]. These compounds show superconductivity properties[21]. Some organic donor molecules such as cobaltocene, can form fully ionic salts with fullerene[22]. C_{60} derivatives are characterized by a small shift to more negative values of the reduction potentials in the cyclic voltammograms relative to C_{60} for the first three reduction waves[18,23,24,25].

For example, the potentials measured ($E_{1/2}$) for N-methyl-3,4-fulleropyrrolidine were -1.05, -1.44, -2.01, -2.42, -3.12 V vs Fc/Fc^{+} [24]. This phenomenon was explained considering that, the saturation of a double bond generated by the functionalization, causes a partial loss of conjugation[6a,18]. A particular case is offered by derivatives termed fulleroids [5,6]-open which are the only derivatives that retains the 60π electron configuration without loss of conjugation, unlike the [6,6]-closed fullerene derivatives[6a,27] or fulleropyrrolidines.

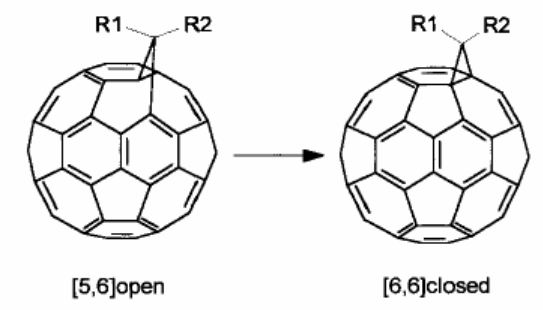

Figure 1.4 *Fulleroid [5,6]open (on the left) and fulleroid [6,6]closed (on the right)[26].*

In donor-acceptor experiments, where both energy and electron transfer processes have been reported, the nature of the spacer was found to play a role[6a]. For instance, through bond electron transfer was shown for dyads 1, 2, 3, whereas formation of a transient intramolecular exciplex was observed for compounds 4, 5[26] (Figure 1.5).

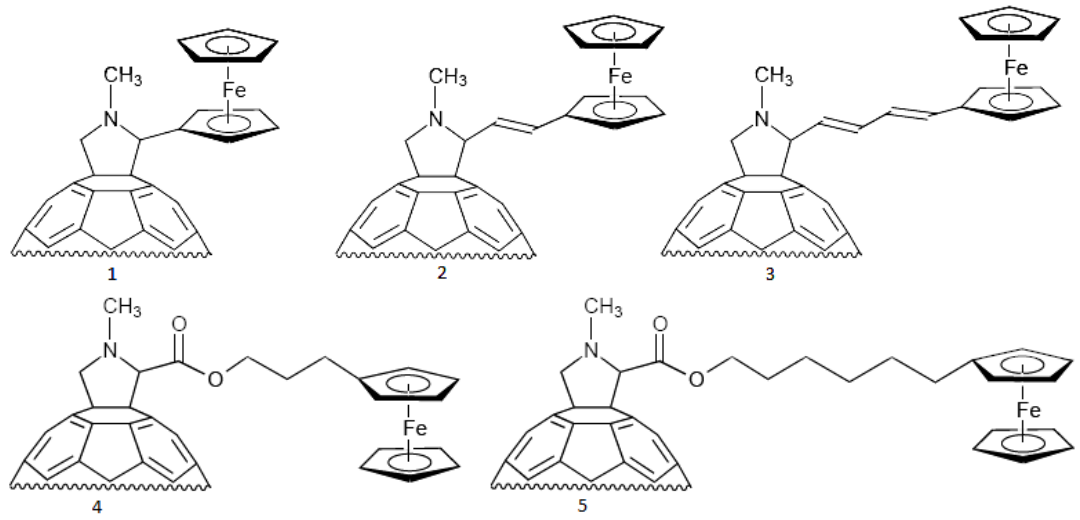

Figure 1.5 *Dyads examples for electron transfer studies.*

While in 1, 2, 3 derivatives, fast charge recombination probably prevents sufficient stabilization, the saturated hydrocarbon bridge in dyads 4, 5 is able to avoid charge recombination and long-lived charge separated states are detected in polar solvents[6a] (Figure 1.5).

Oxidation is far less facile than reduction and it occurs at comparatively high anodic potentials[19]. CV studies showed that the first 1-electron oxidation of C_{60} in 1,1,2,2-tetrachloroethane occurs at a very positive potential, +1.26V vs Fc/Fc^{+}[19].

The difference between the first oxidation and the first reduction of C_{60} at room temperature was calculated to be 2.32 V, which is a measure of the HOMO-LUMO gap of the molecule in solution[19].

C_{60} has four IR active stretching: 1430, 1182, 577, 527cm^{-1} [11]:

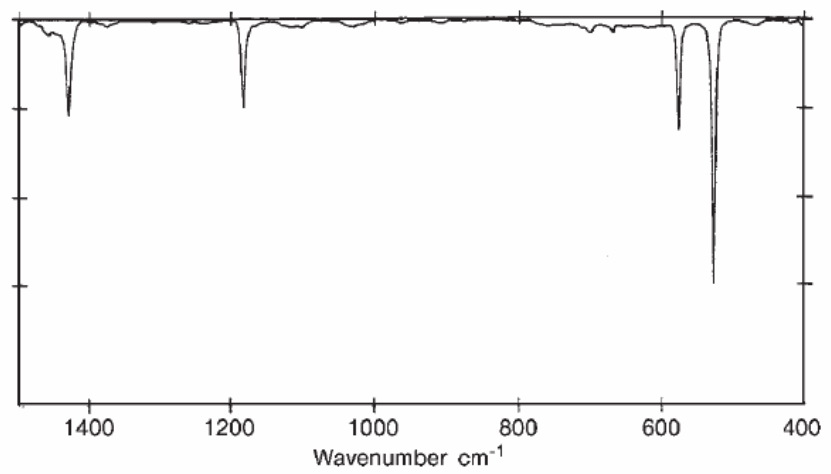

Figure 1.6 *IR spectrum of C_{60} in KBr [1].*

Interesting investigations can be carried out when the C_{60} is covalently linked to a molecule bearing a free radical such as TOAC (2,2,6,6-tetramethylpiperidine-1-oxyl-4-amino-4-carboxylic acid). CV at room temperature in THF on a Pt electrode, using TBAH as supporting electrolite, show five reversible reduction peaks for the fullerene and one irreversible reduction process due to the nitroxide substituent, positioned between the second and third fullerene moiety reduction steps[30]. On the oxidation side, the reversible oxidation of the nitroxide is observed[30]. Coupling between the triplet state of fullerene (generated after photoexcitation) and the doublet state of the nitroxide can be investigated by the TR-EPR (time-resolved electron paramagnetic resonance) technique[16,31,32,33].

1.1.2 About the chemistry of Fullerene C_{60}

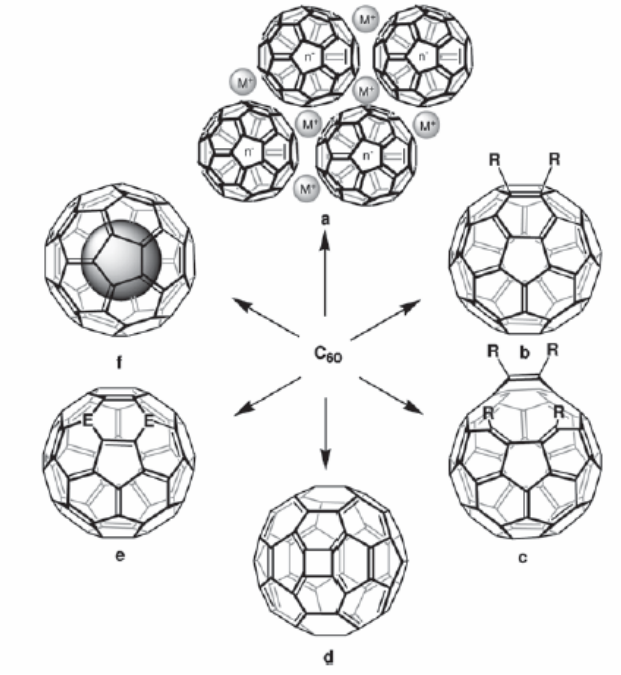

C_{60} posses 30 equivalent double bonds, all sharing the same reactivity which do not contain any hydrogen so that, whereas substitution reactions are not possible[1], redox and addition reactions can lead to several fullerenes derivatives as depicted by figure 1.7:

Figure 1.7 *a) fullerene salts; b) exohedral adducts; c) open cage fullerenes; d) quasi-fullerenes; e) heterofullerenes; f) endohedral fullerenes[1].*

Since pure *p* character of π orbitals is present only when the molecule lies on a plane, a rehybridization of the sp^2 σ and the *p* π orbitals appears to be present in the electronic structure of C_{60} leading to low-lying π^* orbitals with considerable *s* character[35]. As a consequence, C_{60} shows an electrophilic character and it is relatively easy to reduce[1]. All the double bonds are conjugated and enclose in the six member rings. Since they are forced to deviate from planarity[39] (pyramidalization of the sp^2 carbons), an excess of strain is present quantified to be 8 Kcal/mol per carbon[35]. A change towards the sp^3-hybridation promoted by chemical reactions (e.i., addition reactions) is a way for the molecule to release strain and in fact, the fullerene greatly favors reactions that decrease strain[35]. On the other hand, C_{60} is very stable compared with other fullerenes since all the pentagons are isolated by hexagons so that C_{60} is the smallest fullerene to obey the so called "isolated pentagon rule"[36,37] which assures an enhancement of the sphericity of the molecule[38]. When pentagons are adjacent instead, a resonance destabilization together with an increase of strain energy is present as a consequence of the fact that bonds are forced to deviate from planarity[1].

C_{60} behaves such as a fairly localized and electron-deficient polyolefin[1,6a]. In fact, C_{60} tends to form complexes with electron donors[12]. In analogy to olefins, it undergoes cycloadditions[50]. In particular, [3+2] cycloaddition with 1,3 dipole such as azomethine ylide was the synthetic route employed in this work to obtain N-substituted-3,4-fulleropyrrolidines, where the 3,4-bond of a pyrrolidine ring is covalently attached to a 6,6 ring junction of the fullerene moiety. The reaction is regioselective because only the [6,6] bond is attached. Indeed, the [6,6] double bonds of C_{60} exhibit a dienophilic character[40]. Besides, azomethine ylide can be easily generated in situ from several readily accessible materials.

In this work, the 1,3 dipole was obtained by decarboxylating the condensation product of N-substituted glycines with formaldehyde (see experimental part)[41].

The answer to the question "is C_{60} aromatic?"[64] is still debated because there is no suitable model to serve as a reference compound[64]. Several criteria were been taken into account. C_{60} is not planar and does not undergo substitution reactions typical of planar aromatics. On the other hand, from an energetic point of view, it shows an aromatic stability. Calculation of nucleus-independent chemical shift has revealed diatropic hexagons (aromatic molecules sustain diamagnetic ring current) and paratropic pentagons characteristic of antiaromatic molecules so that C_{60} can be defined "ambiguously aromatic"[35]. These two contributions cancel almost exactly and there is virtually no ring-current contribution to the magnetic susceptibility. To quote Haddon[35], "C_{60} molecule posses anomalous magnetic properties but with the reactivity of a continuous aromatic molecule, moderated only by the tremendous strain inherent in the spheroidal structure".

1.1.3 The endofullerene $H_2@C_{60}$

Since fullerenes are hollow molecules it should be possible to trap atoms inside the cage. Such particular fullerenes are called endofullerenes. The symbol @ is used to indicate the atoms in the interior of the fullerene. All atoms listed to the left of the @ symbol are located inside the cage. In this thesis work, $H_2@C_{60}$ endofullerene with encapsulated hydrogen was used. The synthetic approach for obtaining $H_2@C_{60}$ was termed "molecular surgery strategy"[43] that employs the following steps[44]: (1) creating a hole on the C_{60} surface by a cage opening; (2) increasing the size of the hole until its size allows insertion of H_2; (3) insertion of H_2 at 800 atmospheres and at 200°C in a autoclave for 8 hours; (4) closing the hole to regenerate the C_{60} fullerene host with an incarcerated H_2 guest. Upon return to room temperature and atmospheric pressure, the H_2 is incarcerated and stable inside the fullerene[42].

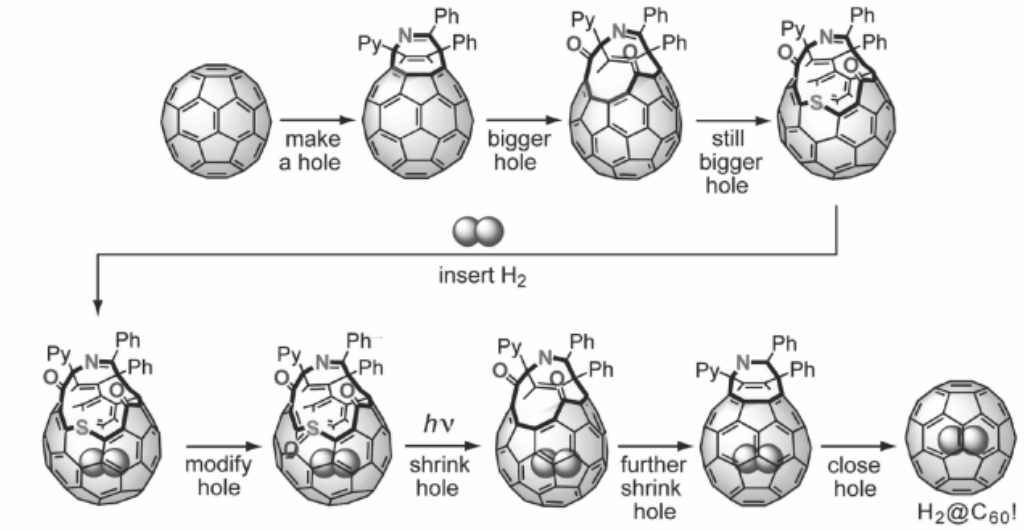

Figure 1.8. *Synthetic scheme for the synthesis of $H_2@C_{60}$ [43].*

Incarceration of H_2 inside C_{60} influences the NMR properties of H_2. For example, the chemical shift of H_2 in organic solvents is typically found at approximately +4.5 ppm, whereas the chemical shift of $H_2@C_{60}$ is found at much higher fields, approximately -1.3 ppm, "to the right of TMS" [45]. The very small downfield shift (0.078 ppm) observed for the ^{13}C NMR signal of $H_2@C_{60}$ (as compared to empty C_{60}) indicates that the electronic property of the fullerene cage is largely unaffected by the encapsulation of H_2[43].

1.2 Nitroxide radicals in solution[49]

Nitroxide free radicals, such as the aminoacid TOAC, have found applications in many fields and in particular, they are commonly used in the study of conformation and structural mobility of peptides and proteins[110] by EPR spectroscopy where they are employed as spin probes and spin traps. The ground state of a nitroxide mono radical is a doublet (s = ½). EPR spectrum of nitroxide

radicals at r.t. and in solution at low viscosity (fast orientational averaging) are characterized by three hyperfine lines (Figure 1.9) due to the coupling of the unpaired electron on the p^{π}_{z} of the nitrogen atom with the nuclear spin $I = 1$ of the nitrogen atom itself (^{14}N). Under the application of a magnetic field B, the degeneracy of the electron spin states $m_s = \pm 1/2$ is lifted and transitions between the spin levels are induced by radiation of the appropriate frequency. The Spin Hamiltonian, also known as Zeeman Hamiltonian, is the following:

$$\hat{H}_s = g\mu_B B\hat{S}_Z$$

where g is called *g-value* ($g_e = 2.00232$ for a free electron), μ_B is the Bohr magneton (9.274×10^{-28} J G^{-1}), B is the magnetic field strength in Gauss and $\hat{S}_Z$ is the z-component of the spin angular momentum operator (the magnetic field defines the z-direction). The difference in energy between the two spin energy levels is:

$$\Delta E = g\mu_B B = h\nu$$

corresponding to the energy, $h\nu$, of a photon required to cause a transition. The unpaired electron interacts with its environment and the details of EPR spectra depend on the nature of those interactions. Because the nitrogen magnetic nuclei interact with the unpaired electron, we have another perturbation of the electron energy which enters in the Spin Hamiltonian with the term $\hat{I}A\hat{S}$ where A is the hyperfine coupling parameter. In solution at low viscosity, due to the rapid molecular tumbling, all the anisotropic interactions are averaged on time. Purely isotropic coupling a_N is responsible for the appearance of multiplets constituted of $(2I+1)$ 3 lines. The Fermi contact interaction, for example, leads to pure isotropic interaction and is due to the non-zero probability to find the electron spin at the same point in space as the nuclear spin. This happens only when the unpaired electron is in an s orbital because this orbital does not have any nodal plane at the nuclei.

The parameters g and the hyperfine splitting factor a are characteristic for every paramagnetic species. In case of nitroxides, g value of 2.0061 and $a_N \sim 15.3$ G [14,30-34] are found. The energy of the transition corresponding to central line in the nitroxide continuos wave EPR spectrum is $g_{ISO}\mu_B B = h\nu$. Since μ_B and h are constant, ν is known (the frequency is fixed and it depends on the instrument) and B can be read from the spectrum, it is thus possible to obtain the g_{ISO} value of the specie under investigation. In the fast orientational averaging, g value is to be regarded as an effective value averaged over all orientations $g_{ISO} = (g_x + g_y + g_z) / 3$. Furthermore, the three line in the spectrum EPR are equally spaced of

$$\Delta B = a_N (g/g_e)$$

Therefore it is possible to obtain the hyperfine parameter a_N once that the g value is calculated.

In this work, an X-band (ν = 9.5 GHz) cw EPR (continuous wave) instrument was employed. For technical reasons, best sensitivity and resolution in EPR is achieved at fixed microwave frequency. The magnetic field is swept and at

the same time modulated with a frequency of 100 KHz. The field modulation causes a signal modulation at the same frequency of 100 KHz. Phase-sensitive detection of this modulation yields the derivative of the absorption spectrum.

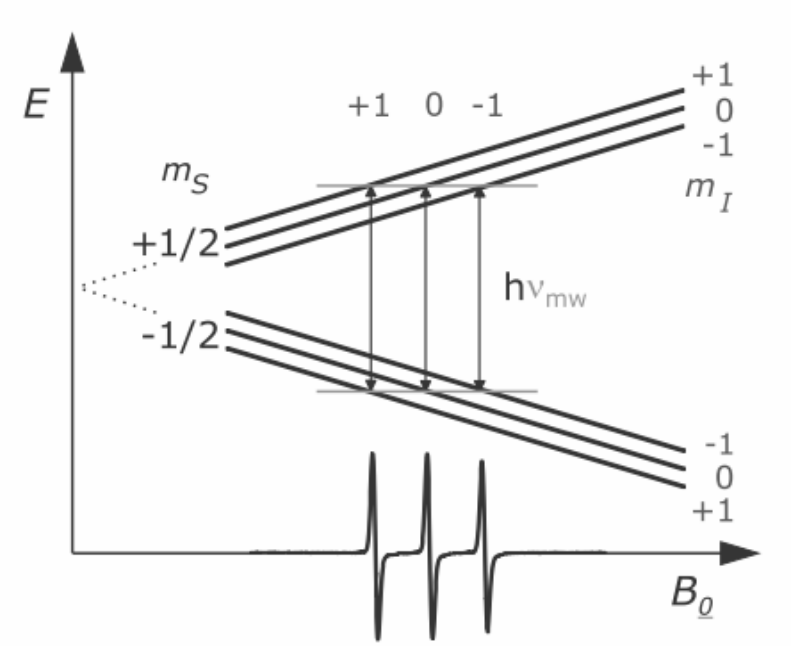

Figure 1.9 *Schematic energy level scheme and cw EPR spectrum of a nitroxide radical in the regime of fast orientational averaging. Only the electron Zeeman and* ^{14}N *hyperfine interactions are here considered.*

1.2.1 About TOAC amino acid

TOAC is an uncoded aminoacid characterized by a piperidinic ring bearing a free radical (the nitroxide group) stabilized by the steric hindrance due to the two next tetrasubstituted carbons that prevents dimerization and by delocalization over the N-O bond[51].

Its synthesis starts from 2,2,6,6-tetramethyilpiperidin-4-one which is converted to 2,2,6,6-tetramethetylpiperidin-1-oxyl-4-one (4-oxo-TEMPO) through oxidation with H_2O_2 in presence of Na_2WO_4 (sodium tungstate).

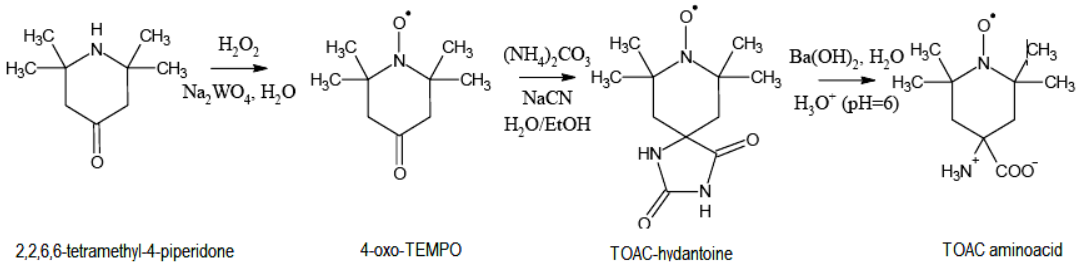

Figure 1.9 *Synthesis scheme of TOAC aminoacid.*

The last step includes the transformation of the ketone intermediate into the spyrohydantoine which is hydrolyzed to aminoacid using $Ba(OH)_2$ in water at 135°C for 48 hours[52].

TOAC is characterized by a weak absorption band (ε = 5-20 L cm^{-1} mol^{-1}) in the visible spectral region (λ = 420-450 nm) assigned to the $n \rightarrow \pi^*$ transition of the nitroxide chromophore[53].

TOAC derivatives can not be characterized by ^{1}H NMR because the paramagnetic center relaxes very fast thus causing strong broadening of NMR lines of nuclei in its vicinity. Even at distances longer than 6 Å, NMR lines may still be broadened beyond detectability[49].

1.3 α-aminoisobutyric acid (Aib) and the 3_{10}-helix

TOAC is tetrasubstituted at the α carbon and likewise Aib, which is another example of C^{α}-tetrasubstituted α-aminoacid, is remarkably rigid and subjected to an elevate restriction to its accessible conformational spaces. As a consequence, it is very efficient to induce β-turn or 3_{10} / α-helical structures in peptides[54]. In particular, very short Aib-homo-peptides (until 6 residues) show a high tendency to assume the 3_{10}-helical structures[55,56].

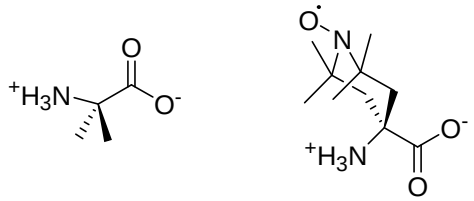

Figure 1.10 *Molecular structures of Aib (on the left) and TOAC (on the right).*

It was demonstrated not only that the tendency of Aib-homopeptides to form β-turns and 3_{10}-helices starts already from the tripeptide[56-61] but also that TOAC follows the same structural tendencies of Aib[62,63]. The 3_{10}-helix and the α-helix are the most commune helices[56] which are substantially different as pointed out in the following chart[56]:

	3_{10}-helix	**α-helix**
ψ	-30°	-42°
Φ	-57°	-63°
Rotation per residue	111°	99°
Number of residues per turn	3.24	3.63
Pitch	6.29 Å	5.67 Å

The parameters above show how the 3_{10}-helix is more elongated and narrower than the α-helix.

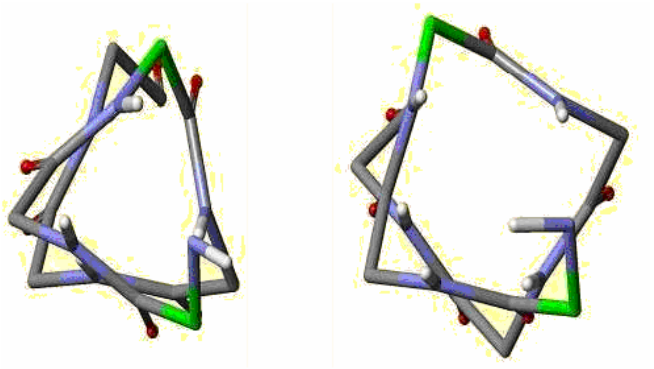

Figure 1.11 *Section of 3_{10}-helix (on the left) and section of α-helix (on the right).*

Besides, the 3_{10}-helix is stabilized by intramolecular H-bond between the C=O group of the residue in the *i*-position and the N-H group of the residue in position *i+3*. For the *α*-helix, it is the N-H group of the residue in position *i+4* involved in the H-bond, instead.

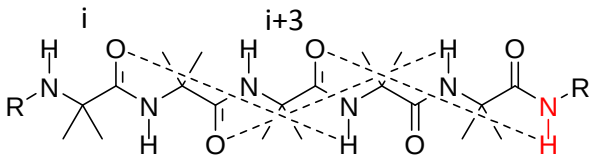

Figure 1.12 *The intramolecular H-bond of an Aib-peptide are depicted with a dotted line.*

It is worthwhile to note that Aib homopeptides posses an high tendency to give raise to structured peptides which is already evident from very short oligomers[62,64,65]. A framework of intramolecular C=O···H-N hydrogen bonds cause C=O and N-H groups to align significantly along the peptide axis. Consequently, 3_{10}-helices are characterized by a strong oriented dipole moment developing along the peptide backbone[62,64,-68]. The unique rigidity of short Aib homopeptides together with the excellent electronic communication provided by the peculiar backbone stiffness qualify them as a successfully spacers or templates in electrochemical and spectroscopic investigations[69]. Molecular spacers are linear structure which enable to locate probes at known distances and positions in the space. The Maran group has previously studied ET reactions across Aib homo-oligopeptides using donor-peptide-acceptor systems in solution[66,67]. Evidence was obtained for a mild distance dependence of the ET rate and even an increase of the rate at a certain peptide length. This outcome was rationalized by considering that while addition of a new *α*-amino acid unit increases the donor-acceptor distance, it also introduces new intramolecular hydrogen bonds that act as efficient ET shortcuts, thereby counteracting the usually observed exponential drop of the ET rate with distance. Theoretical studies supported the general features of this experimental finding[70,71].

1.4 Characteristics of the investigated fullerene-peptides 2+ and 2-

Two couples of fullerene-peptides were synthesized, differing in the direction of the dipole moment: a couple termed *plus* with the positive pole of the dipole moment oriented toward C_{60} and a *minus* couple where the dipole moment is reversed. The name of the fullerene-peptide is given as composed by a number, which refers to the number of intramolecular hydrogen bonds, and a *plus* or *minus* sign, which refers to the orientation of the dipole moment. Each couple is composed by the fullerene-peptide and its reference, that is, the fullerene-peptide-reference where the TOAC residue is substituted by an Aib residue.

a)

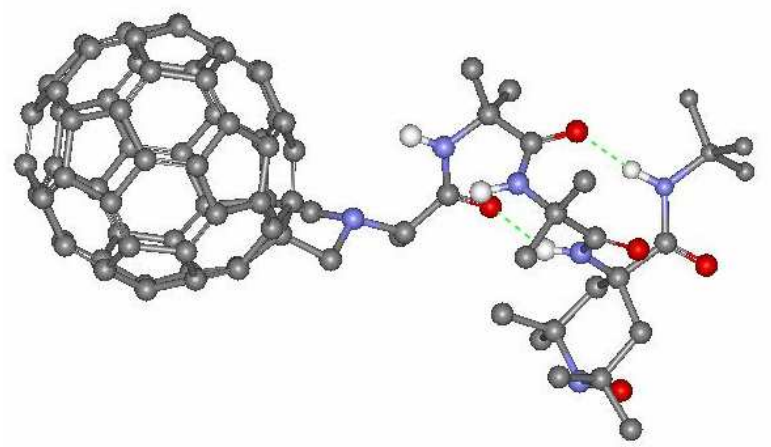

b)

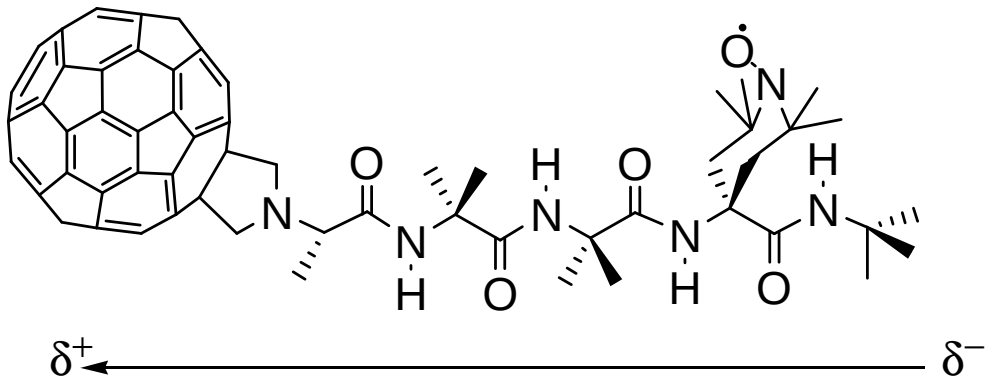

Figure 1.13 *a) secondary structure of fullerene-peptide 2+; b) primary structure of fullerene-peptide 2+.*

Figure 1.15 shows the primary and secondary structure of the fullerene-peptides 2+. In the fullerene-peptide 2+ reference, TOAC is substituted by Aib. The fullerene-peptide 2+ is used in the following discussion to explain the general design of our systems. The head of our system is represented by the fulleropyrrolidine that allows to grasp the fullerene to the peptide via amide bond. On the other terminus, where TOAC is positioned, there is a *tert*-butyl amide group.

Fulleropyrrolidine and TOAC, the only redox active groups in the experimentally applied potential window, are spaced by a small peptide. Figures 1.15 a, b help to understand better the orientation of the dipole. The helicity of the system infers a particular orientation to the aminoacidics residues, orienting all C=O groups toward the C terminus and all N-H groups toward C_{60}. Accordingly, the dipole moment has the *plus* pole by the fullerene moiety.

A *minus* fullerene-peptide was synthesized to investigate the effect of reversing the dipole moment and to compare the results with the *plus* fullerene-peptide. In the *minus* fullerene-peptide the characteristics of the design are the same, but while fulleropirrolidine is now attached to the C terminus that now becomes the head of the fullerene-peptide, the *t*-butyl amide group is on the other terminus that becomes the tail where TOAC is located. Figure 1.16 shows the primary (a) and secondary structure (b) of the fullerene-peptide 2-. In the fullerene-peptide 2- reference, TOAC is substituted by Aib. From the 3D structure we can notice that the C=O groups are now oriented toward C_{60}, while the NH groups are oriented toward the tail of the peptide represented by TOAC. Consequently, the negative pole of the dipole moment is by the fullerene.

a)

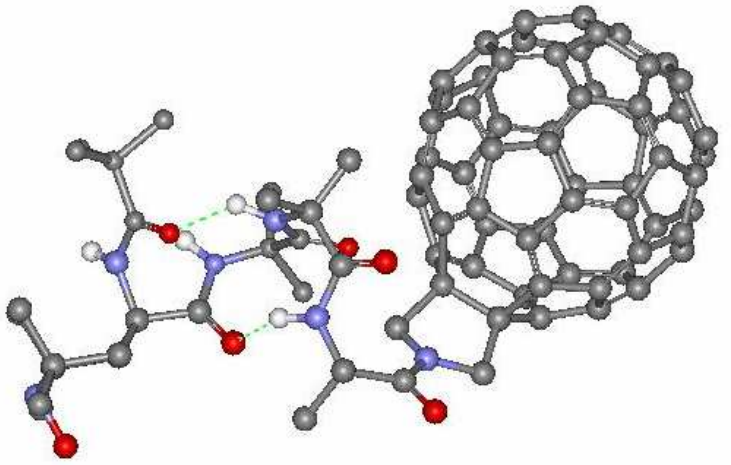

b)

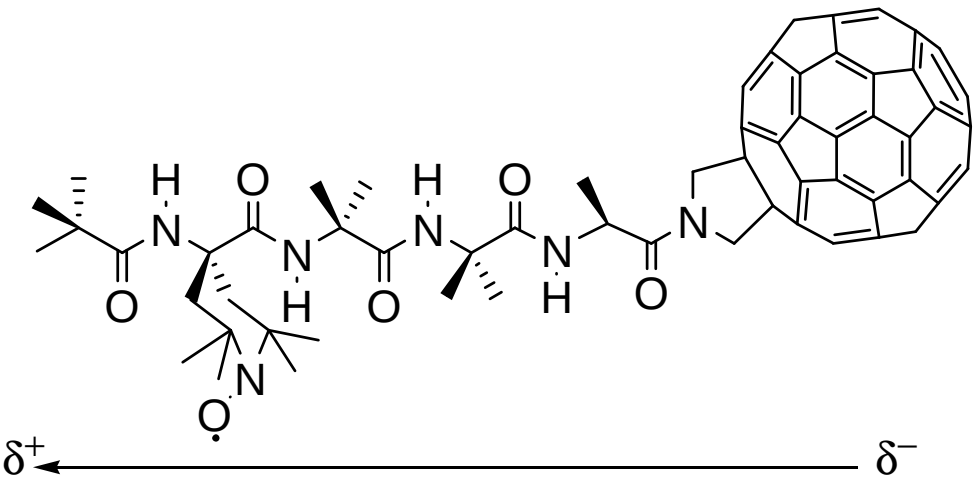

Figure 1.14 *a) secondary structure of fullerene-peptide 2-; b) primary structure of fullerene-peptide 2-.*

To gain a full understanding of investigated compounds, two other peptides-reference 2+ and 2- were synthesized which lack only of the fullerene moiety. These two peptides-reference retain the same number of intramolecular hydrogen bonds of the fullerene-peptides 2+ and 2- and differ from each other only from the position of the TOAC residue which is located on the N-terminus on the peptide-reference 2- and on the C-terminus on the peptide-reference 2+. A complete overview of compounds-set is shown in figure 1.15.

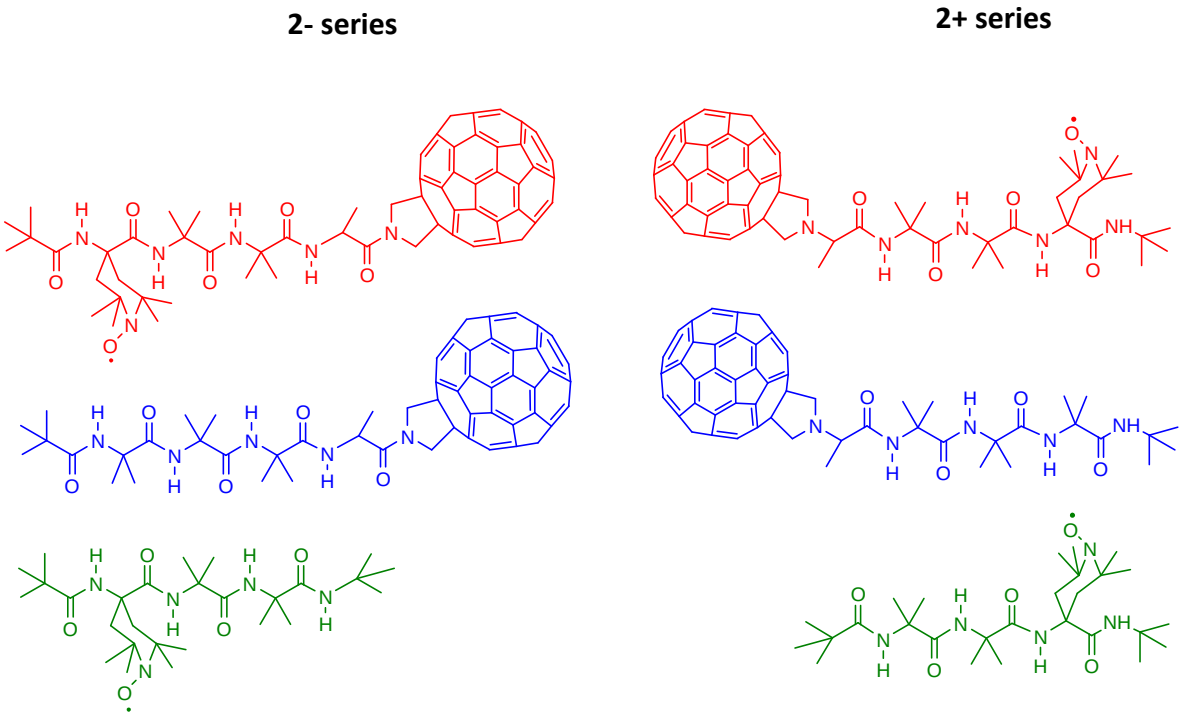

Figure 1.15. *Primary structures of compounds-set. 2- series (from the top): fullerene-peptide 2-, fullerene-peptide-reference 2-, peptide-reference 2-. 2+ series (from the top): fullerene-peptide 2+, fullerene-peptide-reference 2+, peptide-reference 2+.*

In addition, we were provided with some sample of $H_2@C_{60}$ to carry out the synthesis of H_2@fullerene-peptides 2+ and 2-.

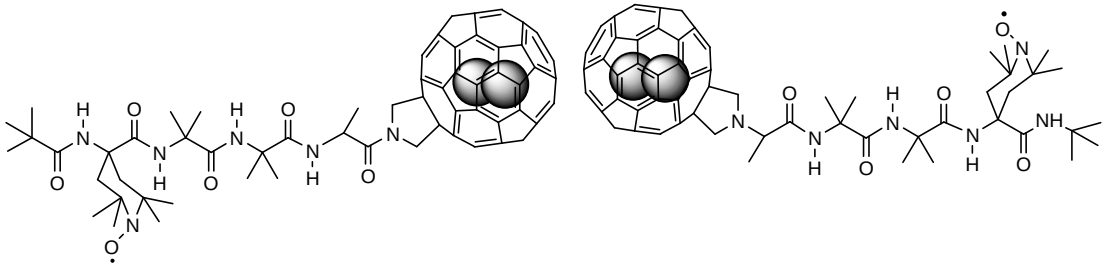

Figure 1.16 *Molecular structures of the endofullerene-peptide 2- (on the left) and 2+ (on the right). The two balls inside the C_{60} cage stand for the hydrogen molecule.*

1.5 Purpose of the thesis

Aim of this Thesis is the synthesis, characterization and investigation of a series of compounds in which fullerenes, peptides, and radicals are coupled. In particular, two series of compounds (shown in the previous paragraph) were synthesized which are characterized by the presence of a fullerene moiety and / or of a nitroxide function covalently linked at the extremity of rigid peptide. The features of the peptide are such that a strong oriented dipole moment, oriented along the main molecular axes, arises. The direction of this peptide dipole is reversed in the two series named 2+ and 2-. The investigation of this two series of compounds could, in principle, elucidate how this electric macrodipole affects the moieties (fullerene and the nitroxide function) located at its extremity.

It is worthwhile to note that Aib homopeptides posses an high tendency to give raise to structured peptides which is already evident from very short oligomers[62,64,65]. The unique rigidity of short Aib homopeptides, provided by the peculiar backbone stiffness, qualify them as a successfully spacers in spectroscopic investigations. Thank to this unique feature, it can be assumed that the nitroxide-C_{60} distance in the fullerene-peptides, obtained from molecular modeling, is a good approximation to the true value. An accurate estimation of the distance is crucial for several investigations where the interactions between the fullerene (or the hydrogen molecule encapsulated inside its cage) and the nitroxide are distance-dependent.

The synthesis of most of the systems and the electrochemical measurements were performed at the University of Padova. Part of the synthesis and some characterization work, in particular ^{1}H NMR experiments, were carried out in the research group of Professor Nicholas J. Turro (Department of Chemistry and Biochemistry of Columbia University, New York). It is worth to say that ^{1}H NMR spectra of nitroxide derivatives are fairly rare in literature since they are more often identified by mass analysis and elemental analysis.

At the Columbia University I also had an outstanding occasion: I was provided with a small amount of $H_2@C_{60}$ and this allowed us to carry out the synthesis of the fullerene-peptides 2+ and 2- employing this precious endofullerene.

2. Experimental

2.1 Chemicals

Unless stated otherwise, all chemicals commercially available were used as received. Fullerene-C_{60} (99.5%), benzyl bromoacetate (96%), Boc-L-Ala-OH (99%), cyanuric fluoride (97%), Z-Ala-OH (99%), sarcosine *tert*-butyl ester hydrochloride (97%), trifluoromethansulfonic acid (99%), 2-bromoisobutyryl bromide (98%), silver trifluoromethanesulfonate (≥99%), silver(I) oxide (99.99%), paraformaldehyde (95%), formaldehyde (water solution 37%), N-triphenylmethyl-glycine (98%), triphenylmethylamine (99%), 2-aminoisobutyric acid (99%), Fmoc-OSu (98%), Fmoc-Aib-OH (99%), N,N-diisopropylethylamine DIEA (99%), $Na_2S_2O_4$ sodium dithionite (85%), 1,2-dichloroethane (HPLC grade, ≥99.8%) were purchased from Sigma-Aldrich. L-Alanine *tert*-butyl ester hydrochloride (99%), ethanol (HPLC grade, ≥99.8%), Palladium on activated charcoal (10% Pd) were purchased from Fluka. EDC·HCl, HOAt were purchased from GL Biochem. $CHCl_3$ (HPLC grade, ≥99.8%), MeOH (HPLC grade, ≥99.8%), toluene (HPLC grade, ≥99.8%) were purchased from HiPerSolv Chromanorm. 1,4-dioxane (99.8%) was purchased from Lab-Scan Analytical Sciences. DCM (HPLC grade, ≥99.5%) was purchased from Carlo Erba Reagents. ACN (HPLC grade, ≥99.9%) was purchased from LiChroSolv. 3-trityl-5-oxazolidinone[73], 3,4-fulleropyrrolidine[24,41], Boc-Ala-Fp[75], Fmoc-TOAC-OH[76], Z-$(Aib)_2$-OMe[81], Z-$(Aib)_3$-OH[81] were synthesized as previously reported. The synthesis of compounds with the endofullerene was performed according to the procedure followed for the synthesis of analogous compounds with the empty fullerene. The ^{1}H NMR signal of the encapsulated hydrogen falls, in all these endofullerene derivatives, at -4.47 ppm to the right of TMS.

2.2 Instrumentations

Separations by flash chromatography were performed using silica gel 60M (0.04 - 0.063 mm, Macherey-Nagel) as stationary phase. Macherey-Nagel TLC-cards (0.2 mm silica gel supported on plastic sheets) were used for TLC analysis and spots were visualized under UV light (λ = 254 nm) and after exposition to iodine vapor and $KMnO_4$ water solution. Reaction residues, dissolved in the minimal amount of solvent, were directly loaded into the column. ^{1}H and ^{13}C NMR spectra were recorded on Bruker AC200 spectrometer operating at 200 MHz and 50 MHz respectively and using a Bruker Ascend operating at 500 MHz. Two-dimensional spectra were obtained from ROESY experiments carried out in deuterochloroform. Chemical shifts are given in parts per million (δ) relative to TMS. ^{1}H-NMR of compounds containing TOAC residue were obtained by mixing 1 mg of compound in 500 µl of ACN-*d3*/D_2O 1:1 with 2 equivalents of $Na_2S_2O_4$ [72]. Splitting patterns are abbreviated as follows: (s) singlet, (d) doublet, (t) triplet, (q) quartet, (m) multiplet.

FT-IR (Fourier transformed Infrared) spectra were recorded on a Perkin-Elmer 1720 X spectrophotometer using either KBr drifts or 1mM – 0.1mM $CHCl_3$ solutions on cells of 1 mm / 10 mm path length. ESI-mass spectra (electron spray ionization) were obtained with a Mariner mass spectra, model ESI-TOF, Perspective Biosystem. MALDI-TOF mass spectra (matrix-assisted laser desorption ionization, time of flight) mass spectrometry experiments were carried out using an Applied Biosystems 4800 MALDI-TOF / TOF spectrometer equipped with a Nd:YAG laser operating at 355 nm. The laser firing rate was 200 Hz and the accelerating voltage was 25 kV. DCTB, trans-2-[3-(4-*tert*-Butylphenyl)-2-methyl-2-propenylidene]malonitrile was employed as matrix. Mp (Melting point) were measured by means of a Leitz device, model Laborlux 12, equipped with a warming table. Mp are not corrected. UV-vis absorbtion spectra were taken in $CHCl_3$ with a Agilent spectrophotometer. The systems concentrations were chosen to provide an optical absorbance *A* near 350 nm of ~ 1.0. The experiments were carried out at room temperature. Steady-state EPR spectra were acquired using a continuous wave Bruker ER 041 XG X-band (ν = 9.75243 GHz) spectrometer.

2.2.1 Electrochemistry

The electrochemical experiments were performed by using an homemade glassy carbon, GC, electrode that was prepared by sharpening a 3 mm diameter Tokai GC-20 rod to obtain a disk with a radius of 0.56 mm. The GC was connected to a copper wire with silver epoxy and then sealed in glass tubing with epoxy (Torr Seal). The electrode was polished using silicon carbide papers (500, 1000, 2400, and 4000), diamond pastes (Struers: 3, 1, and 0.25 μm), alumina (BDH: 0.075 and 0.015 μm), and then stored in ethanol. Before experiments, the electrodes were polished with 0.015 μm alumina, ultrasonically rinsed with ethanol for 5 minutes, washed with acetone, and carefully dried with a cold air stream. The electrodes were electrochemically activated in the background solution by means of several voltammetric cycles at 0.5 V s-1 between the anodic and cathodic potential limits of concern. The electrode areas were determined by measuring the voltammetric current for the oxidation of ferrocene in DMF/0.1 M tetra-n-butylammonium perchlorate, in which ferrocene has a diffusion coefficient of $1.13 \times 10\text{-}5$ cm^2 s^{-1}. Ferrocene Fc (Carlo Erba) was recrystallized by sublimation using a cold finger. A CHI 660c electrochemical workstation was used for both differential pulse voltammetry (DPV) and cyclic voltammetry (CV) experiments. The solvent was 1,2-dichloroethane (DCE, Sigma Aldrich, HPLC grade 99.8%) containing 0.1 M tetra-*n*-butylammonium hexafluorophosphate (TBAH) as the supporting electrolyte. TBAH (Fluka, 99%) was recrystallized from ethanol. For DPV, we used peak amplitude of 50 mV, pulse width of 0.05 s, 2 mV increment per cycle, and pulse period of 0.1 s. For the CV experiments, we employed the feedback correction to minimize the ohmic drop between the working and the reference electrodes. All electrochemical experiments were conducted under an Argon atmosphere in an all-glass microcell that was thermostated at 25 °C. A Pt wire was the counter electrode and an Ag wire was used as a quasi-reference electrode.

The Ag wire was kept in a tube filled with the same electrolyte solution but separated from the main working vessel by a Vycor frit. The behavior of the electrode and the quality of the solvent/electrolyte system was first checked in the background solution by using CV. At the end of each experiment, the reference electrode potential was calibrated against the ferricenium/ferrocene (Fc^+/Fc) couple.

2.3 Synthesis of fullerene-peptide 2-

(Boc-Ala)$_2$O

84 mg (0.44 mmol, 2 equiv) of Boc-Ala-OH were dissolved in 10 mL of anhydrous ACN cooled to 0°C before adding 40 mg of EDC·HCl (0.21 mmol, 1 equiv). The solution was stirred for 30 minutes at 0°C and 4 h at r.t.. Disappearance of Boc-Ala-OH was monitored by TLC (eluent EP/EtOAc 1/1). Afterwards, solvent was removed under reduced pressure and product was immediately used for coupling with fulleropyrrolidine.

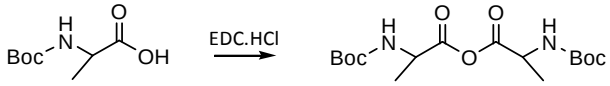

Fmoc-TOAC-(Aib)$_2$-OMe

450 mg (1.34 mmol, 1 equiv) di Z-(Aib)$_2$-OMe was dissolved in 20 ml of MeOH and 50 mg of Pd/C 10% (10% w/w) were added. After stirring for 1 h under hydrogen bubbling, the mixture was centrifuged in order to remove the catalyst and solvent was evaporated under reduced pressure and then under vacuum. 0.7 g di Fmoc-TOAC-OH (1.61 mmol, 1.2 equiv) were suspended in 5 ml of anhydrous DCM and 263 mg (1.93mmol, 1.44 equiv) of HOAt and 370 mg (1.44 mmol, 1.2 equiv) of EDC.HCl were added. The mixture was stirred for 1 h at 0°C until complete dissolution of reagents and then poured into the flask containing H-(Aib)$_2$-OMe and 233 µl (1.34 mmol, 1 equiv) of DIEA. After stirring for 3 days, solvent was evaporated under reduced pressure and the residue was washed with 2x50 ml of a 10% $KHSO_4$ water solution, 30 ml of water, 2x50 ml of a 5% $NaHCO_3$ water solution, 50 ml of water and finally dried over Na_2SO_4. Solvent was evaporated and product was crystallized from EP/EtOAc affording 567 mg (yield 68%) of a yellowish solid. TLC: Fmoc-TOAC-(Aib)$_2$-OMe, eluent $CHCl_3$/EtOH 9/1, R_f 0.7.

Mp: 190-192°C
FT-IR (KBr) (cm^{-1}) 3361, 2986, 2941, 1705, 1522, 1455, 1383, 1251, 1150, 1106, 1028, 909, 737, 642.
^{1}H-NMR (200 MHz, CD_3CN/D_2O 2/1, $Na_2S_2O_4$) 7.85 (m, 2H), 7.63 (m, 2H), 7.39 (m, 4H), 4.47 (m, 2H), 4.26 (m, 1H), 3.57 (s, 3H), 1.35 (m, 24H).
ESI-MS $C_{34}H_{45}N_4O_7$ (MW = 621) *m/z* = 622 $[M+H]^+$

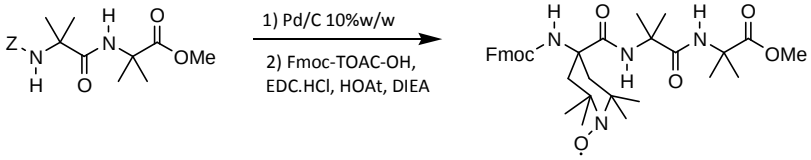

Piv-TOAC-(Aib)$_2$-OMe

400 mg (0.64 mmol, 1 equiv) of Fmoc-TOAC-(Aib)$_2$-OMe were dissolved in 8 ml of ACN and 2 ml of Et_2NH were added. After stirring for 1.5 h, solvent was evaporated and the residue was purified through flash chromatography using DCM/MeOH 9/1 as eluent. Solvent was removed under reduced pressure and under vacuum affording 253 mg of H-TOAC-(Aib)$_2$-OMe (0.63 mmol, 98% yield). Subsequently, the deprotected peptide was dissolved in 20 ml of anhydrous DCM together with 220 µl (1.26 mmol, 2 equiv) of DIEA. 156 µl (1.26 mmol, 2 equiv) of Piv-Cl in 3 ml of anhydrous DCM were added dropwise and the solution was stirred for 1 day. Solvent was removed under reduced pressure and the residue was washed with 3x50 ml of a 10% $KHSO_4$ water solution, 50 ml of water, 3x50 ml of a 5% $NaHCO_3$ water solution, 50 ml of water and finally dried over Na_2SO_4. Solvent was evaporated and product was crystallized from EP/EtOAc affording 230 mg (yield 74%). TLC: Fmoc-TOAC-(Aib)$_2$-OMe, eluent $CHCl_3$/EtOH 9/1, R_f 0.5.

Mp: 253-255°C
FT-IR (KBr) (cm^{-1}) 3398, 3328, 2978, 1729, 1688, 1644, 1529, 1452, 1363, 1302, 1225, 1157, 994, 883, 628.
^{1}H-NMR (200 MHz, CD_3CN/D_2O 2/1, $Na_2S_2O_4$) δ 7.28 (s, 1H), 7.06(d, 2H), 3.58 (s, 3H), 2.34 and 2.37 (two s, 2H), 2.15 and 2.07 (two s, 2H), 1.51 (s, 6H), 1.38 and 1.32 (s, 18H), 1.18 (s, 9H).
ESI-MS $C_{24}H_{43}N_4O_6$ (MW = 483) *m/z* = 484 $[M+H]^+$

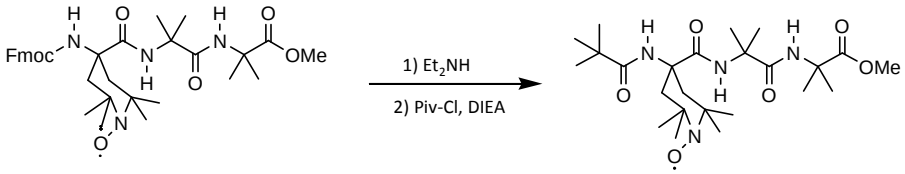

Piv-TOAC-(Aib)$_2$-OH

170 mg (0.27 mmol, 1 equiv) of Piv-TOAC-(Aib)$_2$-OMe were suspended in 2 ml of MeOH and 322 mg (8.04 mmol, 30 equiv) of NaOH in 2 ml of water were added. After stirring for two days, the solution was diluted with EtOAc up to 100 ml and washed with a 3x100 ml of a 10% $KHSO_4$ water solution, 100 ml of water and finally solvent was evaporated under reduced pressure and under vacuum. 82 mg (yield 63%) of a yellowish solid were obtained after crystallization from EtOAc/EP. TLC: Piv-TOAC-(Aib)$_2$-OH, eluent $CHCl_3$/EtOH 9/1, R_f 0.1.

Mp: 242-244°C
FT-IR (KBr) (cm^{-1}) 3308, 2978, 1742, 1644, 1526, 1458, 1383, 1363, 1312, 1221, 1170, 1113, 883, 676, 639, 608.

^{1}H-NMR (200 MHz, CD_3CN/D_2O 2/1, $Na_2S_2O_4$) δ 7.35 (s, 1H), 7.07 (s, 1H), 7.04 (s, 1H), 2.35 and 2.27 (two s, 2H), 2.14 and 2.07 (two s, 2H), 1.51 (s, 6H), 1.39 (m, 12H), 1.32 (s, 6H), 1.17 (s, 9H).
ESI-MS $C_{23}H_{41}N_4O_6$ (MW = 469) *m/z* = 470 $[M+H]^+$

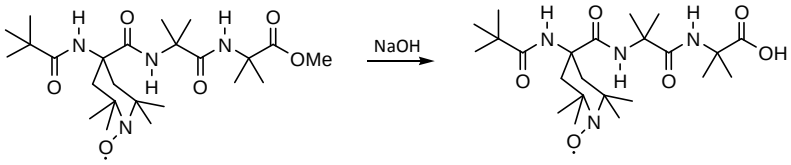

Piv-TOAC-(Aib)$_2$-Ala-Fp

50 mg (0.05 mmol, 1.1 equiv) of Boc-Ala-Fp were dissolved in 15 ml of $CHCl_3$ together with 15 ml of TFA. After stirring for 1 h at r.t., solvent was evaporated and the residue washed with 4x30 ml of Et_2O. 23 mg (0.05 mmol, 1 equiv) of Piv-TOAC-(Aib)$_2$-OH were dissolved in 5 ml of anhydrous $CHCl_3$ and 11 mg (0.06mmol, 1.2 equiv) of EDC·HCl were added. After stirring at r.t. for 1 h, the solution was cooled down to 0°C and poured in the flask containing H-Ala-Fp and 16 µl (0.14 mmol, 3 equiv) of DIEA in 50 ml of anhydrous $CHCl_3$. The mixture was stirred at r.t. for 7 days. Solvent was removed under reduced pressure and the residue was washed with 2 ml of MeOH and then 2 ml of toluene in a centrifuge tube. Subsequently the residue was subjected to flash chromatography, eluent $CHCl_3$, $CHCl_3$/EtOH 200/1, 100/1, 50/1 to afford 11 mg of a brown solid (yield 18%). TLC: Piv-TOAC-(Aib)$_2$-Ala-Fp, eluent $CHCl_3$/EtOH 9/1, R_f 0.4; eluent toluene/EtOH 8/1, R_f 0.2.

IR (1mM, $CHCl_3$) (cm^{-1}) 3466, 3436, 3344, 1661, 1513, 1494, 1456, 1380, 1363.
^{1}H NMR (500 MHz, $CDCl_3$, 10 equivalents PH) 7.72 (d, 1H), 6.70 (s, 1H), 6.40 (s, 1H), 5.75-5.50 (m, 3H), 5.26 (m, 2H), 2.38-2.34 (m, 2H), 2.24-2.21 (m, 2H), 1.68-1.51 (m, 21H), 1.39-1.31 (m, 15H).
MALDI-MS $C_{88}H_{49}N_6O_6$ (MW=1285) *m*/z= 1308 $[M+Na]^+$
UV-vis ($CHCl_3$) λ (ε) 310 (24800), 430 (2700)

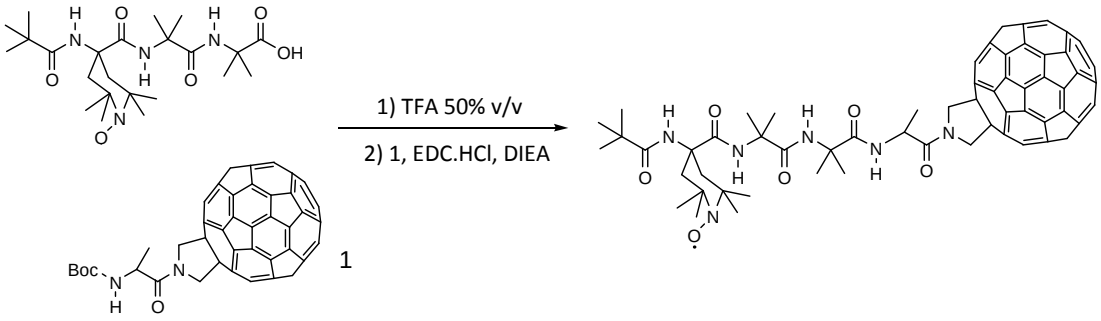

2.4 Synthesis of fullerene-peptide 2+

H-TOAC-NH*t*Bu

To a suspension of 0.5 g (1.15 mmol, 1 equiv) of Fmoc-TOAC-OH in 30 ml of anhydrous DCM, were added 190 mg (1.38 mmol, 1.2 equiv) of HOAt and 265 mg (1.38 mmol, 1.2 equiv) of EDC·HCl. The mixture was stirred for 1 h at 0°C and then 145 µl (1.38 mmol, 1.2 equiv) of *t*Bu-NH_2 in 30 ml of anhydrous DCM were added dropwise. The stirring was continued overnight. Afterwards, the solvent was removed under reduced pressure and the residue oil was dissolved in 16 ml of DCM. Then, 4 ml of *t*Bu-NH_2 were added and the solution was stirred for another 1 h. Finally, solvent was evaporated and product was eluted in flash chromatography with a gradient EP/EtOAc 2/1, 1/1, 1/2 1/3 affording 265 mg of a yellowish solid. Yield 85%. TLC: eluent EP/EtOAc 1/3, R_f 0.5; eluent $CHCl_3$/EtOH 9/1, R_f 0.6.

Mp: 124-126°C
FT-IR (film, DCM) (cm^{-1}) 3395, 3321, 2969, 2928, 1648, 1519, 1452, 1363, 1228.
^{1}H-NMR (200 MHz, CD_3CN/D_2O 2/1, $Na_2S_2O_4$) δ 2.34 and 2.27 (two s, 2H), 1.85 and 1.77 (two s, 2H), 1.50 and 1.44 (two s, 12H), 1.25 (s, 9H).
ESI-MS $C_{14}H_{28}N_3O_2$ (MW = 270) *m/z* = 271 $[M+H]^+$

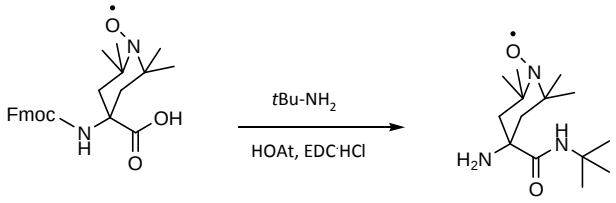

Fmoc-Aib-TOAC-NH*t*Bu

To a suspension of 402 mg (1.24 mmol, 1.2 equiv) of Fmoc-Aib-OH in 10 ml of anhydrous DCM, were added 170 mg (1.24 mmol, 1.2 equiv) of HOAt and 240 mg (1.24 mmol, 1.2 equiv) of EDC·HCl. The mixture was stirred for 1 h at 0°C and then 280 mg of H-TOAC-NH*t*Bu (1.03 mmol, 1 equiv) together with 180 µl (1.03 mmol, 1 equiv) of DIEA were added. After 4 days of stirring, a lot of H-TOAC-NH*t*Bu remained unreacted, thus a stronger coupling agent was employed. Indeed, Fmoc-Aib-F was used and prepared according to the following procedure: 200 mg of Fmoc-Aib-OH were suspended in 5 ml of anhydrous DCM at 0°C. Then 100 µl (1.23 mmol) of pyridine and 100 µl (1.23 mmoles) of cyanuric fluoride were added. After 2 h of stirring, the solution was washed with 3x50 ml of ice cold water and dried over Na_2SO_4. After 3 days of stirring, H-TOAC-NH*t*Bu was still not completely reacted. Solvent was removed under reduced pressure and the residue was subjected to the following work-up: 2x50 ml of a 10% $KHSO_4$ water solution, 30 ml of water, 2x50 ml of a 5% $NaHCO_3$ water solution, 50 ml of water and finally dried over Na_2SO_4. Product was eluted with a gradient EP/EtOAc 5/1, 4/1, 3/1, 2/1, 1/1, 1/2 in flash chromatography. 190 mg of a yellowish solid were thus obtained in 60% of yield. Another 260 mg of product together with an impurity were recovered as well. TLC: Fmoc-Aib-TOAC-NH*t*Bu, eluent $CHCl_3$/EtOH 9/1, R_f 0.8.

Mp: 82-85°C
FT-IR (film, DCM) (cm^{-1}) 3361, 2969, 2244, 1716, 1682, 1526, 1452, 1363, 1255, 1085, 909, 740, 645, 618.
^{1}H-NMR (200 MHz, CD_3CN/D_2O 2/1, $Na_2S_2O_4$) δ 7.87-7.84 (m, 2H), 7.70-7.66 (m, 2H), 7.45-7.36 (m, 4H), 7.18 (s, 1H), 6.98 (s, 1H), 6.69 (s, 1H), 4.41 (m, 2H), 4.35 (m, 1H), 2.21 (m, 2H), 1.46 (s, 6H), 1.38 (s, 12H), 1.27 (s, 9H), 1.24 (m, 2H).
ESI-MS $C_{33}H_{45}N_4O_5$ (MW = 577) *m/z* = 578 $[M+H]^+$

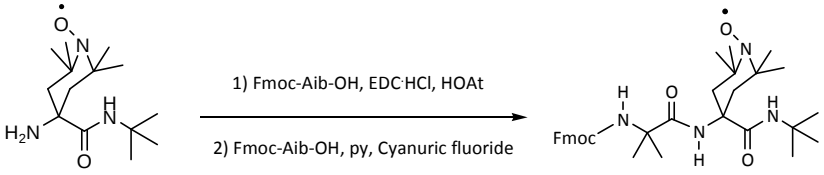

Fmoc-$(Aib)_2$-TOAC-NH*t*Bu

To a suspension of 123 mg (0.38 mmol, 1.5 equiv) of Fmoc-Aib-OH in 5 ml of anhydrous DCM at 0°C, were added 65 µl (0.75 mmol, 3 equiv) of cyanuric fluoride and 65 µl (0.75 mmol, 3 equiv) of pyridine. After 2 h of stirring, the solution was washed with 3x50 ml of ice cold water and dried over Na_2SO_4 and finally added to a solution of 90 mg (0.25 mmol, 1 equiv) of H-Aib-TOAC-NH*t*Bu in 5 ml of anhydrous DCM. 66 µl (50 mg, 0.37 mmol, 1.5 equiv) of DIEA were added and stirring was kept for 4 days. Another 1.5 equivalents of Fmoc-Aib-F were introduced after the second day to consume quantitatively H-Aib-TOAC-NH*t*Bu. Solvent was evaporated and the residue was washed with 2x50 ml of a 10% $KHSO_4$ water solution, 30 ml of water, 2x50 ml of a 5% $NaHCO_3$ water solution and 50 ml of water to be finally dried over Na_2SO_4. Product was eluted with a gradient EP/EtOAc 5/1, 4/1, 3/1, 2/1, 1/1, 1/2, 1/3 in flash chromatography. 100 mg (yield 72%) of a yellowish solid were thus obtained after crystallization from EtOAc/EP. TLC: Fmoc-$(Aib)_2$-TOAC-NH*t*Bu, eluent $CHCl_3$/EtOH 9/1, R_f 0.7.

Mp: 213-215°C
FT-IR (film, DCM) (cm^{-1}) 3348, 2975, 2244, 1675, 1526, 1444, 1357, 1262, 1093, 916, 734, 645.
^{1}H-NMR (200 MHz, CD_3CN/D_2O 2/1, $Na_2S_2O_4$) 7.86-7.83 (m, 2H), 7.68-7.65 (m, 2H), 7.44-7.34 (m, 5H), 7.25 (s, 1H), 7.11 (s, 1H), 6.83 (s, 1H), 4.31 (m, 3H), 2.22 (m, 4H), 1.39 (m, 18H), 1.31 (s, 6H), 1.23 (s, 9H).
ESI-MS $C_{37}H_{52}N_5O_6$ (MW = 662) *m/z* = 663 $[M+H]^+$

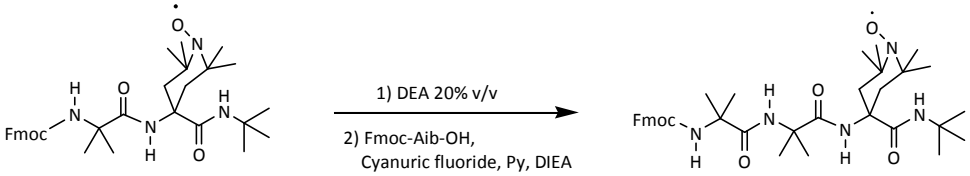

BzO-(CO)-CH_2-NH-$CHCH_3$-COO*t*Bu[77]

20 ml of 1,4-dioxane together with 3 ml of DIEA (16.5 mmol, 3 equiv) were poured into a flask and then, 3 g of HCl·H-Ala-O*t*Bu (16.5 mmol, 3 equiv) were added. The mixture was cooled down to 0°C before adding dropwise over 1 h a solution of 1.26 mg of Br-CH_2-CO-OBz (5.5 mol, 1 equiv) in 30 ml of 1,4-dioxane. Then, 10 ml of ACN were added and the stirring was continued for 3 days at r.t.. After solvent removal under reduced pressure, 100 ml of water were added and the product was extracted with 3x100 ml of EtOAc. The combined organic phases were gathered together and dried over anhydrous Na_2SO_4. Purification was carried out by flash chromatography using EP/EtOAc 4/1 as eluent. Finally, solvent was evaporate under reduced pressure to obtain 953 mg (yield 59%) of a colourless oil. TLC: BzO-(CO)-CH_2-NH-$CHCH_3$-COO*t*Bu, eluent EP/EtOAc 2/1, 0.4.

FT-IR (film, DCM) (cm^{-1}) 3452, 3341, 2977, 2933, 1733, 1459, 1370, 1155, 748, 696.
^{1}H NMR (200 MHz, $CDCl_3$) δ 7.35 (s, 5H), 5.16 (s, 2H), 3.56 (d, 1H), 3.45 (d, 1H) (2H), 3.27 (q, J = 7 Hz, 1H), 2.05 (bs, 1H), 1.45 (s, 9H), 1.29 (d, J = 7 Hz, 3H).
ESI-MS $C_{16}H_{23}NO_4$ (MW = 293) *m/z* = 238 $[M+2H-t\text{Bu}]^+$, 294 $[M+H]^+$.

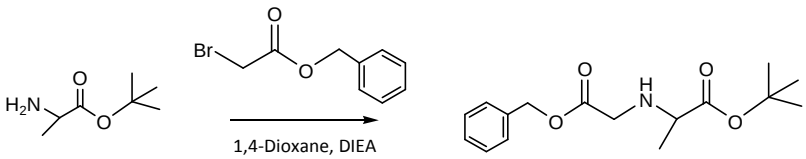

HO-(CO)-CH_2-NH-$CHCH_3$-COO*t*Bu[77]

In 50 ml of MeOH were put 191 mg of Pd/C 10% (20% w/w) and 953 mg (3.24 mmol) of BzO-(CO)-CH_2-NH-$CHCH_3$-COO*t*Bu. The mixture was stirred for 2 hs under H_2 bubbling until disappearance of the substrate (TLC, EP/EtOAc 1/1). Catalyst was removed after centrifugation and solvent was evaporate under reduced pressure. The remaining oil was triturated with Et_2O in order to obtain 457 mg (yield 69%) of a white solid.

Mp 168-171°C
FT-IR (KBr) (cm^{-1}) 3458, 3060, 3004, 1739, 1627, 1586, 1502, 1376, 1251, 1159, 999, 846, 741, 587, 524.
^{1}H NMR (200 MHz, MeOH-*d4*) δ 3.90 (q, J=7.01Hz, 1H), 3.47 (s, 2H), 1.50-1.46 (m, 12H).
ESI-MS $C_9H_{17}NO_4$ (MW = 203) *m/z* = 148 $[M+2H-t\text{Bu}]^+$, 204 $[M+H]^+$.

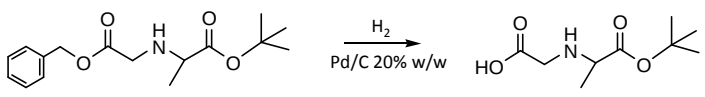

Fp-Ala-O*t*Bu

Similar derivatives are found in references[77,80]. 340 mg (0.47 mmol, 1 equiv) of C_{60} were dissolved in 250 ml of toluene after 10 minutes of sonication and then, 126 mg of HO-(CO)-CH_2-$CHCH_3$-COO*t*Bu (0.61 mmol, 1.3 equiv) together with 71 mg (2.36 mmol, 5 equiv) of paraformaldehyde dissolved in 10ml MeOH were added. After 4 h of reflux, the purple mixture turned into brown. Reaction was monitored by TLC which showed the appearance of a spot with R_f 0.5 in toluene. The mixture was subjected to flash chromatography for purification using Toluene/EP 3/1 as eluent. 136 mg (40% w/w) of unreacted C_{60} were recovered. Crystallization by toluene/ACN afforded 193 mg (yield 46%) of Fp-Ala-O*t*Bu as a brown solid. TLC: Fp-Ala-O*t*Bu, eluent toluene, R_f 0.6; eluent toluene/EP 7/3, R_f 0.3.

FT-IR (KBr) (cm^{-1}) 3428, 2971, 1727, 1636, 1453, 1361, 1263, 1143, 750, 722, 575, 525.
^{1}H NMR (200 MHz, $CDCl_3$) δ 4.62 (s, 4H), 3.93 (q, J = 7 Hz, 1H), 1.76 (d, J = 7 Hz, 3H), 1.64 (s, 9H).
^{13}C NMR (200 MHz, $CDCl_3$) δ 172.08, 155.01, 147.32, 146.17, 145.41, 144.58, 142.63, 141.91, 140.16, 136.40, 81.77, 70.21, 63.75, 59.90, 28.58, 16.90, 15.41.
ESI-MS $C_{69}H_{17}N_1O_2$ (MW = 891) *m/z* = 892 $[M+H]^+$

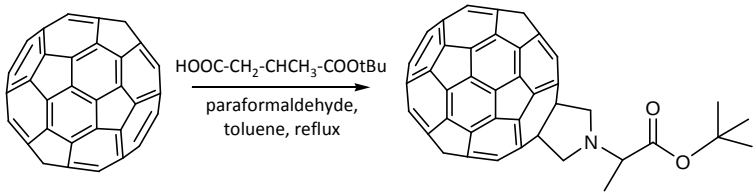

Fp-Ala-$(Aib)_2$–TOAC-NH*t*Bu

50 mg of Fp-Ala-O*t*Bu (0.06 mmol, 1.2 equiv) were dissolved in 6 ml of $CHCl_3$ and 10 ml of TFA together with 250 µl of CF_3SO_3H were added. After 1 h of stirring at r.t., solvent and acid were removed under reduced pressure. The residue was washed several times with Et_2O and dried under vacuum. TLC: Fp-Ala-OH, eluent Toluene/EtOAc 2/1, R_f 0.3; eluent $CHCl_3$/EtOH 9/1, R_f 0.5. 30 mg of Fmoc-$(Aib)_2$-TOAC-NH*t*Bu (0.05 mmol, 1 equiv) and 2 ml of DEA in 8 ml of ACN were stirred for 2 hs at r.t. Solvent was evaporated and the residue was subjected to flash chromatography (eluent DCM, DCM/MeOH 9/1) to afford 19 mg (yield 97%) of H-$(Aib)_2$-TOAC-NH*t*Bu. Fp-Ala-OH was suspended in 30 ml of anhydrous $CHCl_3$ and 10 mg (0.07 mmol, 1.3 equiv) of HOAt and 14 mg (0.07 mmol, 1.3 equiv) of EDC·HCl were added. The mixture was stirred for 1 h and then H-$(Aib)_2$-TOAC-NH*t*Bu in 5 ml of anhydrous $CHCl_3$ together with 12 µl (0.07 mmol, 1.3 equiv) of DIEA were added. The mixture was stirred for 5 days at r.t. and then, solvent was removed under reduced pressure. The residue was washed with 2 ml of MeOH followed by 2 ml of toluene in a centrifuge tube. Finally, flash chromatography was performed using $CHCl_3$, $CHCl_3$/EtOH 200/1, 100/1, 70/1, 40/1, 25/1 as eluent to afford 10 mg (yield 18%) of a brown solid. TLC: Fp-Ala-$(Aib)_2$-TOAC-NH*t*Bu, eluent $CHCl_3$/EtOH 9/1, R_f 0.6; eluent toluene/EtOH 8/1, R_f 0.2.

IR (1 mM, $CHCl_3$) (cm^{-1}) 3456, 3436, 3357, 1670, 1514, 1458, 1380, 1363.
^1H NMR (500 MHz, $CDCl_3$, 50 equivalents PH) 8.18 (s, 1H), 6.57 (s, 1H), 4.52 (m, 4H), 3.8 (q, J = 7 Hz, 1H), 2.49 (m, 2H), 2.28 (m, 2H), 1.72 (d, J = 7 Hz, 3H), 1.60-1.52 (m, 12H), 1.36 (s, 9H), 1.26-1.22 (m, 12H).
MALDI-MS $C_{88}H_{49}N_6O_6$ (MW = 1257) *m/z* = 1258 $[M+H]^+$
UV-vis ($CHCl_3$) λ (ε) 310 (23400), 430 (3000)

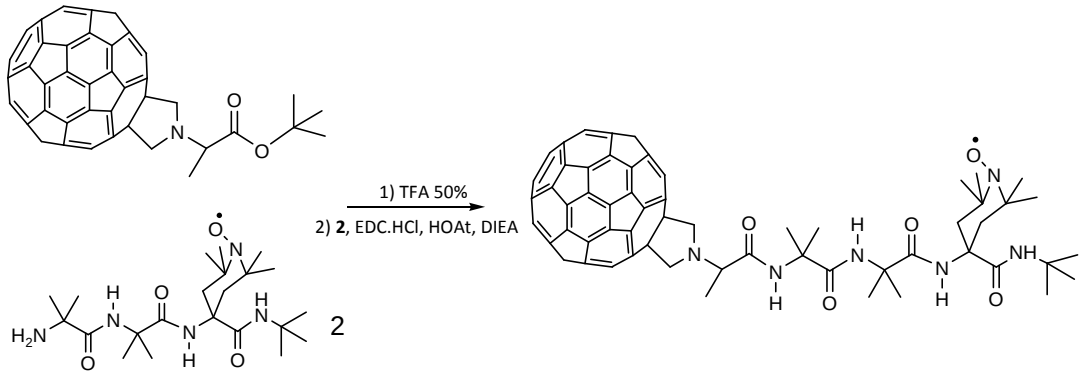

2.4 Synthesis of fullerene-peptide-reference 2-

Boc-$(Aib)_3$-OMe

The Z protecting group was removed under catalytic hydrogenation: a mixture of 1 g of Z-$(Aib)_2$-OMe (3.1 mmol, 1.2 equiv) and 200 mg of Pd/C 10% (20% w/w) in 50 ml of MeOH was stirred for 2 hs under hydrogen bubbling. Disappearance of reagent was monitored by TLC ($CHCl_3$/EtOH 14/1). Catalyst was discharged after centrifugation and solvent was evaporated under reduced pressure and under vacuum. TLC: Z-$(Aib)_2$-OMe, eluent CH_3Cl/EtOH 9/1, R_f 0.7; H-$(Aib)_2$-OMe, eluent $CHCl_3$/EtOH 9/1, R_f 0.4. 456 mg (2.6 mmol, 1 equiv) of Boc-Aib-OH, 389 mg (2.9 mmol, 1.1 equiv) of HOAt and 548 mg (2.9 mmol, 1.1 equiv) of EDC·HCl in 5 ml of anhydrous DCM were stirred at r.t. for two hs before being poured into the flask containing H-$(Aib)_2$-OMe (3.1 mmol, 1.2 equiv) dissolved in 5 ml of anhydrous DCM together with 445 µl (2.6mmol, 1 equiv) of DIEA. After 3 days of stirring at r.t., solvent was evaporated and the residue was washed with 3x50 ml of a 10% $KHSO_4$ water solution, 50 ml of water, 3x50 ml of a 5% $NaHCO_3$ water solution, 50 ml of water and finally dried over Na_2SO_4. Solvent was evaporated and product was crystallized from EP/EtOAc affording 255 mg (yield 25%) of a white solid. TLC: Boc-$(Aib)_3$-OMe, eluent $CHCl_3$/EtOH 9/1, R_f 0.6.

Mp: 197-200°C
FT-IR (KBr) (cm^{-1}) 3380, 3304, 2983, 2937, 1725, 1694, 1659, 1530, 1460, 1387, 1314, 1170, 1083, 758, 650.
^1H NMR (200 MHz, $CDCl_3$) δ 7.43 (s, 1H), 6.43 (s, 1H), 4.88 (s, 1H), 3.69 (s, 3H), 1.47 (m, 27H).
ESI-MS $C_{18}H_{33}N_3O_6$ (MW = 387) *m/z* = 388 $[M+H]^+$

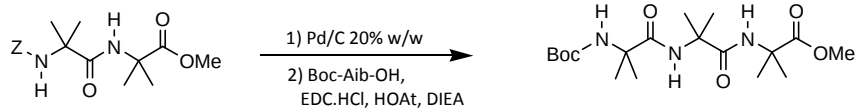

Piv-(Aib)$_3$-OMe

To remove Boc protection, 245 mg (0.66 mmol, 1 equiv) of Boc-Aib$_3$-OMe were dissolved in 2 ml of DCM together with 2 ml of TFA. After stirring for 1 h, solvent was evaporated under reduced pressure and under vacuum. TFA$^-$H-Aib$_3$-OMe thus obtained was dissolved in 20 ml of anhydrous DCM together with 230 µl of DIEA (1.32 mmol, 2 equiv). Then, a solution of 162 µl of Piv-Cl (1.32 mmol, 2 equiv) in 5 ml of anhydrous DCM was added dropwise. The solution was stirred for 1 day. Solvent was removed under vacuum and the residue was subject to flash chromatography (eluent, EP/EtOAc 1/3). 56 mg (yield 24%) of a white solid were obtained. TLC: Boc-Aib$_3$-OMe, eluent CH_3Cl/EtOH 9/1, R_f 0.5.

Mp: 175-177°C
IR (KBr) (cm^{-1}) 3393, 3348, 3304, 2985, 1726, 1682, 1637, 1533, 1459, 1155, 756.
^{1}H NMR (200 MHz, $CDCl_3$) δ 7.30 (s, 1H), 6.22 (s, 1H), 5.95 (s, 1H), 3.69 (s, 3H), 1.49-1.47 (m, 18H), 1.21 (s, 9H).
ESI-MS $C_{18}H_{33}N_3O_5$ (MW = 371) *m/z* = 372 $[M+H]^+$

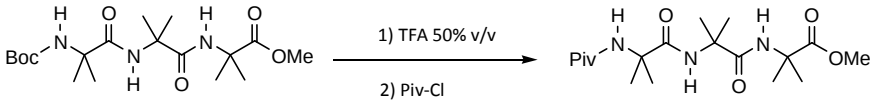

Piv-(Aib)$_3$-OH

56 mg (0.16 mmol, 1 equiv) of Boc-(Aib)$_3$-OMe were dissolved in 0.8 ml of MeOH together with 0.8 ml of a 6 N water solution of NaOH (30 equiv). The solution was stirred for 2 days and then diluted with 50 ml of EtOAc. The mixture was washed with a 3x30 ml of a 10% $KHSO_4$ water solution and with 2x30 ml of water. The organic phase was dried over Na_2SO_4 and solvent was evaporated under reduced pressure to afford 34 mg of a white solid (yield 60%).

Mp: 235-238°C
IR (KBr) (cm^{-1}) 3421, 3303, 3059, 3000, 1733, 1688, 1651, 1518, 1458, 1384, 1317, 1233, 1206, 1169, 666.
^{1}H NMR (200 MHz, CD_3CN) δ 7.52 (s, 1H), 6.87 (s, 1H), 6.66 (s, 1H), 1.46 (s, 6H), 1.38 (s, 6H), 1.33 (s, 6H), 1.17 (s, 9H).
ESI-MS $C_{17}H_{31}N_3O_5$ (MW = 357) *m*/z = 358 $[M+H]^+$

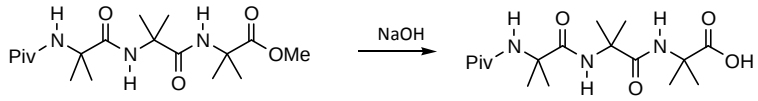

Piv-(Aib)$_3$-Ala-Fp

44 mg (0.05 mmol, 1 equiv) of Boc-Ala-Fp were dissolved in 15 ml of DCM together with 15 ml of TFA.

After stirring for 1 h at r.t., solvent and acid were evaporated and the residue washed with 4x30 ml of Et_2O and then dried under vacuum. 22 mg (0.06 mmol, 1.3 equiv) of Piv-$(Aib)_3$-OH were dissolved in 5 ml of anhydrous $CHCl_3$ and 11 mg (0.06 mmol, 1.3 equiv) of EDC·HCl were added. After stirring at r.t. for 1 h, the solution was cooled down to 0°C and poured in the flask containing H-Ala-Fp and 20 µl (0.18 mmol, 3 equiv) of DIEA in 50 ml of anhydrous $CHCl_3$. The mixture was stirred at r.t. for 7 days and then solvent was removed under reduced pressure. The residue was washed with 2 ml of MeOH, then with 2 ml of toluene in a centrifuge tube. Subsequently, flash chromatography was performed using $CHCl_3$, $CHCl_3$/EtOH 200/1, 100/1, 50/1, 40/1 as eluent to afford 9 mg of a brown solid (yield 16%). TLC: Piv-$(Aib)_3$-Ala-Fp, eluent $CHCl_3$/EtOH 9/1, R_f 0.5; eluent toluene/EtOH 8/1, R_f 0.2.

IR (1 mM, $CHCl_3$) (cm^{-1}) 3437, 3329, 1662, 1512, 1456, 1380, 1362.
^{1}H NMR (200 MHz, $CDCl_3$) δ 7.75 (d, 1H, J=8.1Hz), 7.51 (s, 1H), 6.20 (s, 1H), 5.97 (s, 1H), 5.72 (m, 1H), 5.51 (m, 2H), 5.21 (m, 2H), 1.65-1.50 (m, 21H), 1.25 (s, 9H).
^{13}C NMR (50 MHz, $CDCl_3$) δ 179.29, 174.98, 173.56, 173.08, 146.27, 145.39, 144.56, 142.67, 142.13, 140.14, 129.04, 58.65, 57.57, 57.20, 56.91, 47.29, 27.38, 25.65, 25.32, 17.63
MALDI-MS $C_{82}H_{39}N_5O_5$ (MW = 1173) *m*/z = 1196 $[M+Na]^+$
UV-vis ($CHCl_3$) λ (ε) 310 (24800), 430 (2700)

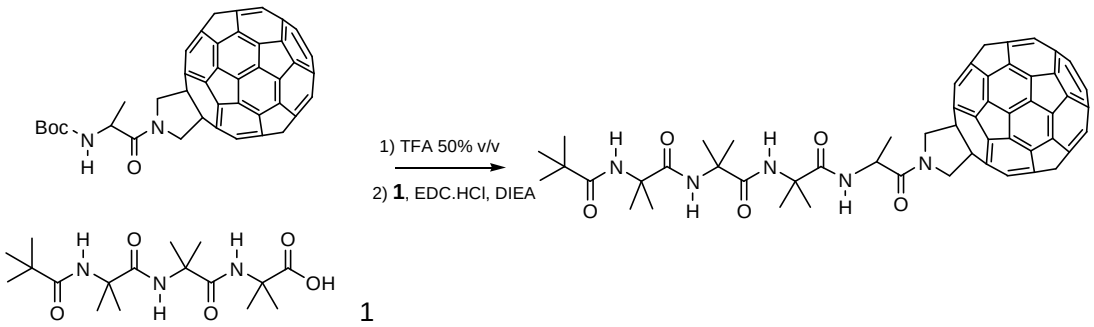

1

2.6 Synthesis of fullerene-peptide 2+ reference

Z-$(Aib)_3$-NH*t*Bu

1 g (2.46 mmol, 1 equiv) of Z-$(Aib)_3$-OH and 566 mg (2.95 mmol, 1.2 equiv) of EDC·HCl were dissolved in 10 ml of DCM. Then, 3 µl (7.38 mmol, 3 equiv) of *t*Bu-NH_2 were added and the solution was stirred for 10 hs at r.t.. Solvent was evaporated under reduced pressure and the residue was dissolved in EtOAc and washed with a 3x100 ml of a 10% $KHSO_4$ water solution, 100 ml of water and finally dried over Na_2SO_4. Organic solvent was evaporated under reduced pressure and the residue was purified through flash chromatography using a gradient EP/EtOAc 1/1, 1/2, 1/3, 1/4. Crystallization from EtOAc/EP afforded 813 mg (yield 72%) of a white solid. TLC: Z-$(Aib)_3$-NH*t*Bu, eluent CH_3Cl /EtOH 9/1, R_f 0.4.

Mp: 184-186°C
FT-IR (KBr) (cm^{-1}) 3437, 3332, 2989, 2940, 1715, 1666, 1540, 1453, 1363, 1268, 1226, 1167, 1094, 919, 730, 699, 618.

^{1}H NMR (200 MHz, $CDCl_3$) δ 7.35 (m, 5H), 7.08 (s, 1H), 6.72 (s, 1H), 6.27 (s, 1H), 5.39 (s, 1H), 5.10 (s, 2H), 1.46 (s, 12H), 1.36-1.32 (m, 15H).
ESI-MS $C_{24}H_{38}N_4O_5$ (MW = 462) *m/z* = 463 $[M+H]^+$

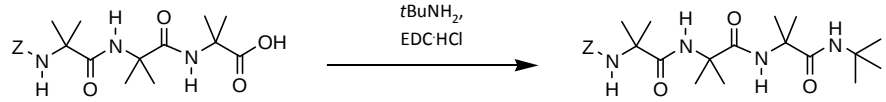

Fp-Ala-(Aib)$_3$-NH*t*Bu

25 mg of Z-(Aib)$_3$-NH*t*Bu (0.05 mmol, 1.2 equiv) were dissolved in 50 ml of MeOH and 5 mg of Pd/C 10% (20% w/w) were added. The mixture was stirred for 2 h under hydrogen bubbling and then centrifuged in order to remove the catalyst. 40 mg (0.04 mmol, 1 equiv) of Fp-Ala-O*t*Bu was dissolved in 15 ml of $CHCl_3$ and 10 ml of TFA were added together with 250 µl of CF_3SO_3H. The mixture was stirred at r.t. for 1 h until complete disappearance of reagent (TLC: eluent toluene). Solvent was evaporated and the brown solid thus obtained was washed several times with Et_2O and dried under vacuum. Subsequently, it was precipitated in 30 ml of anhydrous $CHCl_3$, cooled down to 0°C and 8 mg (0.06 mmol, 1.3 equiv) of HOAt and 11 mg (0.06 mmol, 1.3 equiv) of EDC·HCl were added. The mixture was stirred for 1 h and then H-(Aib)$_3$-NH*t*Bu (1.2 equiv) in 5 ml of anhydrous $CHCl_3$ together with 5 µl (0.04 mmol, 1 equiv) of DIEA were added. The mixture was stirred for 2 days and then, flash chromatography was performed using $CHCl_3$, $CHCl_3$/EtOH 200/1, 100/1, 70/1, 40/1, 25/1 as eluent. 10 mg (yield 20%) of a brown solid were obtained. TLC: Fp-Ala-(Aib)$_3$-NH*t*Bu, eluent $CHCl_3$/EtOH 9/1, R_f 0.5, eluent toluene/EtOH 8/1, R_f 0.2.

FT-IR (1 mM, $CHCl_3$) (cm^{-1}) 3460, 3434, 3358, 1672, 1514, 1458, 1380, 1362.
^{1}H NMR (200 MHz, CD_2Cl_2) δ 8.17 (s, 1H), 7.32 (s, 1H), 6.74 (s, 1H), 6.35 (s, 1H), 4.56 (s, 4H), 3.80 (q, J = 7 Hz, 1H), 1.76 (d, J = 7 Hz, 3H), 1.56-1.44 (m, 18H), 1.33 (s, 9H).
^{13}C NMR (50 MHz, $CDCl_3$) δ 174.05, 172.82, 172.20, 153.92, 147.50, 146.32, 145.74, 145.42, 144.62, 143.26, 142.83, 142.08, 140.39, 136.01, 69.78, 64.25, 60.73, 57.03, 50.85, 28.76, 26.25, 25.45, 25.05, 15.33.
MALDI-MS $C_{81}H_{39}N_5O_4$ (MW = 1145) *m/z* = 1146 $[M]^+$
UV-vis ($CHCl_3$) λ (ε) 310 (23400), 430 (3000)

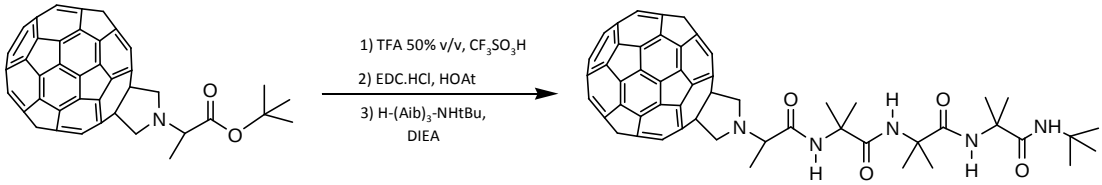

2.9 Synthesis of peptide-reference 2-

Piv-TOAC-(Aib)$_2$-NH*t*Bu

To a solution of 20 mg of Piv-TOAC-(Aib)$_2$-OH (0.04 mmol, 1 equiv) in 5ml of anhydrous ACN were added 10 mg of EDC·HCl (0.05 mmol, 1.3 equiv).
The solution was stirred at r.t. for 3 h and then 14 µl of *t*Bu-NH_2 (0.13mmol, 3.2 equiv) were added. The solution was stirred at 70°C for 4 days, then the solvent was

evaporated under reduced pressure. The residue was dissolved in 10ml of DCM and washed with 2x10 ml of a 10% $KHSO_4$ water solution, 10 ml of water, 2x10 ml of a 5% $NaHCO_3$ water solution and 10 ml of water to be finally dried over Na_2SO_4. Crystallization from EtOAc / Hexane afforded 9 mg of a yellowish powder (yield 40%). TLC: Piv-TOAC-$(Aib)_2$-NH*t*Bu, eluent $CHCl_3$ / EtOH 9/1, R_f 0.4.

FT-IR (1 mM, $CHCl_3$) (cm^{-1}) 3459, 3437, 3360, 1679, 1663, 1520, 1454, 1380, 1362.
^1H NMR (500 MHz, $CDCl_3$, 10 equivalents PH) 6.98 (s, 1H), 6.69 (s, 1H), 6.63 (s, 1H), 6.14 (s, 1H), 2.11 (m, 4H), 1.48 (s, 6H), 1.40 (s, 6H), 1.36 (s, 9H), 1.31 (s, 6H), 1.23 (s, 15H).
FAB-MS $C_{27}H_{50}N_5O_5$ (MW = 524) *m/z* = 525 $[M+H]^+$

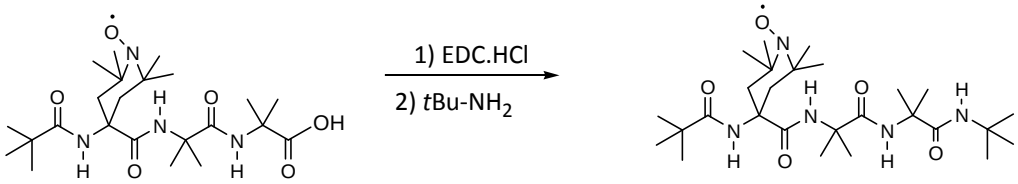

2.10 Synthesis of peptide-reference 2+

Piv-$(Aib)_2$-TOAC-NH*t*Bu

7 mg of Fmoc-$(Aib)_2$-TOAC-NH*t*Bu (0.01 mmol, 1 equiv) and 2ml of DEA in 8 ml of ACN were stirred for 1 h at r.t. Solvent and DEA were then removed under reduced pressure. The residue was dissolved in 2 ml of DCM and subjected to flash chromatography with $CHCl_3$, $CHCl_3$/EtOH 9/1 as eluent. H-$(Aib)_2$-TOAC-NH*t*Bu was dissolved in 2 ml of anhydrous DCM and 3 µl of Piv-Cl (0.02 mmol, 2 equiv) together with 2 µl of pyridine (0.02 mmol, 2.3 equiv) in 1ml of anhydrous DCM were added. The solution was stirred at r.t. for 1 day, then solvent was removed under reduced pressure. The residue was dissolved in 5ml of DCM and washed with 2x10 ml of a 10% $KHSO_4$ water solution, 10 ml of water, 2x10 ml of a 5% $NaHCO_3$ water solution and 10 ml of water to be finally dried over Na_2SO_4. Crystallization from EtOAc / Hexane afforded 1.4 mg of a yellowish powder (yield 23%). TLC: Piv-$(Aib)_2$-TOAC-NH*t*Bu, eluent $CHCl_3$/EtOH 9/1, R_f 0.5.

FT-IR (1 mM, $CHCl_3$) (cm^{-1}) 3466, 3438, 3367, 1679, 1663, 1520, 1454, 1380, 1362.
^1H NMR (500 MHz, $CDCl_3$, 50 equivalents PH) 6.27 (s, 1H), 5.91 (s, 1H), 2.46 (m, 2H), 2.27 (m, 2H), 1.47, 1.32, 1.20. The assignments of the four NH protons was not possible due to the quencher signals. The aliphatic region was not clearly resolved.
FAB-MS $C_{27}H_{50}N_5O_5$ (MW = 524) *m/z* = 525 $[M+H]^+$

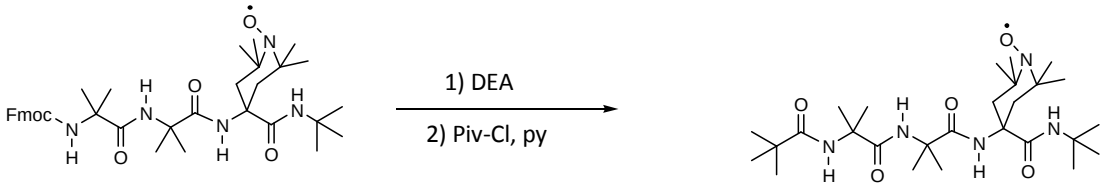

2.11 Synthesis of Boc-TOAC-NH*t*Bu

The starting material Boc-TOAC-OH was previously prepared according to procedure for the synthesis of Fmoc-TOAC-OH. To a suspension of 100 mg (0.32 mmol, 1 equiv) of Boc-TOAC-OH in 20 ml of anhydrous DCM, were added 56 mg (0.41 mmol, 1.3 equiv) of HOAt and 79 mg (0.41 mmol, 1.3 equiv) of EDC·HCl. The mixture was stirred for 1 h at 0°C and then 89 µl (0.8 mmol, 2.5 equiv) of *t*Bu-NH_2 in 5 ml of anhydrous DCM were added dropwise. The stirring was continued overnight. Afterwards, the solvent was removed under reduced pressure and the residue oil was dissolved in 30 ml of EtOAc. The organic phase was washed with 2x30 ml of a 10% $KHSO_4$ water solution, 30 ml of water, 2x30 ml of a 5% $NaHCO_3$ water solution, 30 ml of water and finally dried over Na_2SO_4. Solvent was evaporated and product was crystallized from EP/EtOAc affording 97 mg of an orangey solid. Yield 85%. TLC: eluent EP/EtOAc 1/1, R_f 0.5.

^{1}H-NMR (200 MHz, CD_3CN/D_2O 2/1, $Na_2S_2O_4$) δ 6.81 (s, 1H), 2.26 – 2.19 (m, 2H), 1.99 – 1.93 (s, 2H), 1.48 (s, 9H), 1.36 - 1.34 (s, 12H), 1.22 (s, 9H).
ESI-MS $C_{19}H_{36}N_3O_4$ (MW = 370) *m*/*z* = 371 $[M+H]^+$

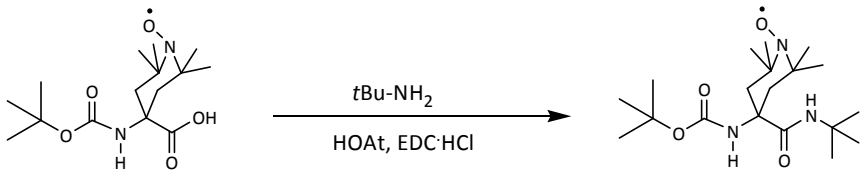

3. Results and discussion

3.1 Synthetic approach

All the peptides were synthesized by standard solutions procedures adding one residue per time to the peptide chain. The *t*-butyl amides (*t* = *tert*) of the P-protected peptides (P = protecting group) P-(aminoacid)$_3$-NH*t*Bu, are obtained by condensation of P-aminoacid-OH with the appropriate H-(aminoacid)$_{n-1}$-NH*t*Bu segments. Amide coupling between the N$^{\alpha}$-deprotected peptides H-(aminoacid)$_3$-NH*t*Bu with Fp-Ala-OH (Fp = fulleropyrrolidine), freshly prepared by hydrolysis of the t-butyl ester, affords Fp-Ala-(aminoacid)$_3$-NH*t*Bu. The carboxilyc acids of the Piv-protected peptides (Piv = pivaloyl or *t*butyl-carbonyl) Piv-(aminoacid)$_3$-OH, are obtained by condensation of P-aminoacid-OH (P = protecting group) with the appropriate H-(aminoacid)$_{n-1}$-OE segments (E = ester) followed by reaction with Piv-Cl after removing of N$^{\alpha}$-protection and final hydrolysis of ester. Amide coupling between peptides Piv-(aminoacid)$_3$-OH with H-Ala-Fp, freshly prepared by removal of the Boc protection (Boc = *t*-Butyloxycarbonyl), yields Piv-(aminoacid)$_3$-Ala-Fp. Whereas the amino function was protected by means of urethanes (Z = benzyloxycarbonyl, Fmoc = 9-fluorenylmethoxycarbonyloxy, Boc), methyl esters and *t*-butyl esters were used for the carboxylic function. Activation of the carbonyl was carried out employing EDC·HCl / HOAt. In some case, cyanuric fluoride was also used. Unlike Ala, Aib and TOAC are achiral aminoacids so that no racemization issue were taken into account. On the other hand, their steric hindrance is responsible for prolonged reaction times and low yields compared with other less hindered aminoacids. The functionalization of C_{60} was performed by the Maggini-Prato reaction, by decarboxylating the condensation product of N-substituted glycines with formaldehyde. The 1,3 dipole thus obtained in situ is trapped by the fullerene in a [3+2] cycloaddition giving N-substituted-3,4-fulleropyrrolidines.

3.1.1 Protection of the amino group

Fmoc is the only urethane that can be utilized when TOAC is present. Fmoc is removed using DEA 50% v/v and TOAC is stable under basic conditions as its synthesis can suggest. The removal conditions for the Z group are not compatible with the free radical which would be reduced after the catalytic hydrogenation. TFA 50% v/v cleaves the Boc moiety but, it is known that under acidic conditions, TOAC undergoes a disproportion process leading to two derivatives. The oxidated product was found to be an oxidating agent[82].

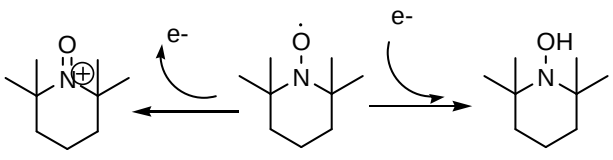

Figure 3.1 *Disproportion products of TOAC under acidic conditions.*

Besides, Fmoc-tagged amino acids are easy to follow under UV lamp thanks to the fluorenyl cromophore. However, this urethane owns two disadvantages. Not only the coupling conditions (presence of a free primary amine) are not so different from the deprotecting conditions but also the side product of the deprotection, dibenzofulvene, is a mild electrophile which must be disposed of, thus introducing a further step of work. Z group was used during the synthesis of peptides-references instead. Z derivatives are fairly stable and easy to follow under UV lamp. Boc group was employed when C_{60} was present since acidic conditions are compatible with fullerene, unlike catalytic hydrogenation and basic conditions. Indeed, C_{60} is reactive towards nucleophiles such as primary and secondary amines.

3.1.2 Protection of the carboxylic function

In analogy to Boc, *t*-butyl ester was exploited because it can be hydrolyzed under acidic conditions. Methyl ester was used during the synthesis of Piv-$(Aib)_3$-OH since it can be hydrolyzed under basic conditions which are orthogonal to the Z and Boc groups.

3.1.3 Carboxyl activation

In this work, the formation of the amide bond is catalyzed by the couple EDC·HCl / HOAt.

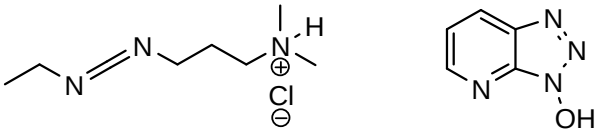

Figure 3.2 *Chemical structure of EDC·HCl (on the left) and HOAt (on the right).*

The carbodimide promotes the formation of an activated ester intermediate between the carboxylic group of the N^{α}-protected and the HOAt. The catalytic effect of the HOAt is due to the anchimeric assistance given to both nitrogen atoms N2 and N7 for nucleophilic attack to the amine group[83].

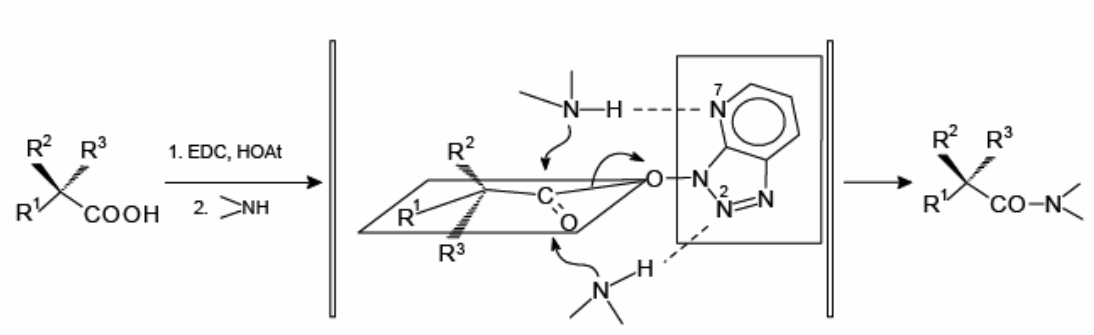

Figure 3.3 *Nucleophilic attack assisted by HOAt that activates the carboxylic group.*

In some case, a stronger activating agent was employed. Cyanuric fluoride is a mild fluorinating agent able to transform carboxylic acids in acyl fluorides[84].

Figure 3.4 *Chemical structure of cyanuric fluoride.*

Acyl fluorides are stable in presence of *t*-butyl, Boc, Fmoc, Trityl protection and are greater stable than the corresponding acyl chlorides to exposition to water. Besides, they do not undergo fast cyclization to oxazolone (Leuch's anhydride) such as Fmoc/Boc N-protected aminoacid bromides[85] do. This effect is even more facilitated with Aib by the presence of the two α-methyl substituents ("gem-dimethyl effect")[84]. Thus, different protecting groups than urethanes must be used when acyl bromide /chloride are to be employed.

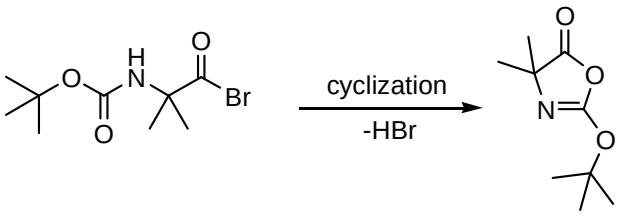

Figure 3.5 *The oxygen of the carbonyl group of Boc attacks the acyl bromide to give the oxazolone.*

3.1.4 N-substituted-3,4-fulleropyrrolidines

There are several ways to functionalize the fullerene exploiting its tendence to behave like a reactive 2π component in cycloaddition[1]. The [6,6] double bonds are dienophilic which enables the molecule to form five-membered rings covalently through [3+2] cycloadditions with 1,3 dipolarophiles[1]. Azomethine ylides are 1,3 dipoles, planar species, which can be easily generated *in situ* from several readily accessible materials obtained by decarboxylating the condensation product of N-substituted glycines with formaldehyde[41,73,86]. The broad acceptance of this method (the Maggini-Prato reaction) is explained by the good selectivity (only the 6,6 bond is attacked) and a wide range of addends and functional groups that are tolerated[1,41]. Other methods were not suitable to the synthesis of our systems either because strong conditions are required (e.i. Bingel reaction), or because complicated equilibrium between the [6,5]-open and [6,6]-closed structures of [60]fullerene takes place (e.i. addition-thermal decomposition of diazo compounds)[1]. Furthermore, the Maggini-Prato reaction does not require particular functional groups, to stabilize the intermediate responsible for the cycloaddition, that can interfere with the electrochemical investigation and allows us to obtain the fullerene-peptides 2+ and 2- only by modifying the substituent at the nitrogen atom of glycine.

Indeed in the reaction, the amino function of an N-substituted glycine attacks the carbonyl group of the aldehyde giving the corresponding imine. Subsequently, the oxygen O-H of the carboxyl function attacks the carbon of the imino function affording the oxazolidinone which can be isolated in the case of 3-trityl-5-oxazolidinone[73]. Under refluxing toluene, the oxazolidinone intermediate decarboxilates thus generating the 1,3 dipole which is trapped by the C_{60}. The cycloaddition product is an N-substituted pyrrolidine ring covalently linked to the C_{60}.

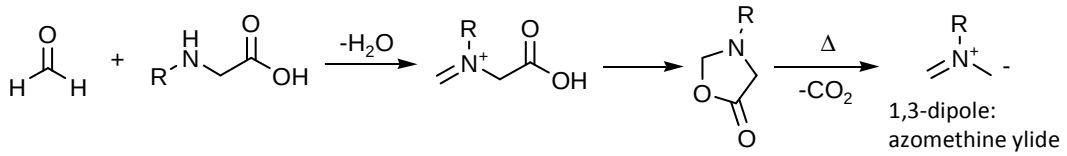

Figure 3.6 *Generation of azomethine ylide.*

Nucleophilic substitution of Bromo-benzyl-acetate by H-Ala-O*t*Bu, followed by catalityc hydrogenation of the benzyl ester, gives the corresponding N-substituted glycine in 68% of yield. 1 equivalent of this derivative together with 5 equivalents of paraformaldehyde and 1 of C_{60} under refluxing toluene for 3 hours affords Fp-Ala-O*t*Bu in 45% of yield. When Trt-Gly-OH (Trt = triphenylmethyl) is mixed with aqueous formaldehyde in EtOH, 3-trityl-5-oxazolidinone[73] is produced and can be isolated and used for the cycloaddition with C_{60}. The product is a 3,4-fulleropyrrolidine protected at the nitrogen atom with the trityl moiety. Removal of the trityl moiety followed by amide coupling with $(Boc\text{-}Ala)_2O$ affords Boc-Ala-Fp[75] in 35% of overall yield.

Trityl, Boc and *t*-butyl ester were chosen to protect the amino and carboxylic function because they can be removed under acidic condition. In fact, C_{60} is not compatible with basic conditions[74,107] employed to hydrolyze methyl esters. It is known that C_{60} is reactive towards nucleophiles such as cyanide[23], amines[4,74], hydroxide[87]. In case of secondary and primary amines, the addition starts with a single electron transfer to give the C_{60} radical anion, followed by the covalent bond formation and proton transfer[74]. N-propylamine, n-dodecylamine, *t*butyl-amine, ethylenediamine, morpholine have been observed to react with neutral C_{60} in solution to give amino addition compounds of the type $C_{60}H_n(NRR')$[88]. Neither catalytic hydrogenation used to remove benzyl esters can be applied when the fullerene is present.

3.2 The fullerene-Aib-peptide and the attempts for its synthesis

The synthesis of a fullerene-peptide, where the alanine residue was originally an Aib residue, was also attempted.

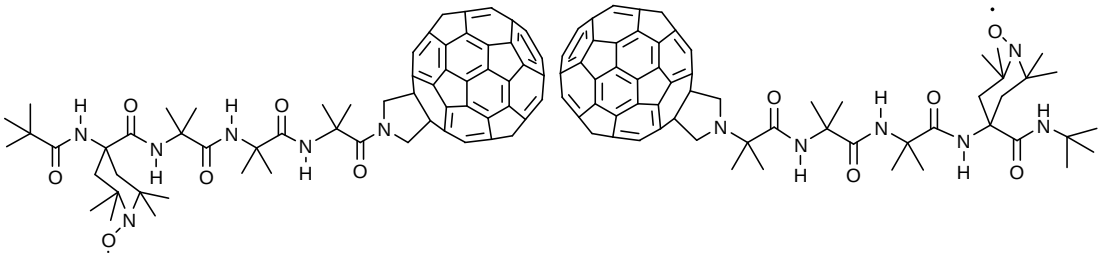

Figure 3.7 *Fullerene-Aib-peptide 2- (on the left) and 2+ (on the right).*

Peptide synthesis employing Aib is characterized by long time reactions and low yields because of the high steric hindrance at the α-carbon. In this case, the coupling is even more challenging because the nitrogen of fulleropyrrolidine is not a good nucleophile due to the inductive and steric effect brought about by the buckyball[109]. Many strategies were tried out but no one could afford the desired products fullerene-Aib-peptide 2- and 2+. This strategies will be now described in detail:

-nucleophilic attack to the saturated carbon of α-bromoamides
-use of activated ester and anhydride
-use of acyl chloride/bromide
-novel strategy through fulleroproline

3.2.1 Nucleophilic attack to the saturated carbon of α-bromoamides

It is known that in 2-bromoamides, the bromine can be displaced by nucleophiles through an S_N2 mechanism bringing the configuration at the α-carbon inverted. When silver oxide Ag_2O is added, the reaction rate speeds up and no inversion is observed. It was postulated that Ag_2O behaves both as Lewis acid and Bronsted base because from one hand, Ag weakens the Br-C^{α} bond and on the other, the oxygen contributes to break the N-H bond thus generating an aziridonic intermediate which is very reactive and undergoes attack by the nucleophile[89,90,91].

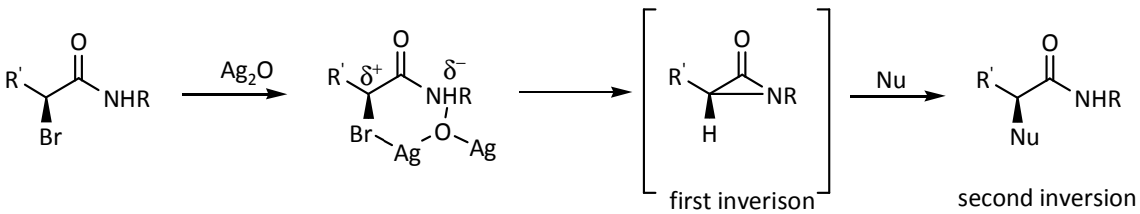

Figure 3.8 *Nucleophlic substitution at the α-carbon in 2-bromoamides promoted by silver oxide. The retention of the configuration at the α-carbon is explained invoking the mechanism depicted above.*

Even silver triflate $Ag^+CF_3SO_3^-$ is able to catalyse this reaction with the difference that it promotes the configuration inversion at the α-carbon[91].

The synthesis of derivatives 1 and 2 (Figure 3.9) was attempted according to the synthetic strategic described before regarding the nucleophilic attack at the α-carbon of 2-bromoamides.

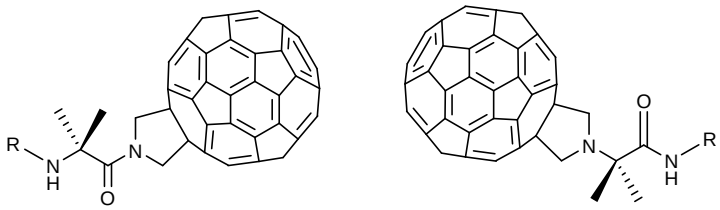

Figure 3.9 *Derivative 1 (on the left) and derivative 2 (on the right).*

Derivative 1 and 2 (Figure 3.9) are respectively the precursors for the synthesis of fullerene-Aib-peptides 2- and 2+ where the R group can be a removable group or the peptides itself. In order to obtain the derivative 1, the following route was followed. Firstly, reaction between fulleropyrrolidine and α-bromo-α-dimethyl-acylbromide afforded Br-Aib-Fp in quantitative yield.

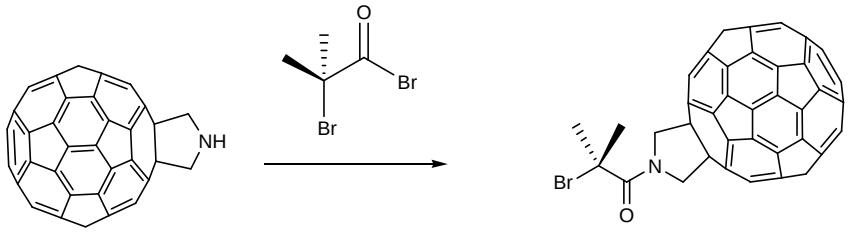

Figure 3.10 *Reaction between fulleropyrrolidine and Br-isobutyric-acylbromide afforded Br-Aib-Fp.*

Secondly, because Br-Aib-Fp is a tertiary α-bromo-amide which can in principle undergo nucleophilic attack at the α-carbon promoted by silver triflate, ammonia and Trt-NH_2 were used as nucleophiles. Trt-NH_2 was also employed in the place of NH_3 because:

-it is more soluble in toluene than NH_3
-it is a solid and its concentration can be controlled
-in case derivative 1 was obtained, the amino group was protected by the trityl moiety which can be removed under acidic condition

To a solution of 20 mg of fulleropyrrolidine (0.03 mmol, 1 equiv) in 50 ml of toluene at 0°C were added 10 µl (18 mg, 0.08 mmol, 3 equiv) of $BrC(CH_3)_2COBr$. After stirring for 1 h at r.t., solvent was evaporated under reduced pressure and the residue was subjected to flash chromatography using toluene as eluent. 23 mg (quantitative yield) of Br-Aib-Fp as a brown solid were thus obtained. TLC Br-Aib-Fp, eluent toluene, R_f 0.3. ^{1}H NMR (200MHz, $CDCl_3$) δ 5.68 (s, 4H); 2.27 (s, 6H). 20 mg (0.02 mmol, 1 equiv) of Br-Aib-Fp and 23 mg (0.11 mmol, 5 equiv) of $AgClO_4$ were dissolved in 50 ml of toluene and the solution was bubbled at r.t. with ammonia gas generated mixing 50 g of NaOH and 67 g of NH_4Cl in another flask. The gas flow was forced to pass through two tubes containing NaOH pallets and anhydrous $NaSO_4$ to

remove water traces. Even after 20 days of bubbling under stirring at r.t. and 1 day at 60°C, no reaction took place since Br-Aib-Fp was recovered after flash-cromatography unchanged (as ^{1}H NMR spectrum demonstrated).

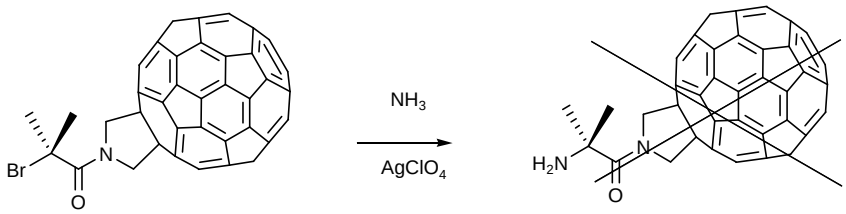

Figure 3.11 *Reaction scheme for the synthesis of H-Aib-Fp.*

When a toluene solution of 20 mg of Br-Aib-Fp (0.02 mmol, 1 equiv) and 11 mg (0.04 mmol, 2 equiv) of Trt-NH_2 together with 40 mg (0.13 mmol, 6 equiv) of SilverTriflate (Triflate = $CF_3SO_3^-$) was refluxed for two days, Br-Aib-Fp was quantitatively transformed into product (TLC, eluent toluene/EtOAc 9/1). Unfortunately, ^{1}H-NMR spectrum revealed that the product was not derivative 1 but the corresponding unsatured-α,β-amide. TLC product, eluent toluene/EtOAc 9/1, R_f 0.4. ^{1}H NMR (200MHz, $CDCl_3$) δ 5.59 (s, 2H), 5.47 (s, 4H), 2.21 (s, 3H).

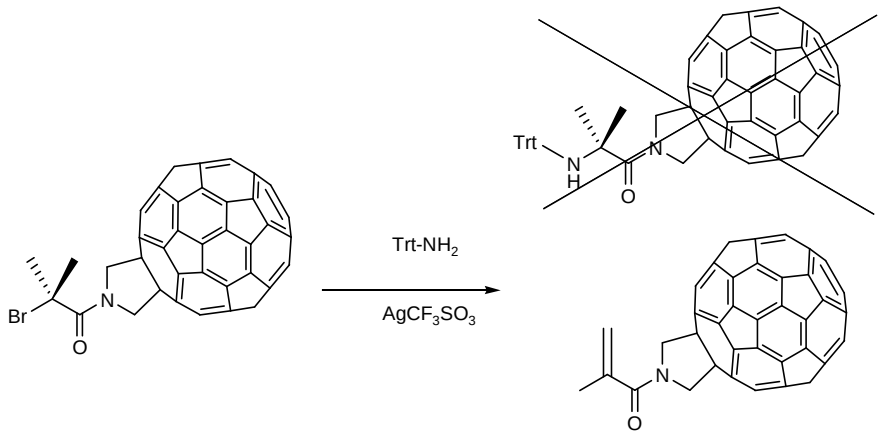

Figure 3.12 *Reaction scheme for the synthesis of Trt-Aib-Fp. The reaction gave the unsatured-α,β-amide.*

In order to obtain derivative 2 (Figure 3.9) instead, Fp-Aib-NHR, fulleropyrrolidine was stirred together with 2-Br-N-benzyl-propanamide in presence of silver oxide.

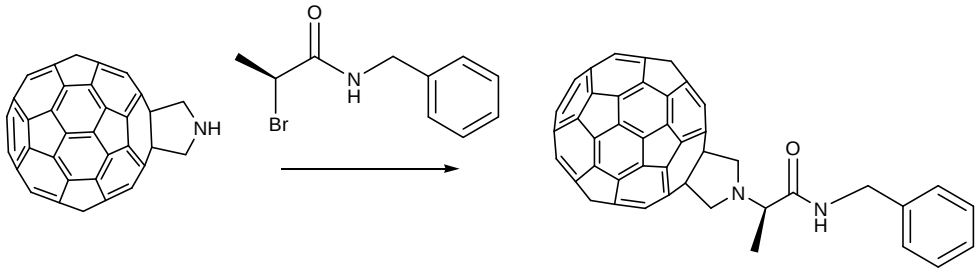

Figure 3.13 *Reaction between 2-Br-N-Benzyl-propanamide was expect to give the corresponding substitution product Fp-Ala-NHBenzyl.*

To a 4 ml toluene solution of 50 mg (0.06 mmol, 3 equiv) of fulleropyrrolidine, 20 mg (0.09 mmol, 4 equiv) of Ag_2O and 5 mg (0.02 mmol, 1 equiv) of 2-Br-N-Benzyl-propanamide were added. After 3 weeks of sonication at r.t. no product was detected on TLC employing toluene/EtOAc 1/1 and EP/EtOAc 1/1 as eluents. Same negative outcome was reached when 2-Br-N-Benzyl-butyramide was used. To a 5 ml toluene solution of 20 mg (0.03 mmol, 1 equiv) of fulleropyrrolidine, 12 mg (0.05 mmol, 2 equiv) of Ag_2O and 13 mg (0.05 mmol, 2 equiv) of 2-Br-N-Benzyl-butyramide were added. Product was detected only after 3 weeks of sonication at r.t. and flash chromatography was performed for purification using toluene/EtOAc 9/1 as eluent. Unfortunately, protonic NMR spetrum showed no compatible peak with the expected product Fp-Aib-NHBenzyl.

These attempts were carried out to see if the strategy employing 2-bromoamides was feasible for the synthesis of fullerene-peptide 2+ according to the following reaction scheme:

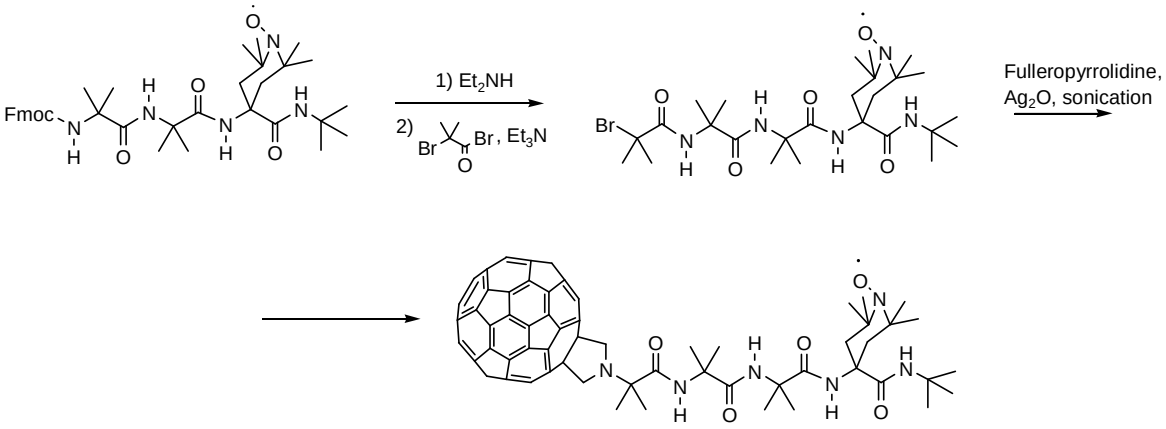

Figure 3.14 *Reaction scheme for the synthesis of fullerene-peptide 2+ through the nucleophilic substitution at the α-carbon of α-bromo-amides assisted by silver oxide.*

3.2.2 Use of the activated ester and anhydride

The synthesis of derivative 1 (Figure 3.9), P-Aib-Fp (P = protecting group), was attempted also using the activating couple EDC·HCl / HOAt. To a suspension of 15 mg (0.08 mmol, 1.2 equiv) of Boc-Aib-OH in 5 ml of anhydrous DCM at 0°C, 17.4 mg (0.09 mmol, 1.4 equiv) of EDC·HCl and 12 mg (0.09 mmol, 1.4 equiv) of HOAt were added. After stirring at r.t. for 1 h, the solution was added to a 50 ml toluene solution of 50 mg (0.06 mmol, 1 equiv) of fulleropyrrolidine together with 16 µl (0.09 mmol, 1.4 equiv) of DIEA. After stirring for 1 week at r.t. and 1 week at 60°C, no product was detected on TLC (TLC, eluent toluene, EtOAc 9/1). The amide bond formation between Aib and fulleropyrrolidine was also attempted by using $(Boc\text{-}Aib)_2O$. To a suspension of 26 mg (0.13 mmol, 2 equiv) of Boc-Aib-OH in 5 ml of anhydrous DCM at 0°C, 15 mg (0.08 mmol, 1.2 equiv) of EDC·HCl were added. After stirring at 0°C for 30 minutes and 2 hs at r.t., the solution was added to a 50 ml toluene solution of 50 mg (0.06 mmol, 1 equiv) of fulleropyrrolidine together with

22 µl (0.13 mmol, 2 equiv) of DIEA. After stirring at r.t. for 1 week, no product was detected on TLC using toluene/EtOAc 9/1 as eluent.

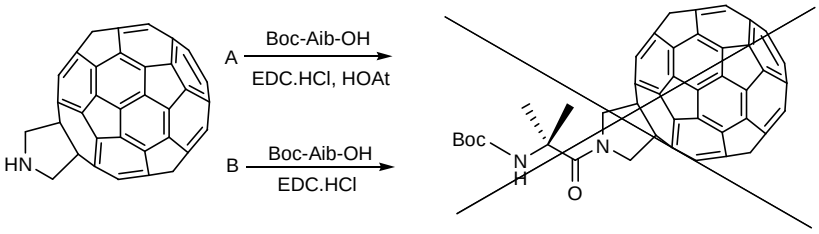

Figure 3.15 *Reaction scheme for the synthesis of Boc-Aib-Fp through the activated ester (A) and anhydride (B).*

3.2.3 Use of acyl chloride / bromide

Cyanuric fluoride was also employed to activate the carboxylic function of Aib in order to obtain Boc-Aib-Fp. To a suspension of 20 mg (0.10 mmol, 1.5 equiv) of Boc-Aib-OH in 5 ml of anhydrous DCM at 0°C, were added 43 µl (40 mg, 0.29 mmol, 4.5 equiv) of cyanuric fluoride and 43 µl (23 mg, 0.29 mmol, 4.5 equiv) of pyridine. After 2 hours of stirring at r.t., the solution was washed with 3x50ml of iced water and dried over $NaSO_4$ and finally added to a solution of 50 mg (0.06 mmol, 1 equiv) of Fp in 50 ml of toluene together with 17 µl (0.10 mmol, 1.5 equiv) of DIEA. After stirring at r.t. for 1 h, product was separated through flash chromatography however protonic NMR revealed no peak compatible with Boc-Aib-Fp.

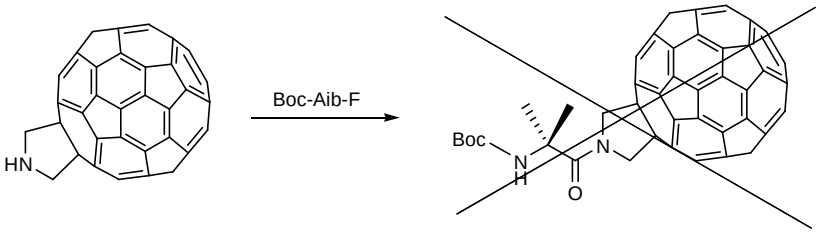

Figure 3.16 *Reaction scheme for the synthesis of Boc-Aib-Fp through acyl fluoride.*

Fmoc/Boc N-protected aminoacids bromide/chloride undergo fast cyclization and therefore require particular N-protections such as sulfonamides and azides[85].

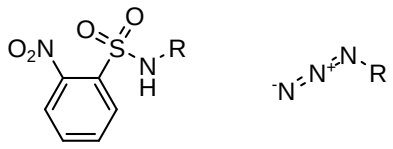

Figure 3.17 *"o-Nbs" orto-nitro-sulphonamide (on the left) and azide (on the right).*

These protecting groups are not able to take part in the cyclization as urethanes do[85]. They can be respectively introduced using *o*-Nbs[106] chloride and CF_3-SO_2-N_3[85]. Then, the carboxylic group of the amino acid can be treated with 1-bromo-N,N-2-trimethyl-1-propenylamine[92] to be transformed into the corresponding acyl bromide.

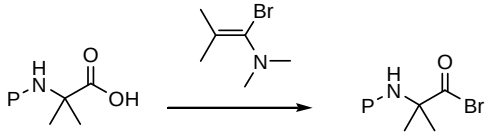

Figure 3.18 *1-bromo-N,N-2-trimethyl-1-propenylamine is the brominating agent. P is the protecting group.*

Removal of *o*-Nbs can be accomplished after exposition to K_2CO_3/thiophenol in DMF whereas the azide group is transformed into the amino group after reduction with Ph_3P in THF[85]. The synthesis of an N_3-Aib-Br or *o*-Nbs-Aib-Br was not attempt because:

- the synthesis of the brominating agent is not an easy task[92]
- the removal condition of N_3 and o-Nbs have never been tried in presence of fullerene
- fulleropyrrolidine is not soluble in DMF and THF, solvents required during the deprotection step

3.2.4 A novel strategy through fulleroproline

The experimental outcomes demonstrate that the amide bond formation between Aib and fulleropyrrolidine can not be obtained by means of the synthetic routes described before. Thus, the design of the fullerene-Aib-peptides was modified in the following way:

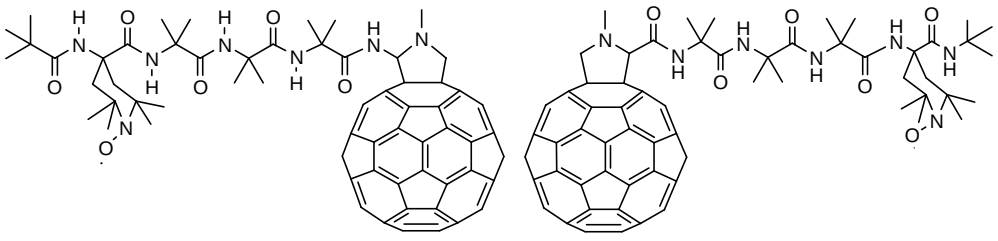

Figure 3.19 *Modified fullerene-peptides 2+ (on the right) and 2- (on the left). The peptide is attached to the C_{60} moiety through a fulleroproline residue.*

The idea was to synthesize Fpr-O*t*Bu (Fpr=fulleroproline) and then to hydrolyze the *t*-butyl ester to get Fpr-OH. Fpr-OH could react with the N-terminal peptide to give the fullerene-Aib-peptide 2+.

Besides Fpr-OH has a carboxylic function which can be converted into a primary amino group *via* Curtius rearrangement (Figure 3.25), to afford N-methyl-2-amino-3,4-fulleropyrrolidine Fpr-NH_2. Subsequently, Fpr-NH_2 could react with the COOH-terminal peptide to give the fullerene-Aib-peptide 2-.

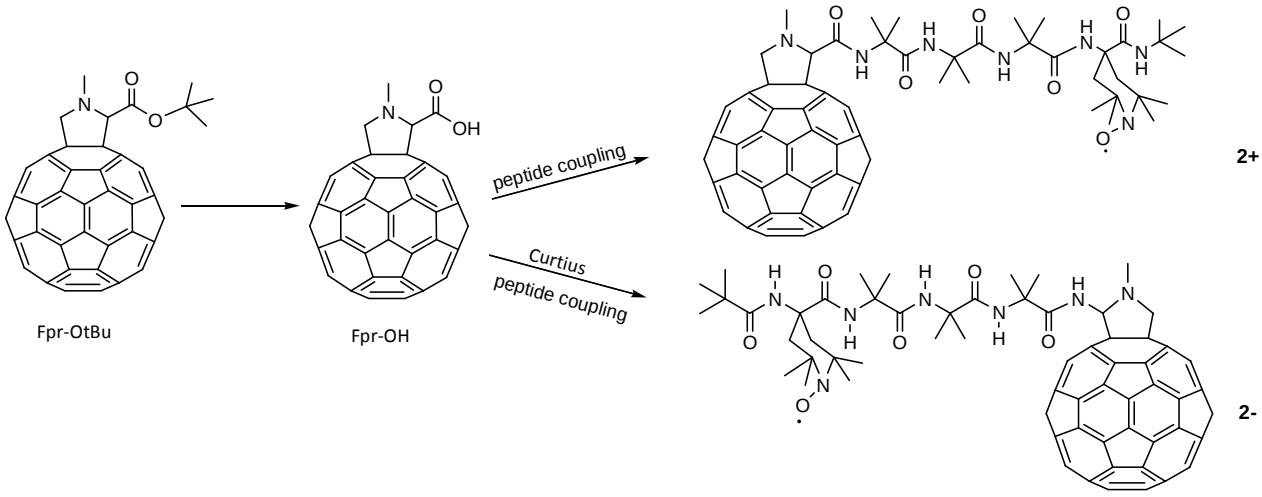

Figure 3.20 *The strategy through fulleroproline.*

3,4-fulleropyrrolidine has a secondary amino group whereas Fpr-NH_2 bears a primary amino group. Therefore, the peptide coupling between the COOH-terminal peptide and Fpr-NH_2 was expected to be easier, compared with the coupling between fulleropyrrolidine and Aib, because less hindered.

According to the experimental part described in the references[93,94], the following was the synthetic strategy tried to get the fullerene-peptide 2+ and 2- through fulleroproline:

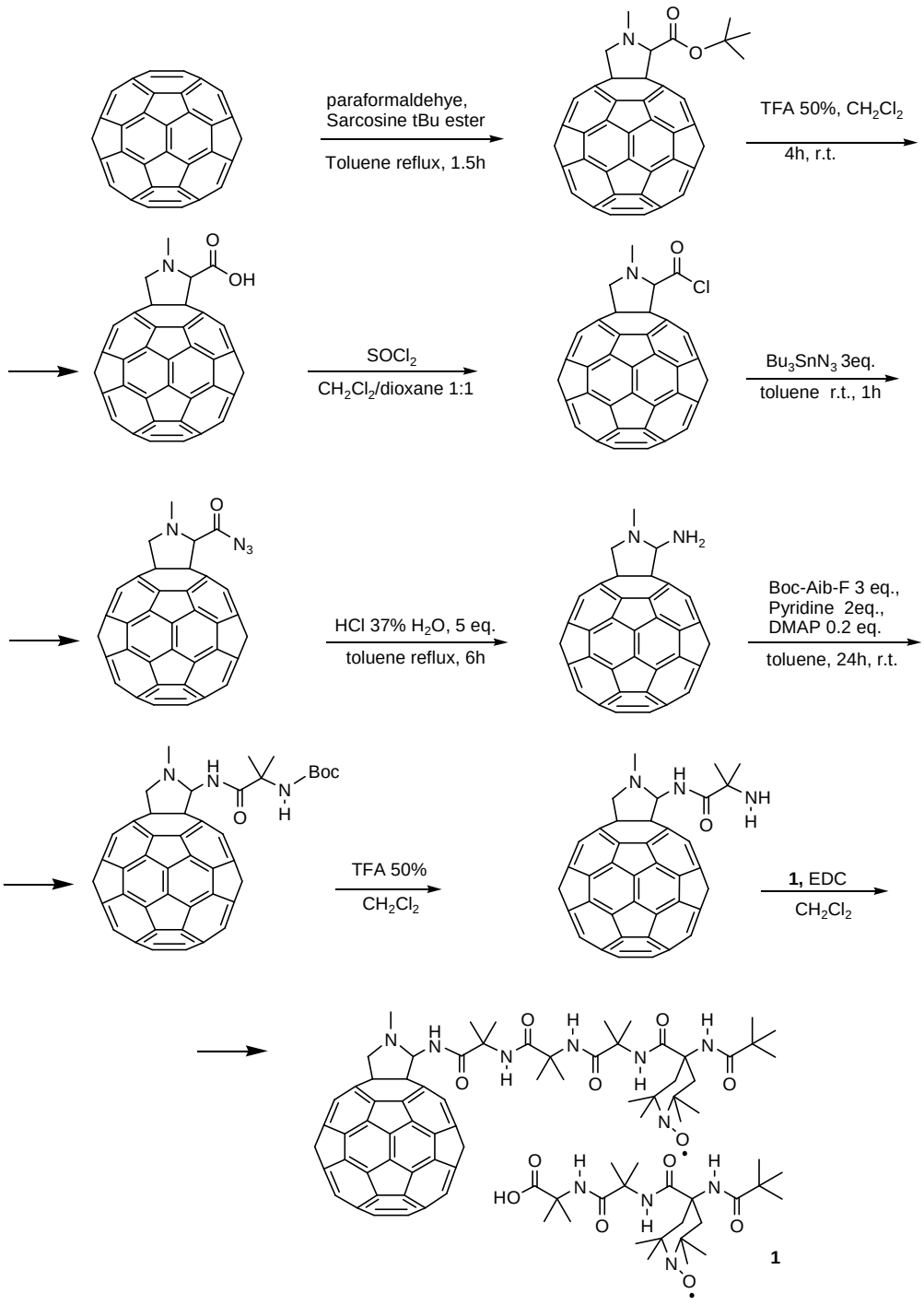

Figure 3.21 *Strategy for the synthesis of modified fullerene-peptide 2-.*

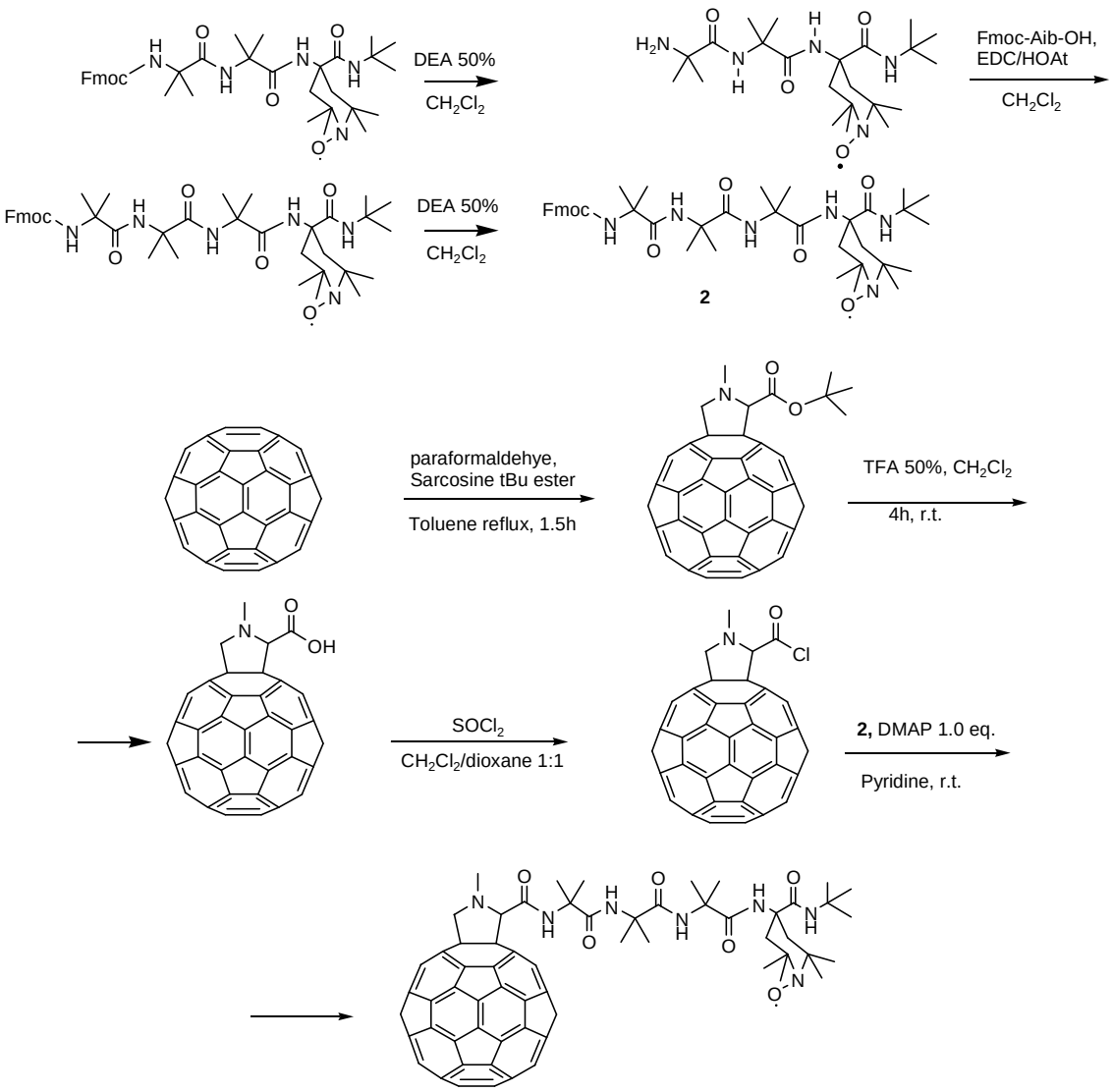

Figure 3.22 *Strategy for the synthesis of the modified fullerene-peptide 2+.*

Fpr-O*t*Bu and **Fpr-OH** were synthesized as previously reported[95,96].

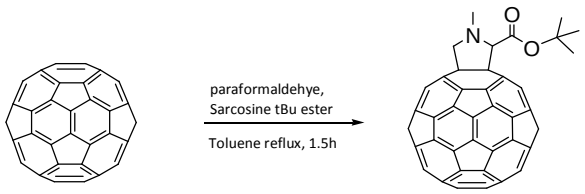

Figure 3.23 *Reaction scheme for the synthesis of Fpr-OtBu.*

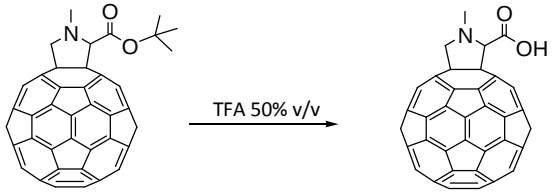

Figure 3.24 *Reaction scheme for the synthesis of Fpr-OH.*

N-methyl-2-amino-3,4-fulleropyrrolidine

250 mg (0.30 mmol, 1 equiv) of Fpr-OH were suspended in a 200 ml solution of DCM/dioxane 1/1. 25 ml (300 mmol, 1000 equiv) of Cl_2SO were added and the mixture was refluxed for 24 hs. Solvent and thionyl chloride in excess were removed under vacuum. 200 mg (0.24 mmol, 1 equiv) of the residue were subsequently suspended in 20 ml of toluene at 0°C and treated with 197 µl (0.71 mmol, 3 equiv) of Bu_3SnN_3 dropwise according to the experimental part of reference[94]. The mixture was stirred for 2 days at r.t. and the solvent remained uncoloured, then refluxed for 1 day in presence of 5 ml of water to decompose the expected azide. Solvent was removed under reduced pressure but unfortunately the residue was not soluble in any solvent so that it was not possible to characterize the product. The synthetic project of the fullerene-peptide 2+ and 2- through fulleroproline was thus rejected.

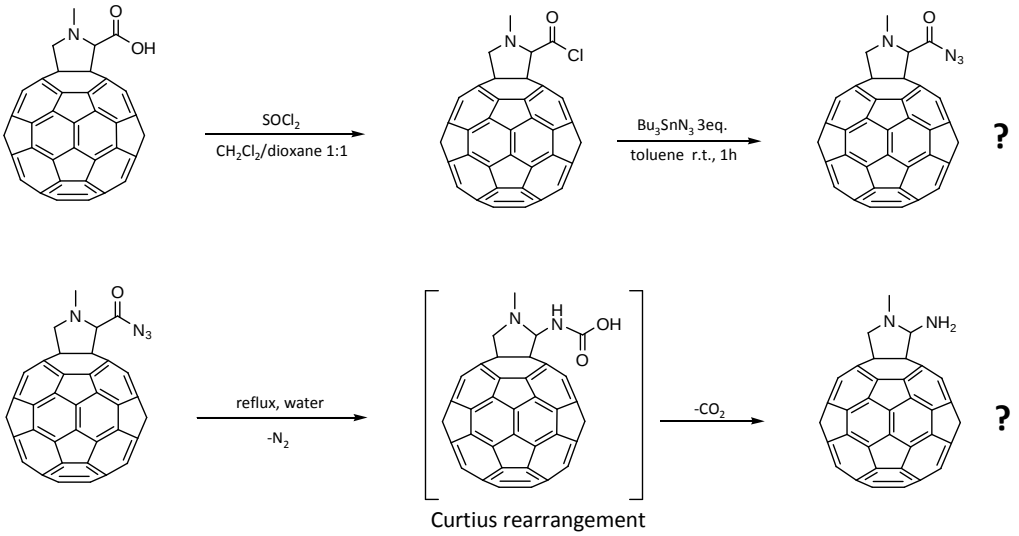

Figure 3.25 *Reaction scheme followed to try to obtain the derivative N-methyl-2-amino-3,4-fulleropyrrolidine via Curtius rearrangement .*

3.3 Investigation and Characterization in solution

The fullerene-peptides were found to be soluble in chlorinated solvents such as $CHCl_3$ and 1,2-dichloroethane. The solubility slightly decreases in DCM. However, these molecules are insoluble in more polar solvents or toluene. The synthesized molecules were characterize by mass spectrometry, FT-IR and NMR spectroscopies. The mass spectra show the expected molecular peak for both fullerene-peptides 2+ and 2- (Figures 3.26 a, b). The analyte was dissolved in CCl_4 containing DCTB to obtain a 0.1 mM solution with a 1:1000 analyte/matrix ratio. 2 µL of solution were drop-cast onto the sample plate and air-dried. The spectra were recorded by MS-Reflector mode in the positive mode.

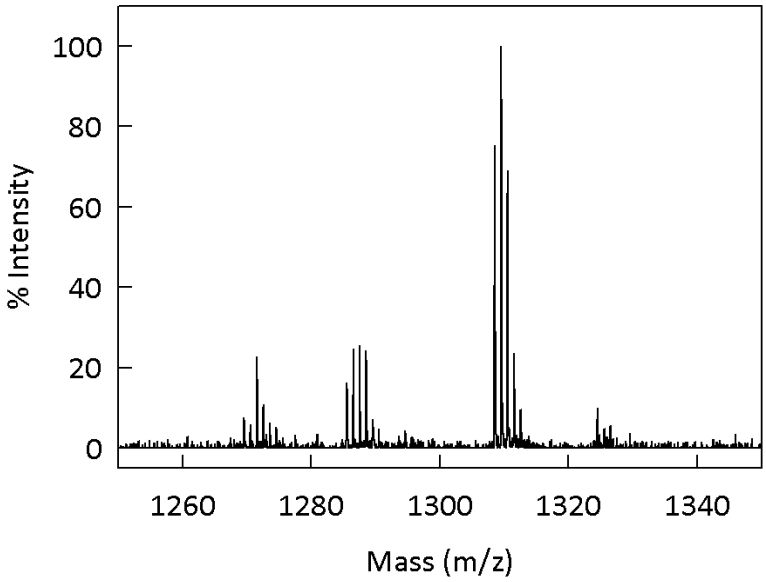

Figure 3.26 a. *MALDI –TOF mass spectrum of fullerene-peptide 2-.*

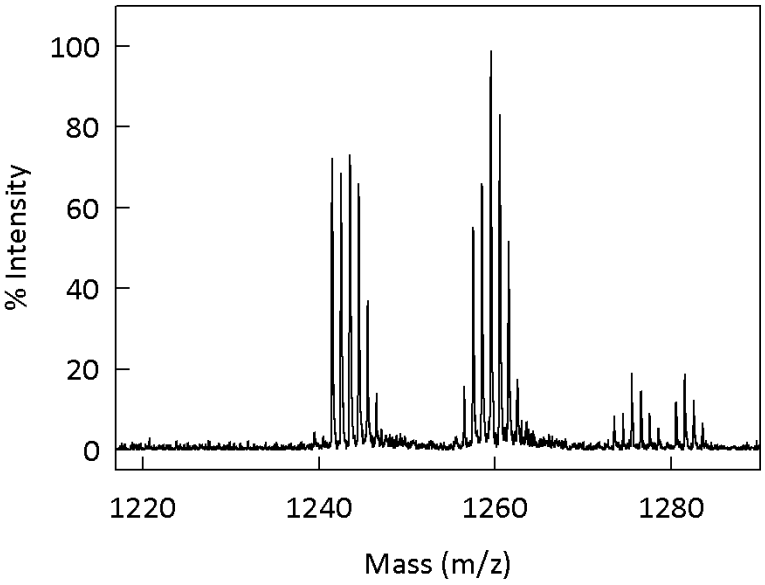

Figure 3.26 b. *MALDI-TOF mass spectrum of fullerene-peptide 2+.*

3.3.1 FT-IR characterization of the 2+ and 2- systems

FT-IR absorption spectra were recorded in $CHCl_3$ at 23°C which is a solvent of low polarity having no propensity to behave as a hydrogen-bond acceptor, and the analysis focused on the N - H and C = O stretching modes. The N - H stretching region (amide A, 3500 ÷ 3200 cm^{-1}) is composed by a high-energy region corresponding to the NH groups that are not involved in hydrogen bonds and a low-energy region pertaining to NH groups involved in intra- and inter-molecular hydrogen bonds[99]. For the amide A stretching region, the FT-IR spectra of the investigated systems (Figure 3.27 a) reveal a strong absorption band in the range 3369 ÷ 3329 cm^{-1} and a weaker band at 3469 ÷ 3439 cm^{-1} assigned to N-H bonded and N-H free groups, respectively [97].

Information on peptide conformation is also found in the amide I and amide II regions. Amide I, which corresponds to the C = O stretching, occurs at 1662 ÷ 1666 cm^{-1} for fully stable 3_{10}-helices, whereas the amide II band, which is more complex with an important contribution from N-H bending and C-N stretching vibrations, is expected at 1531 ÷ 1533 cm^{-1} [99] for fully formed 3_{10}-helices. In the amide I region, a strong band in the range 1678 ÷ 1662 cm^{-1} is observable in figure 3.27 b, typical for the carbonyl in helical peptides[98]. The systems 2+ and 2- possess 4 NH groups belonging to tetrasubstituted residues (Aib, TOAC) and in a previous IR absorption study, it was possible to show that Aib homooligomers with 4 NH groups are characterized by 69% of intramolecular H-bonds of the 3_{10} -helix type[60]. These data highlight the great efficiency of the Aib unit in stabilizing folded and helical species even in very short peptides[99].

Now we will focus on the comparison among the various spectra. The IR spectra in figures 3.27 a, b clearly disclose the similarity of the fullerene-peptide 2+ with its fullerene-peptide-reference and its peptide-reference. Noteworthy, however, a marked difference is evident in the free NH band for the peptide-reference 2+ which results more intense in comparison with the free NH band for the fullerene-peptides 2+ and fullerene-peptide-reference 2+: this suggests a possible deviation on the number of free NH groups. Unlike the 2+ series, the peak position of the fullerene-peptides 2- spectrum does not match those of the spectra of the fullerene-peptide-reference 2- and peptide-reference 2- in the amide A region. Whereas the free NH band occurs at the same wavenumber for the three compounds, a red shift is observable for the bonded NH band as one goes from the peptide-reference, to the fullerene-peptide and to the fullerene-peptide-reference. It appears that the interactions involving the NH groups in the 2- series are of different strenght. This observed increase in bond strength for the bonded NH could be accounted for by two reasons. Firstly, in the 2- series, the negative pole of the macrodipole is on the fullerene, which is known to be electro-deficient[1,6a]. In principle, C_{60} should not influence the peptide helical structure as previously observed in other reports[75,105] but in this particular case, a strong oriented dipole moment is located along the main axes of the compound. Preliminary results obtained on the experimental determination of the dipole moments of series of Aib homooligomers indicated that the peptide dipole moment linearly increases with the number of Aib units. This outcome also implies that these peptides are indeed stiff even when short.

For peptides with one, two and three intramolecular hydrogen bonds, 8.22, 10.79 and 12.34 D were determined, respectively[120]. Therefore, by helping to spread the negative charge density of the negative side of the macrodipole, the C_{60} moiety could play a role in the stabilization of the peptide secondary structure. Secondly, it appears that in the *minus* series, the substitution of the TOAC residue with an Aib residue brings about an effect on the NH groups interaction frameworks displayed by the red shift of the bonded NH in the FT-IR spectra of fullerene-peptide 2- and fullerene-peptide-reference 2-. The absence of any band shift in the FT-IR spectra of the *plus* series would thus point to a higher sensitivity of the peptide secondary structure of the *minus* series, compared with the *plus* series, to change of the chemical surround.

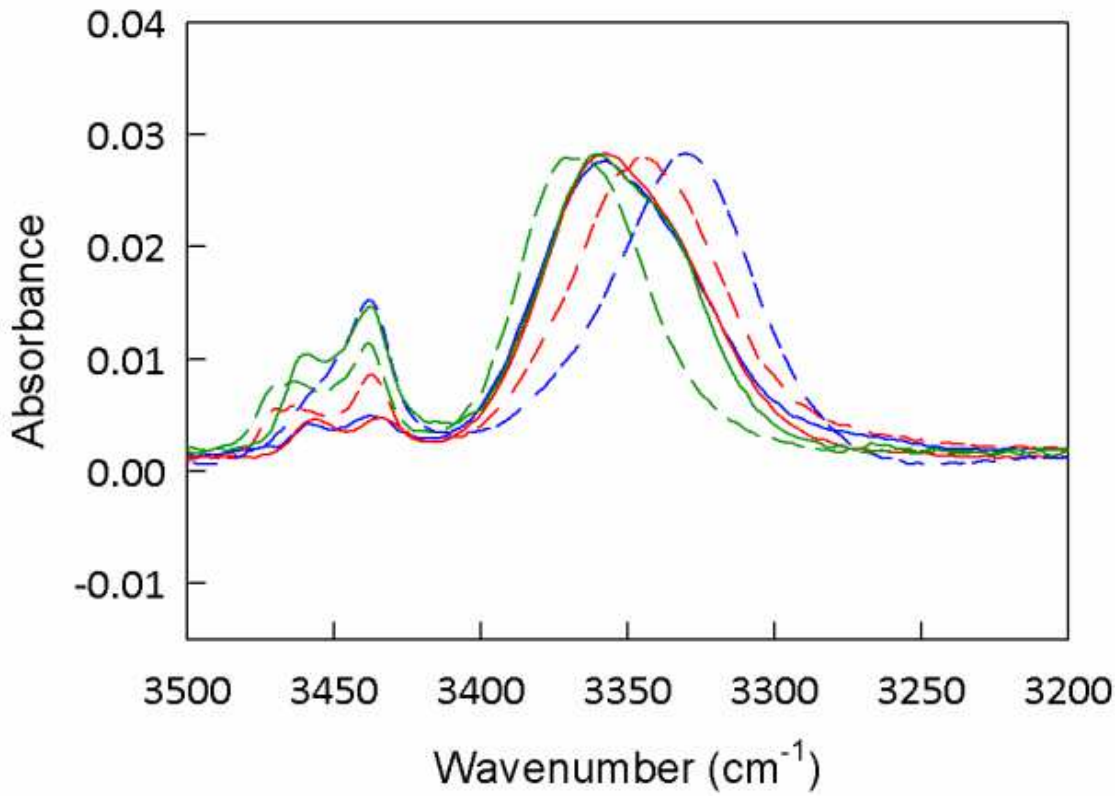

Figure 3.27 a. *FT-IR spectrum of systems 2+ and 2- in the amide A stretching region. 2- system in dashed line. 2+ system in continue line. Fullerene-peptide, fullerene-peptide-reference, peptide-reference. Spectra are normalized by taking into account the N-H band of intramolecularly H-bonded peptides.*

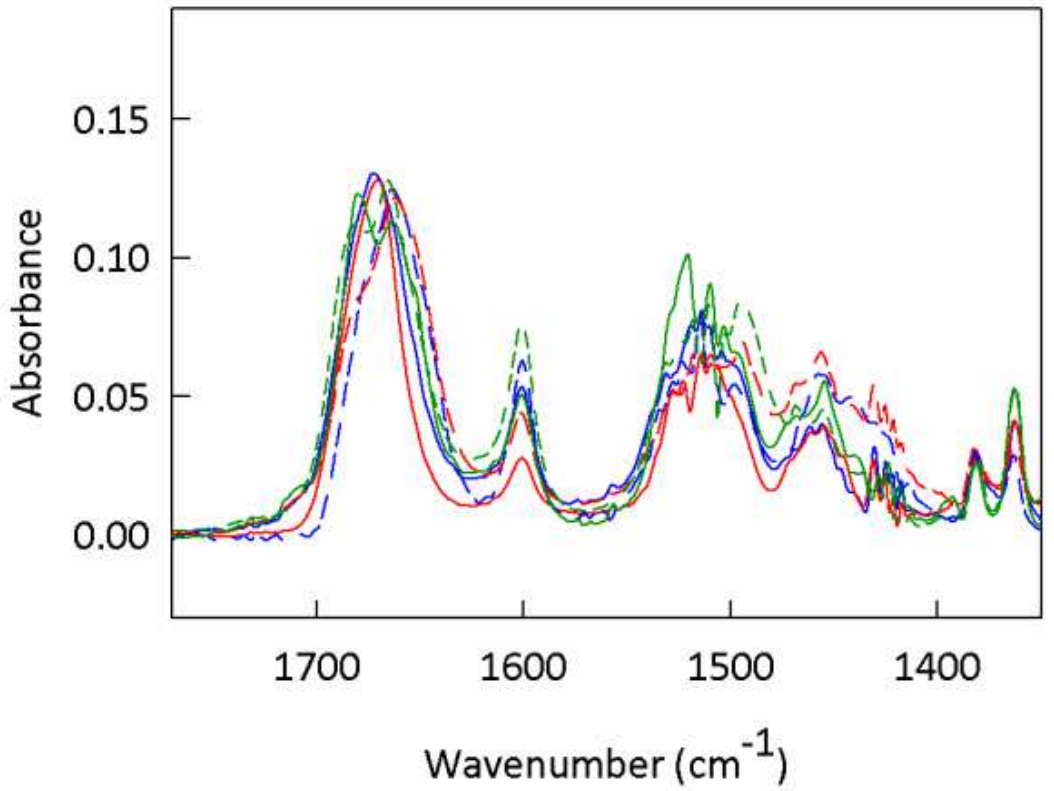

Figure 3.27 b. *FT-IR spectrum of systems 2+ and 2- in the amide I and II stretching region. 2- system in dashed line. 2+ system in continue line. Fullerene-peptide, fullerene-peptide-reference, peptide-reference. Spectra are normalized by taking into account the C=O band.*

3.3.2 ^{1}H NMR characterization of fullerene-peptides-reference 2+ and 2-

^{1}H NMR of 2 mM fullerene-peptides-reference 2- and 2+ (Figures 3.30 and 3.31) were acquired at r.t. using $CDCl_3$ as the solvent. CD_2Cl_2 however, was employed for the fullerene-peptide-reference 2+ because one signal perfectly overlaps with the signal of the residual $CHCl_3$ when $CDCl_3$ is used.

^{13}C NMR spectra of 3 mM fullerene-peptides-reference 2+ and 2- in $CDCl_3$ show a cluster of peaks in the aromatic region 153 ÷ 136 ppm, typical of fullerene carbons[22].

Being $CHCl_3$ the only solvent that reasonably dissolves the fullerene-peptides, circular dichroism measurements can not be exploited to obtain structural information because any absorptions under 220 nm is covered. However, above 220 nm no otpically active band was observed for the fullerene-peptide-reference 2+ in a 1 mM $CHCl_3$ solution.

2D ROESY (Rotating-Frame Overhauser Effect Spectroscopy) spectra and ^{1}H NMR titrations were performed to obtain information on the secondary structure assumed by the fullerene-peptides in solution. Bidimensional ^{1}H NMR spectra of the fullerene-peptides-reference 2+ and 2- were obtained in $CDCl_3$ and allowed for complete proton assignment. Through-space connectivities of the *$C^{\beta}H$ (i - 1) → NH (i)* type (between the methyl protons of an Aib and the amide proton of the following residue) and *NH (i) → NH (i + 1)* type were used for the assignment of the proton resonances. In particular, it was possible to determine unambiguously the identity of the four amide protons both for the fullerene-peptides-reference 2+ and 2-. By providing information on the through-space connectivities, useful insights into the peptide secondary structure could be obtained. The section of the ROESY spectrum of fullerene-peptides-reference 2- and 2+ in figures 3.33 a, b and 3.34 a, b show evident NH (*i*) → NH (*i+1*) connectivities (red lines), indicative of an highly folded conformation of the peptide[104,105].

Besides, to test the participation of the amide protons in intramolecular hydrogen bonds, the evolution of the ^{1}H NMR spectra of fullerene-peptides-references 2+ and 2- were studied as a function of the good H-bond acceptor Me_2SO-*d6* [60].

Figure 3.35 clearly shows two classes of NH protons for the fullerene-peptide-reference 2-: the first class, N(1)H and N(2)H, includes protons whose chemical shifts are remarkably sensitive to the addition of the H-bonding acceptor solvent Me_2SO-*d6*; the second class N(3)H and N(4)H includes those displaying a behavior characteristic of shielded protons (very modest sensitivity of the chemical shifts to the solvent composition). The absence of effects brought about on the N(3)H and N(4)H protons points to the failure of Me_2SO-*d6* to disrupt the intramolecular H-bonds involving them.

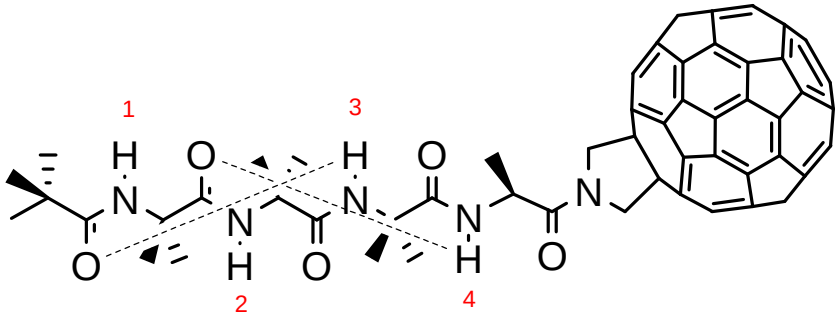

Figure 3.28. *Molecular structure of the fullerene-peptide-reference 2- where the intramolecular hydrogen bonds are evidenced.*

Since in the 3_{10} –helix, the formation of stable intramolecular H-bonds starts from the N(3)H proton, it can thus be inferred that the fullerene-peptide-reference 2- adopts such an ordered secondary structure.

As far as the fullerene-peptide-reference 2+ is concerned, figure 3.36 again shows two class of protons: not shielded N(2)H (its chemical shift is sensitive to the Me_2SO-d_6 addition) and two shielded amide protons N(3)H and N(4)H.

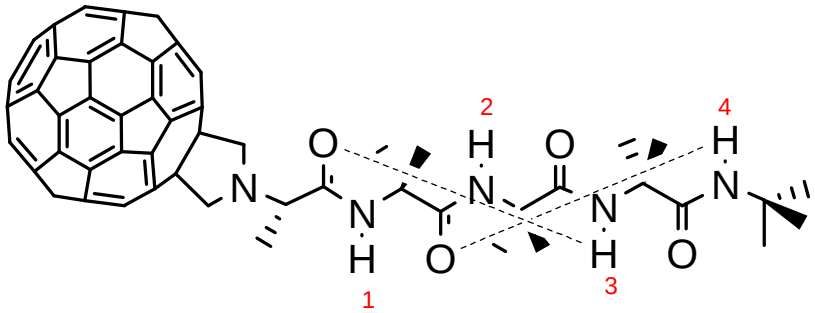

Figure 3.29. *Molecular structure of the fullerene-peptide-reference 2+ where the intramolecular hydrogen bonds are evidenced.*

From figure 3.36, it is clear how the N(1)H shows an anomalous behavior. Not only its chemical shift is not consistent for a free NH group but also its chemical shift only slightly increases with Me_2SO-d_6 addition. This trend is not in line with the normal behavior of Aib homopeptides for which the sensitivity of the N(1)H protons is notably higher than that of the N(2)H protons. The insensitivity of the N(1)H chemical shift to the addition of Me_2SO-d_6 suggests how this proton can be engaged in some sort of interaction. This observation is consistent with the FT-IR spectrum of fullerene-peptide-reference 2+ (Figure 3.27). The band of the free NH in the amide A region results less intense compared with the corresponding band in the peptide-reference 2+ FT-IR spectrum. The peptide-reference 2+ only lacks of the C_{60} moiety and retains the same number of NH groups; therefore, the decrease in intensity of the free NH band can be accounted for a lower number of free NH groups in comparison with the number of free NH groups present in the peptide-reference 2+.

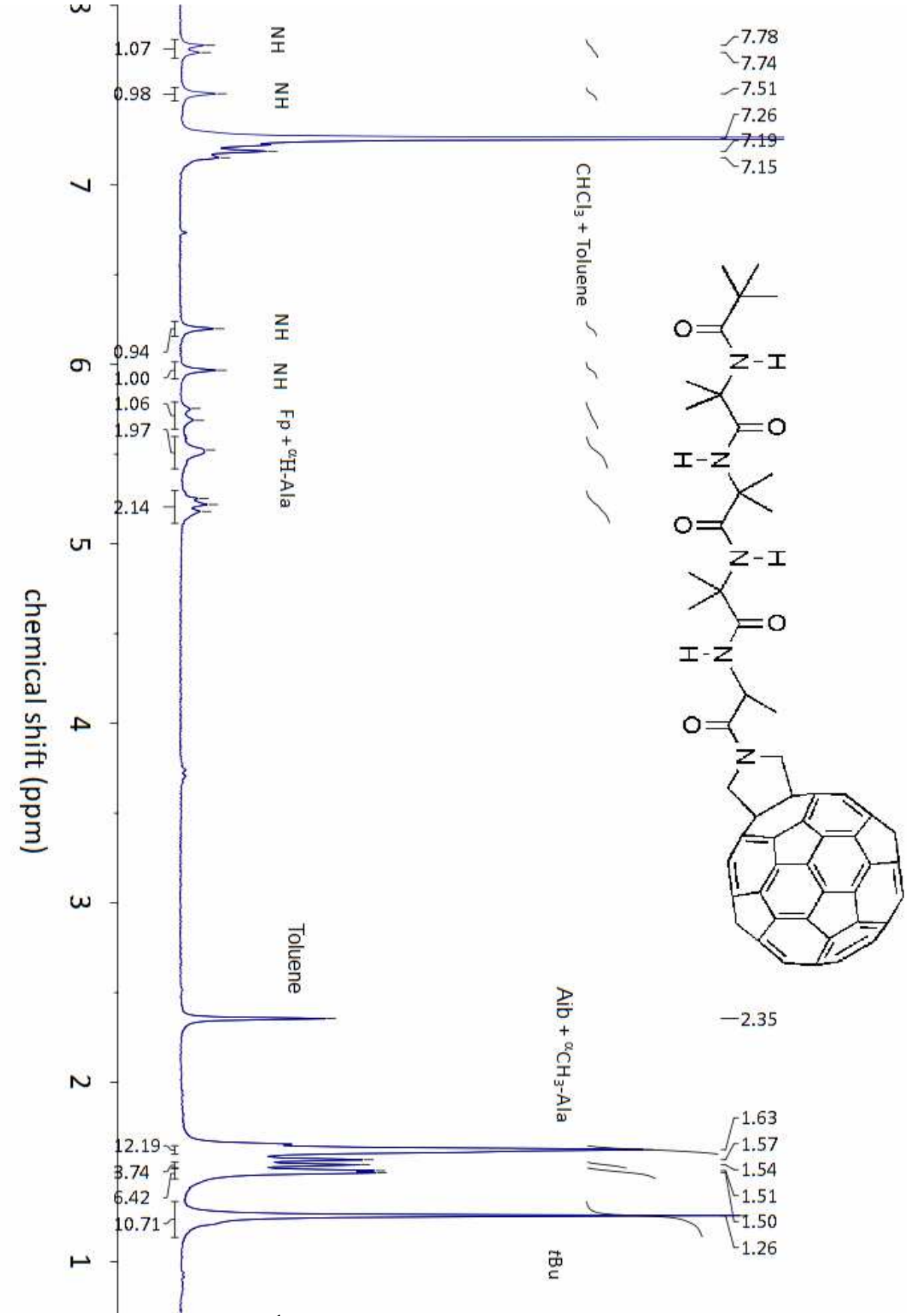

Figure 3.30. *200 MHz ^{1}H NMR spectrum of fullerene-peptide-reference 2- in $CDCl_3$, 20°C, 2 mM.*

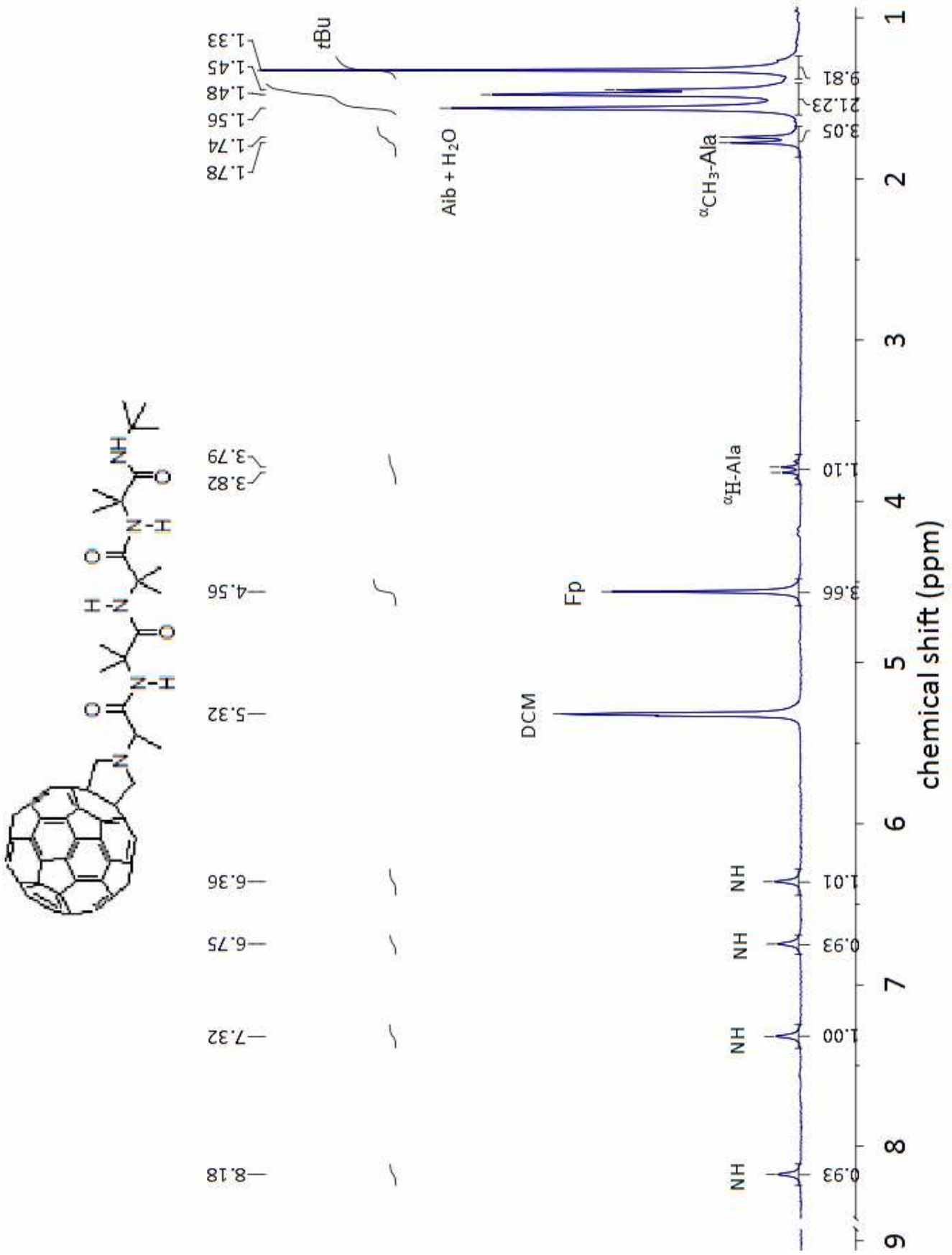

Figure 3.31. *200 MHz* ^{1}*H NMR of fullerene-peptide- reference 2+ in* CD_2Cl_2*, 20°C, 2 mM.*

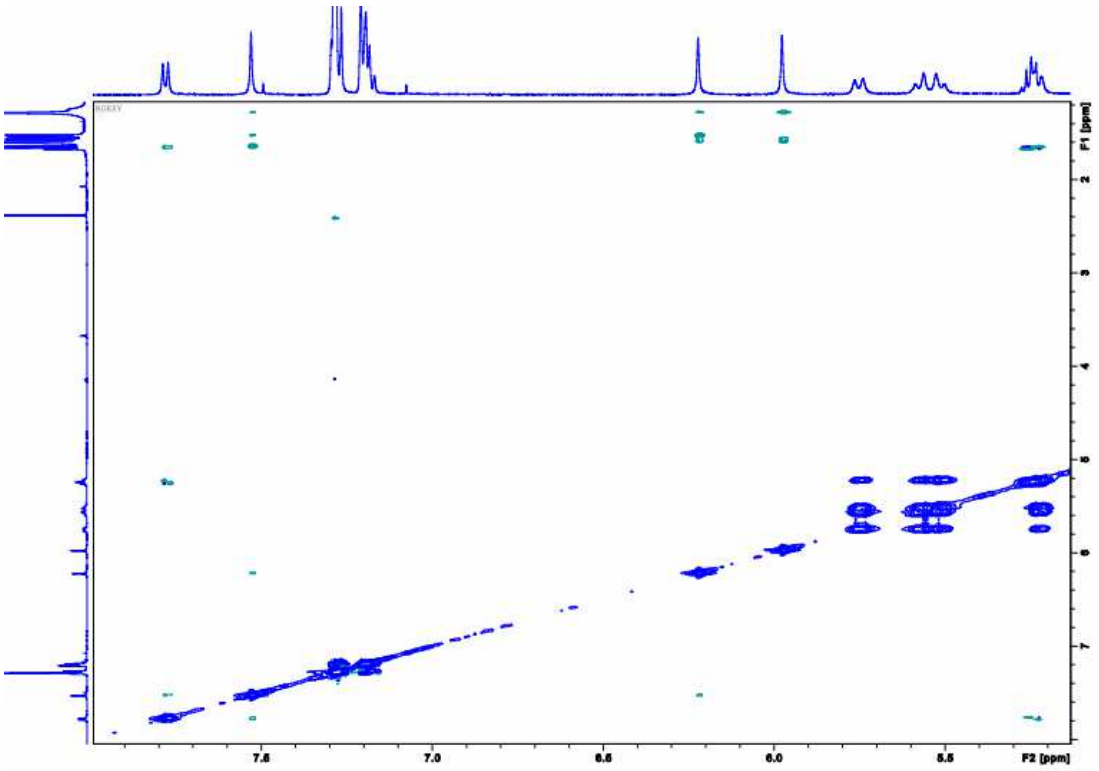

Figure 3.33 a. *Full 2D ROESY spectrum in $CDCl_3$ of 3 mM fullerene-peptide-reference 2-.*

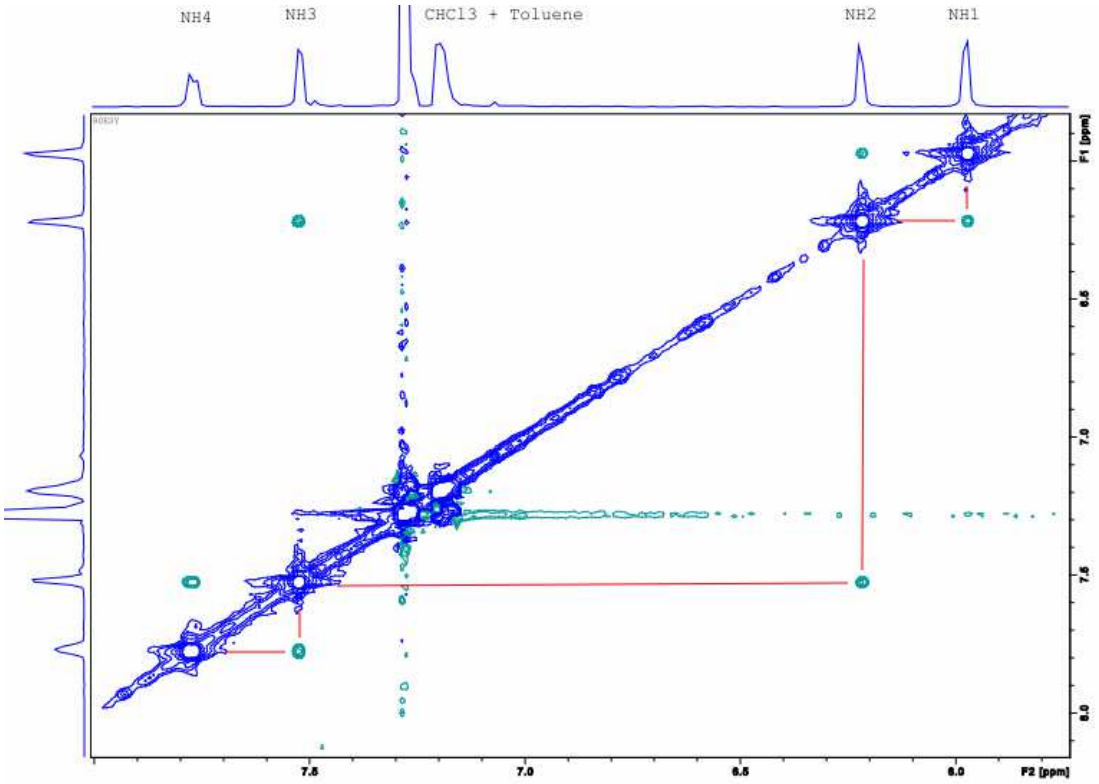

Figure 3.33 b. *2D ROESY spectrum in $CDCl_3$ of 3 mM fullerene-peptide-reference 2- in the NH protons resonance region.* NH (*i*) → NH (*i+1*) connectivities are shown (red lines).

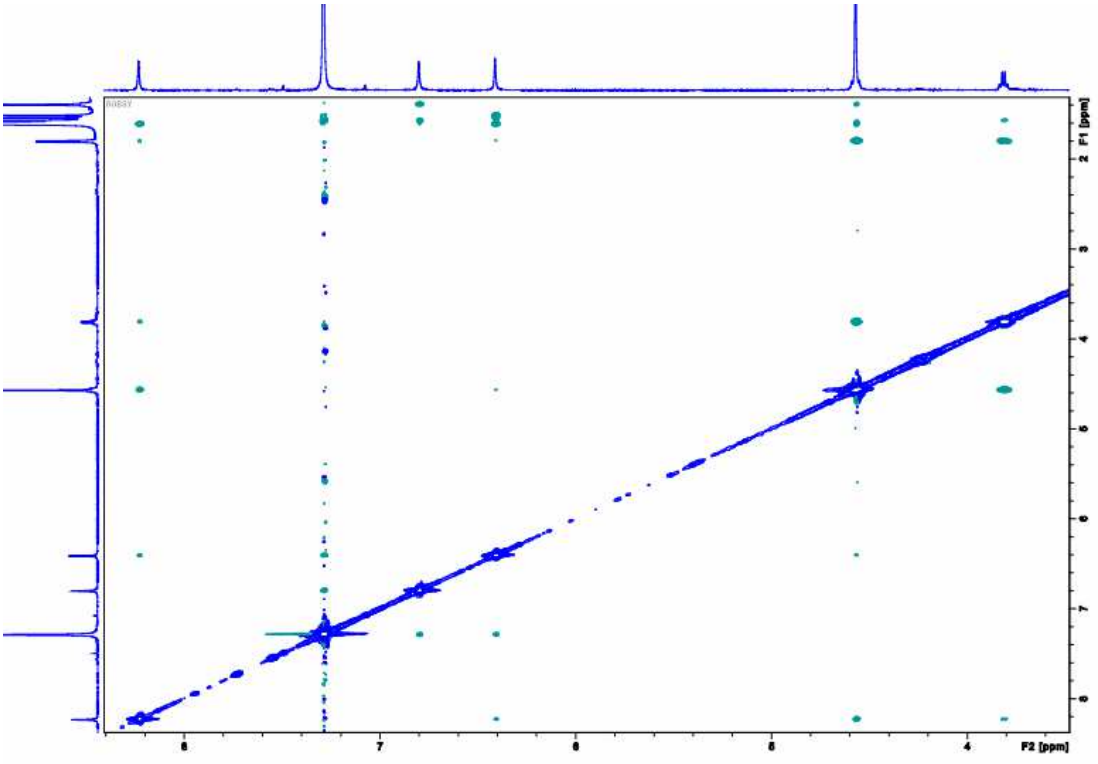

Figure 3.34 a. *Full 2D ROESY spectrum in $CDCl_3$ of 3 mM fullerene-peptide-reference 2+.*

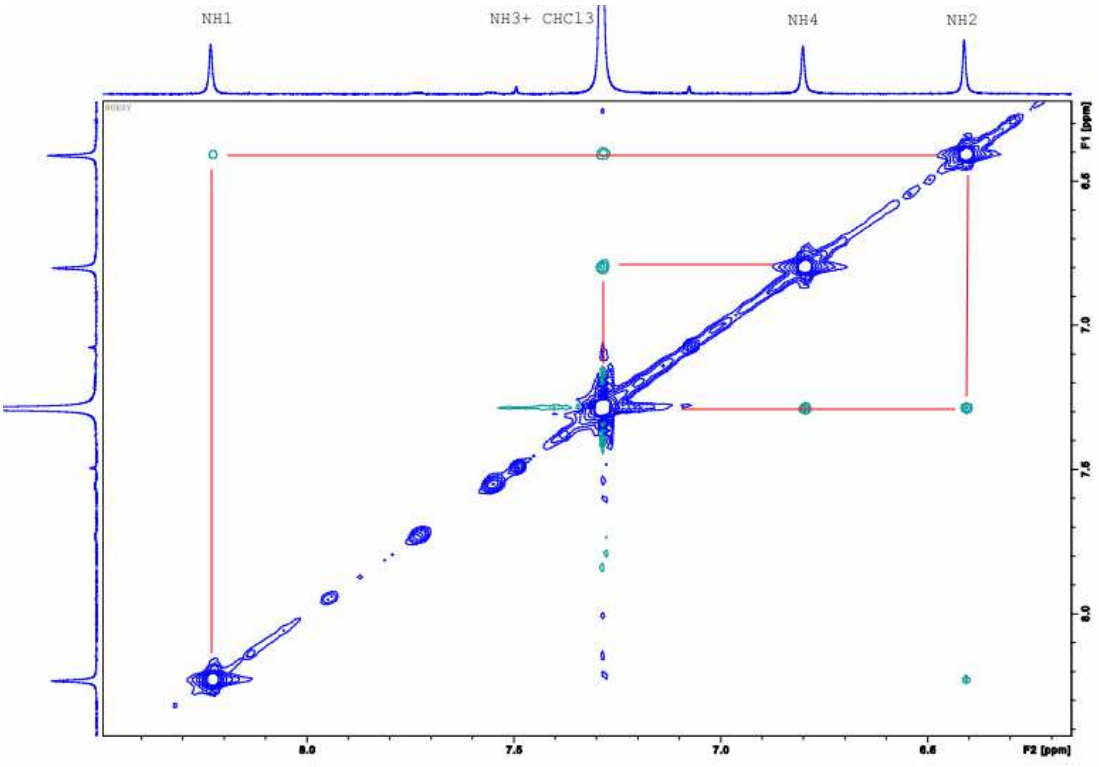

Figure 3.34 b. *2D ROESY spectrum in $CDCl_3$ of 3 mM fullerene-peptide-reference 2+ in the NH protons resonance region.* NH (*i*) → NH (*i+1*) connectivities are shown (red lines).

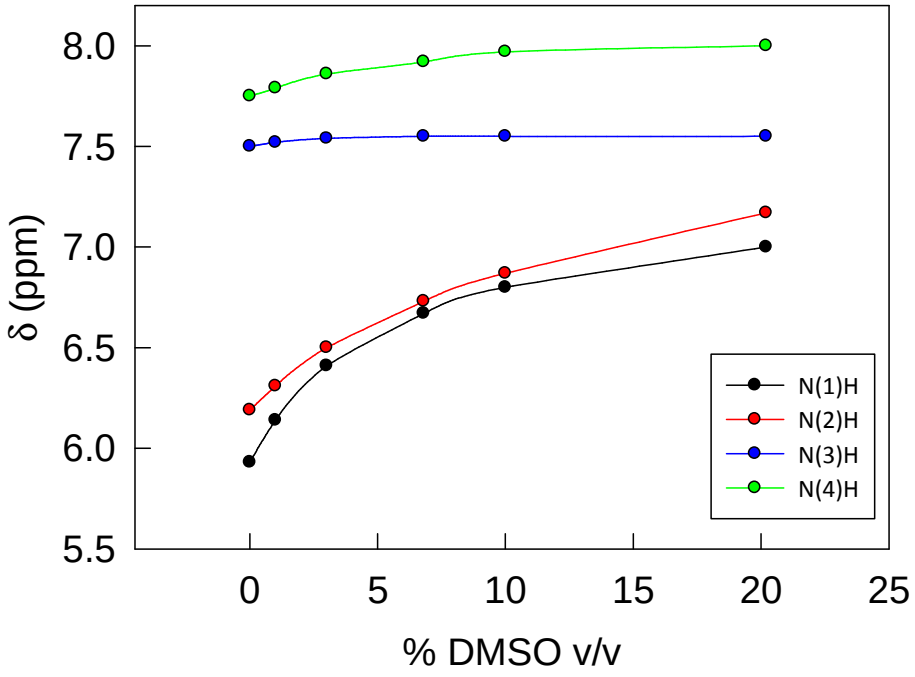

Figure 3.35. *^{1}H NMR titration in $CDCl_3$: Variation of the chemical shifts of the four amide protons of 1 mM fullerene-peptide-reference 2- as a function of the addition of Me_2SO-d6.*

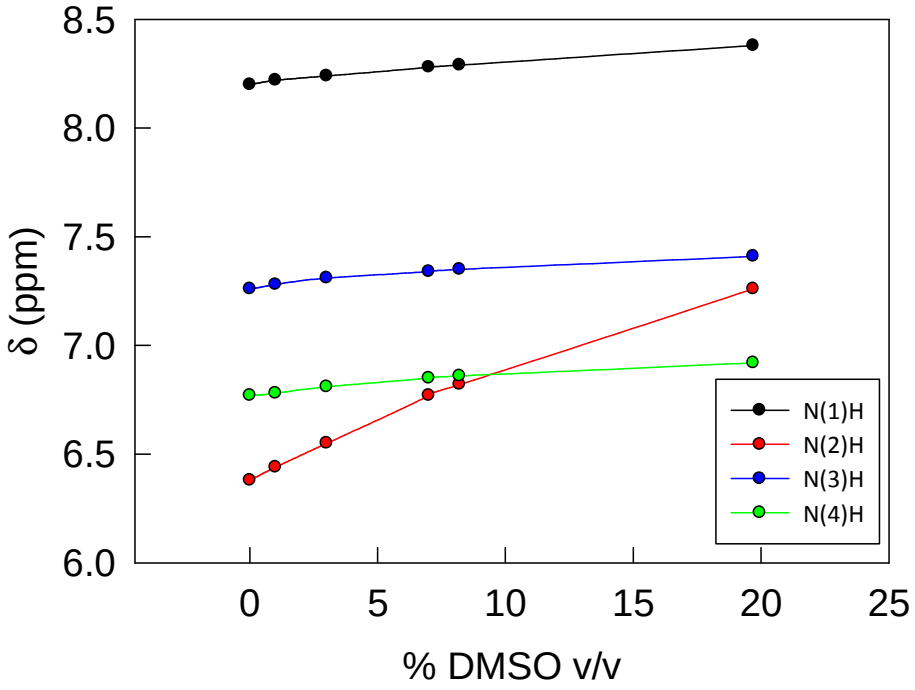

Figure 3.36. *^{1}H NMR titration in $CDCl_3$: Variation of the chemical shifts of the four amide protons of 1 mM fullerene-peptide-reference 2+ as a function of the addition of Me_2SO-d6.*

3.3.3 Quenching of the systems bearing the nitroxide monitored by cw EPR

The presence of the free radical in the 2+ and 2- systems bearing the nitroxide was proved by cw EPR spectra which show the typical three lines pattern of the nitroxide due to the ^{14}N (I = 1) nuclei hyperfine coupling with a g value of 2.0061 and a_N ~ 15.3 G [14,30-34] (Figures 3.39 a, b). The measurement of g was performed by measuring B at the zero of the first derivative signal of the central line of the EPR spectrum. It is worth stressing that here we wanted only a qualitative measurement of g and a_N since many factors concur to determine these two parameters such as temperature, signal distortions, frequency counter accuracy, stability of the frequency and of the magnetic field and other instrumental factors, limits on the accuracy of the natural constants (h, β_e)[49]; therefore, a standard is required when a precise determination is sought. In EPR spectra of 2+ and 2- series, further splitting by the protons of the methyl substituents and by the methilene protons of the piperidinic ring are not resolved[30]. Without entering into details, the three EPR lines show different widths because of the uncomplete averaging of anisotropic hyperfine interactions and the g tensor.[49] Spectra were acquired in $CHCl_3$, 0.05 mM concentration so that interactions between paramagnetic centers should be negligible; this was done to avoid line broadening by spin-spin interaction. Microwave losses and sample heating due to non-resonant absorption of the electric component by the electric dipoles of solvent was reduced by employing capillaries 2x3 mm o.d. Diphenylhydrazine (PH)[100] was used to quench (here quench is meant as the change of the redox state of the native radical) the free radical according to the following reaction scheme:

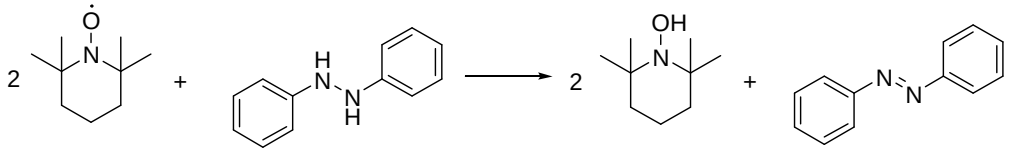

Figure 3.37. *Reaction scheme for the reduction of the nitroxide.*

Various alternative mechanisms for the reduction of nitroxides by PH were been proposed[101]. In the mechanism depicted in figure 3.38, the nitroxide forms an H-complex with PH, in which the oxygen atom of the nitroxide donates a lone pair to a hydrogen atom of the PH NH-group. According to this scheme, formation of the final product, hydroxylamine, requires transfer of an electron from the lone pair of the PH nitrogen atom to the nitrogen atom of the nitroxyl group with concerted or subsequent proton transfer from the NH-group to the nitroxide oxygen atom.

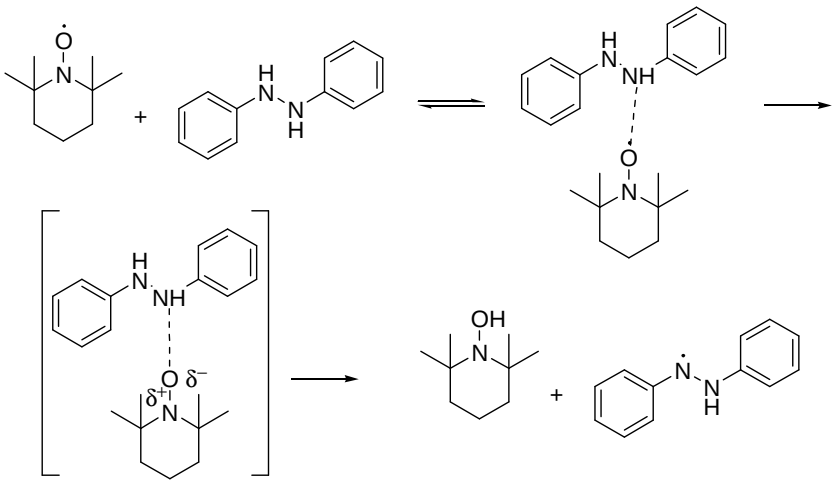

Figure 3.38. *Possible reaction mechanism for the reduction of the nitroxide through PH.*

The most likely alternative appears to be the following: an NH group of PH attaches to a π-orbital of nitroxide through the σ-bond of a hydrogen atom, forming a π-σ type complex. In this case there are fewer steric hindrances than in the previous case. The π-complex lies on the reaction coordinates of hydrogen atom transfer. However, when passing through the reaction coordinates, the system can jump over the complex state.

PH solutions in $CDCl_3$ were freshly prepared prior to each series of experiments, and used within a 30 minutes. Quenching was monitored by cw-EPR. Digital double integration of the EPR signal was performed: two integrations (a "running" one to obtain the signal in absorption and a "numerical" one to yield simply a number) were needed to obtain the desired area from the experimentally obtained first-derivative profile. The area is of particular interest since it is proportional to the number of nitroxide in the sample[49]. Therefore, the ratio between the area of the EPR signal before and after addition of the quencher provides a measure of the amount of quenched nitroxide in the sample. Several EPR spectra were recorded at different times, after addition of the quencher to the solution containing the sample (Figures 3.39 a, b). The plot of figure 3.40 show the percent of quenched nitroxide over time. It is important to stress that we did not want a precise quantification of the nitroxide concentration in solution but only a qualitative idea of how fast the nitroxide was reduced. In fact, the area of the EPR signal is affected not only by the number of nitroxide moieties in the sample but also by other factors such as temperature, applied magnetic field magnitude *B*, microwave frequency, the amplitude B_1 of the microwave magnetic field effective at the sample, the overall spectrometer gain[49] and, as already stressed, the use of a standard would be required for quantitative determination.

The reduction reaction was observed to be reversible. Indeed, when the integral of EPR signal reached the minimum value, corresponding to the *plateau* in the graph "% nitroxide quenched" against "time" (Figure 3.40), the integral does not decrease anymore, on the contrary, a slight increase is observed. In fact, it is known that the N-hydroxy-amine is oxygen sensitive[72].

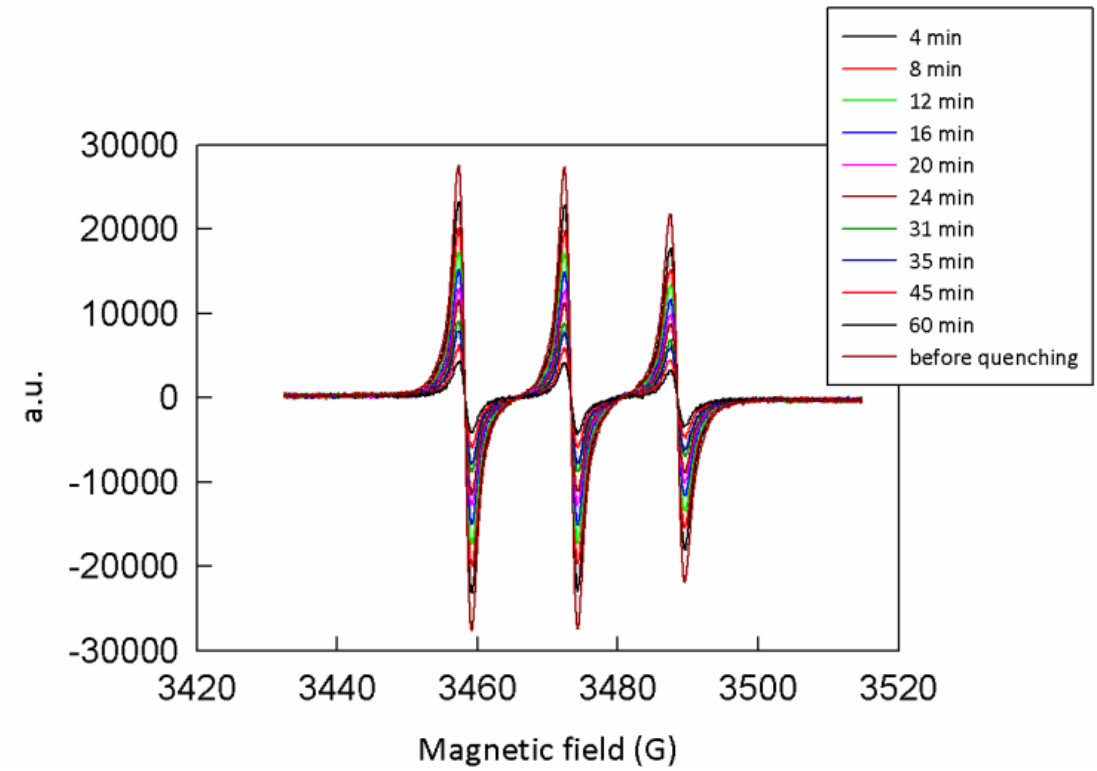

Figure 3.39 a. *cw EPR spectrum of fullerene-peptide 2- in a 0.05 mM $CHCl_3$ solution monitored over time after have added 10 equivalents of PH at r.t, microwave attenuation 10 dB.*

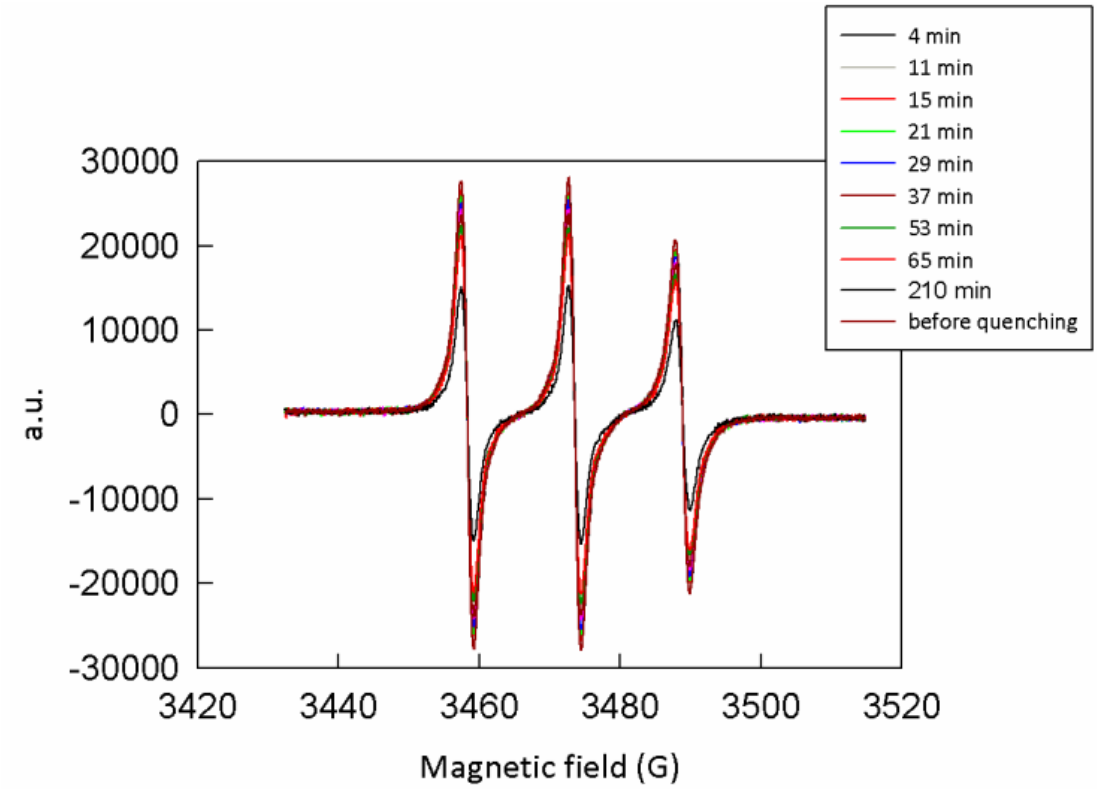

Figure 3.39 b. *cw EPR spectrum of fullerene-peptide 2+ in a 0.05 mM $CHCl_3$ solution monitored over time after having added 10 equivalents of PH at r.t., microwave attenuation 10 dB.*

The reduction kinetic is here shown:

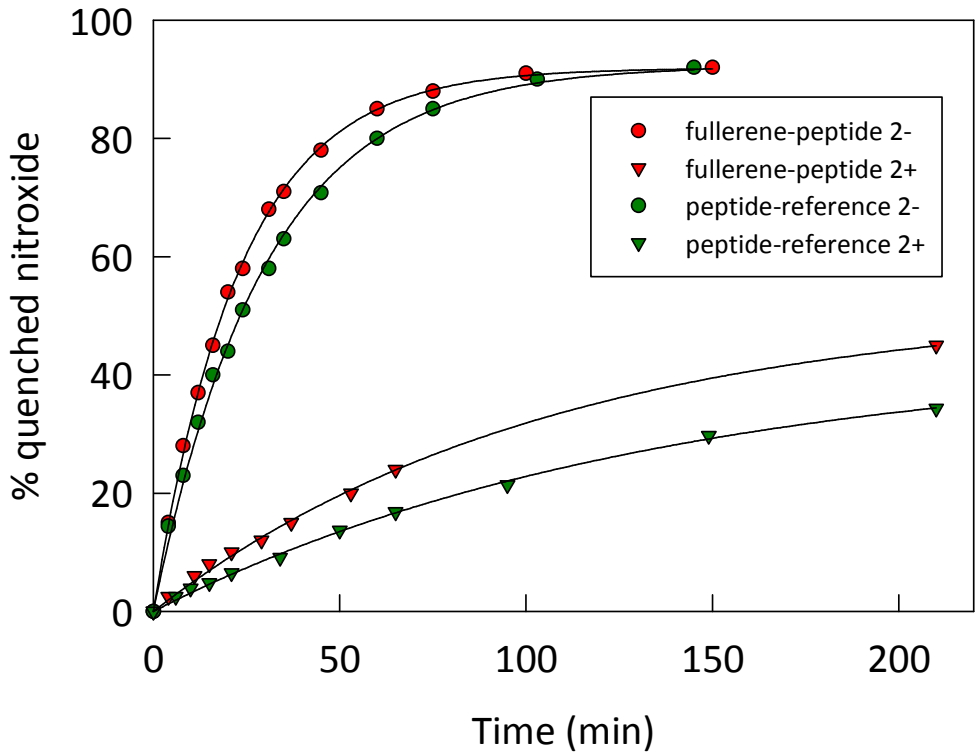

Figure 3.40. *Reduction kinetic for the 2- and 2+ series under the same conditions; 0.05 mM $CHCl_3$ solution with 10 equivalents of PH, r.t.*

	k (min^{-1})	k_{2-} / k_{2+}
Fullerene-peptide 2-	0.043	*4.5*
Fullerene-peptide 2+	0.0095	
Peptide-reference 2-	0.033	*4.5*
Peptide-reference 2+	0.0074	

The graph in figure 3.40 shows that, under the same conditions, the fullerene-peptide 2+ is reduced four times slower than the fullerene-peptide 2- where the sign of dipole moment is reversed and the *plus* sign of the dipole is on the TOAC. Same behavior is observed in the two peptides-reference which only lack of the C_{60} moiety and retain the same number of NH groups. The origin of this rate difference can be ascribed to the opposite direction of the macrodipole moment associated with the peptide helical structure. In the *plus* series, negative charge density is located on TOAC. In principle, this charge could yield the reduction process more difficult, acting like an electro-donating group attached on TOAC. In the *minus* series the situation is reversed and here the positive charge of the macrodipole is on TOAC thus affecting favorably the reduction process, acting like an electro-withdrawing group attached on TOAC.

It is also worth noting that the systems bearing the fullerene are reduced faster by a factor of 1.3 compared with their peptides-reference. It is known that

the buckyball behaves such as a fairly localized and electron-deficient polyolefin[1,6a] and tends to form complexes with electron donors[12]. The possible formation of a transient complex between PH and the π-system of the fullerene could explain the catalytic effect observed on the reaction.

3.3.4 ^{1}H NMR characterization of systems bearing the nitroxide

TOAC derivatives can not be characterized by ^{1}H NMR because the paramagnetic center relaxes very rapidly, thereby causing strong broadening of NMR lines of nuclei in its vicinity. Even at longer distances than 6Å NMR lines may still be broadened beyond detectability[49]. Well resolved NMR spectra can be acquired after quenching of the free radical. To this purpose, PH was used. Spectra were acquired in $CDCl_3$ at r.t. before and after quenching, to show the appearance of peaks. A comparison with the corresponding references was also done. In the spectra of the quenched systems (Figures 3.42, 3.43, 3.44, 3.45), the following peaks located at 5.58, 6.85, 7.21, 7.53, 7.93 ppm belong to the oxidated PH and to PH present in excess. Besides PH is known to produce by-products[111].

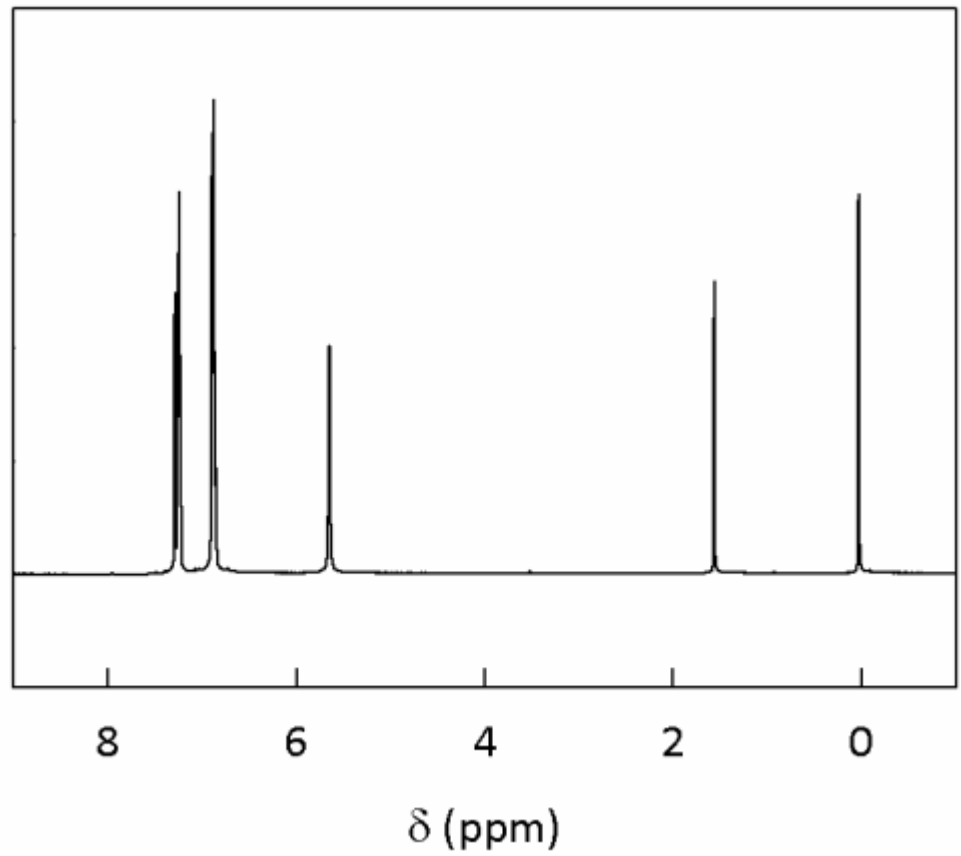

Figure 3.41. *^{1}H NMR of 2 mM PH in $CDCl_3$, r.t.*

For the 2+ system 50 equivalents of PH were used instead of 10, according to the kinetic study (Figure 3.40) which showed a slower quenching for the 2+ system compared with the 2- system.

Before quenching, the ^{1}H NMR spectra of the systems bearing the nitroxide show a bunch of broad and unresolved peaks in the aliphatic region. No other signal is observable. After quenching, peaks related to the expected products appear resolved and in good agreement with the corresponding fullerene-peptides-reference peaks (Figures 3.42, 3.43, 3.44, 3.45).

The peaks corresponding to the methylene groups of the TOAC piperidinyl ring appear at 2.4 ppm for the fullerene-peptide 2+ (Figure 3.43) and at 2.3 ppm for the fullerene-peptide 2- (Figure 3.42) in good agreement with the corresponding peaks of the peptides-reference 2+ and 2- (Figures 3.44 and 3.45). The resonances of the four TOAC methyl groups fall at higher fields, i.e., at 1.24ppm for the fullerene-peptide 2+ and at 1.35 ppm for the fullerene-peptide 2- (Figures 3.42 and 3.43).

It is possible to observe that, in the ^{1}H NMR spectrum of the peptide-reference 2+ (Figure 3.45), the N(1)H amide proton peak is shifted to high fields and no singlet is observable at 8.2 ppm, similarly to the ^{1}H NMR spectra of fullerene-peptide 2+ and fullerene-peptide-reference 2+ (Figure 3.43). Finally, the fulleropyrrolidine and alanine peaks ($^{\alpha}H$ and $^{\alpha}CH_3$) are not visible in the ^{1}H NMR spectrum of peptide-reference 2+ and 2- (Figures 3.44 and 3.45).

^{1}H NMR titration was not possible for the systems 2+ and 2- bearing the nitroxide because the presence of the quencher signals in the aromatic region of the NMR spectrum covers the amide protons peaks of the systems 2+ and 2- so that it is not possible to follow their shifts. It is known, however, that TOAC and Aib share the same structural tendencies when in peptides and thus a reasonable assumption is that the fullerene-peptides should retain the same conformations of their corresponding fullerene-peptides-reference. As previously suggested by FT-IR analysis (Figures 3.27 a, b) whereas this assumption appears as valid for the 2+ series, for the 2- series the substitution of the TOAC residue with the Aib residue appears to affect significantly the interactions involving the NH groups.

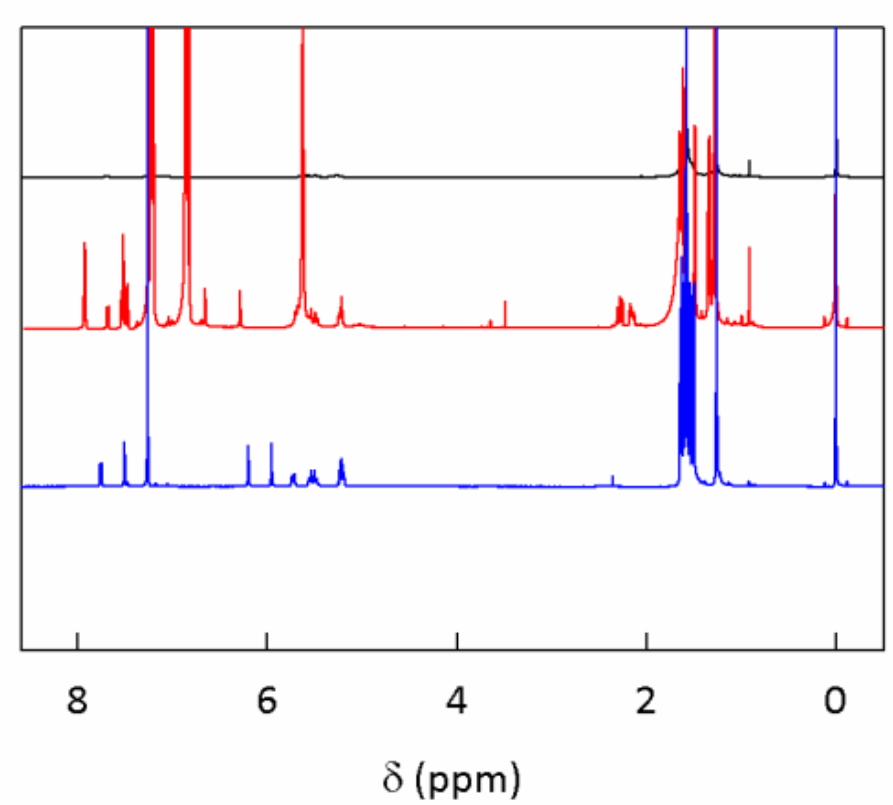

Figure 3.42 a. *500 MHz ^{1}H NMR of fullerene-peptide 2- before and after quenching with 10 equivalents of PH, fullerene-peptide-reference 2-, in $CDCl_3$, r.t., 2 mM.*

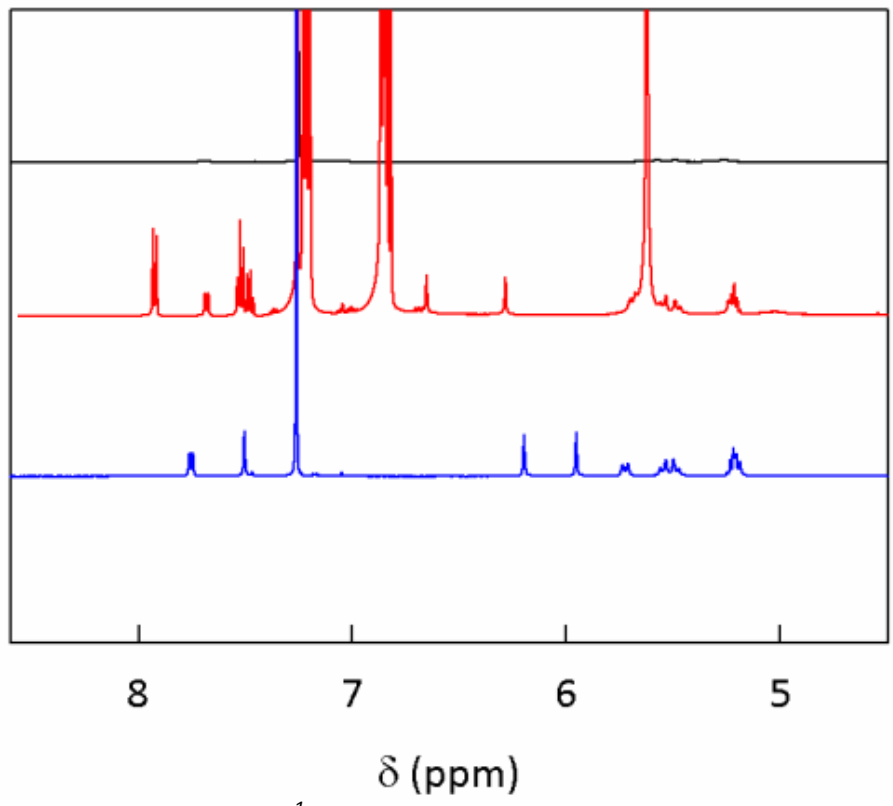

Figure 3.42 b. *Partial 500 MHz ^{1}H NMR of fullerene-peptide 2- before and after quenching, fullerene-peptide-reference 2-, in $CDCl_3$, r.t., 2 mM. NH resonances region.*

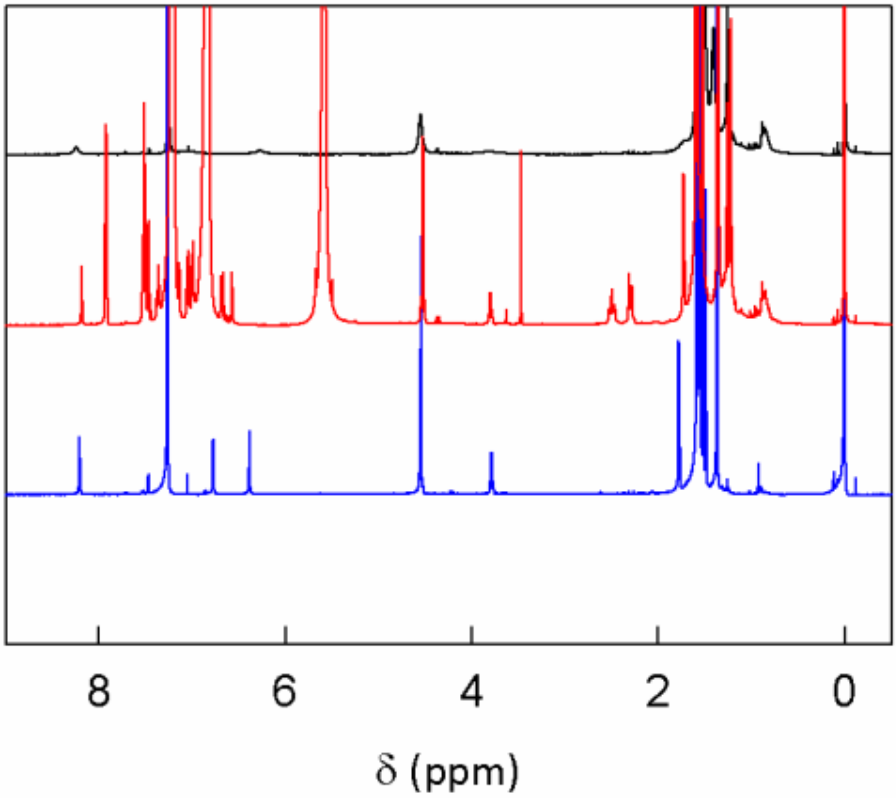

Figure 3.43 a. *500 MHz ^{1}H NMR of fullerene-peptide 2+ before and after quenching with 50 equivalents of PH, fullerene-peptide-reference 2+, in $CDCl_3$, r.t., 2 mM.*

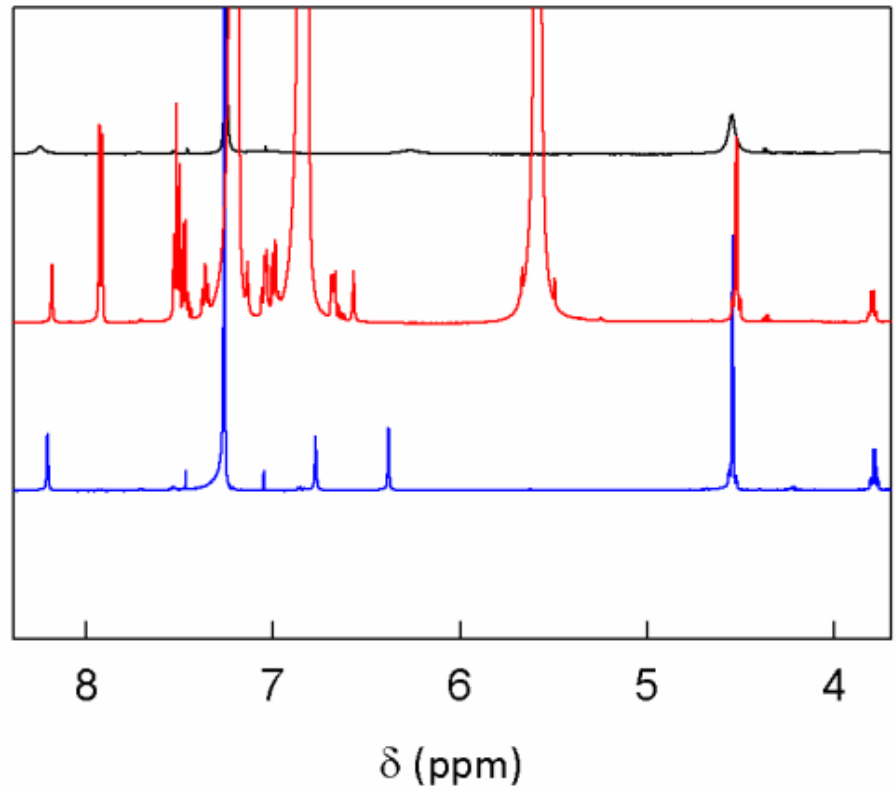

Figure 3.43 b. *Partial 500 MHz ^{1}H NMR of fullerene-peptide 2+ before and after quenching, fullerene-peptide-reference 2+, in $CDCl_3$, r.t., 2 mM. NH resonances region.*

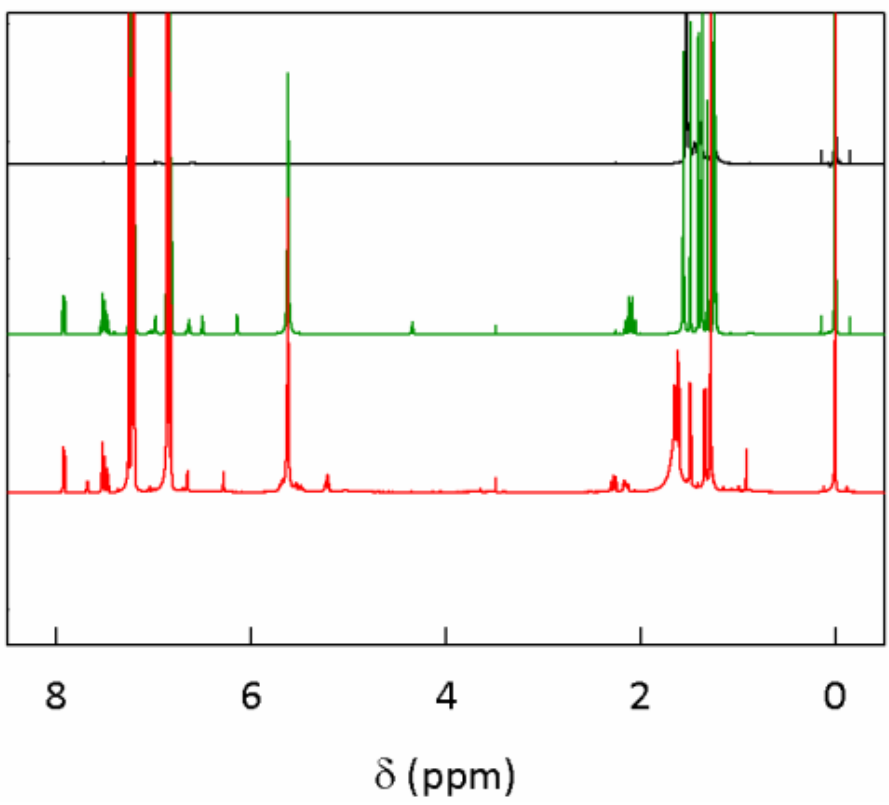

Figure 3.44 a. *500 MHz ^{1}H NMR spectrum of peptide-reference 2- before and after quenching with 10 equivalents of PH, fullerene-peptide 2- after quenching with 10 equivalents of PH, in $CDCl_3$, r.t., 2 mM.*

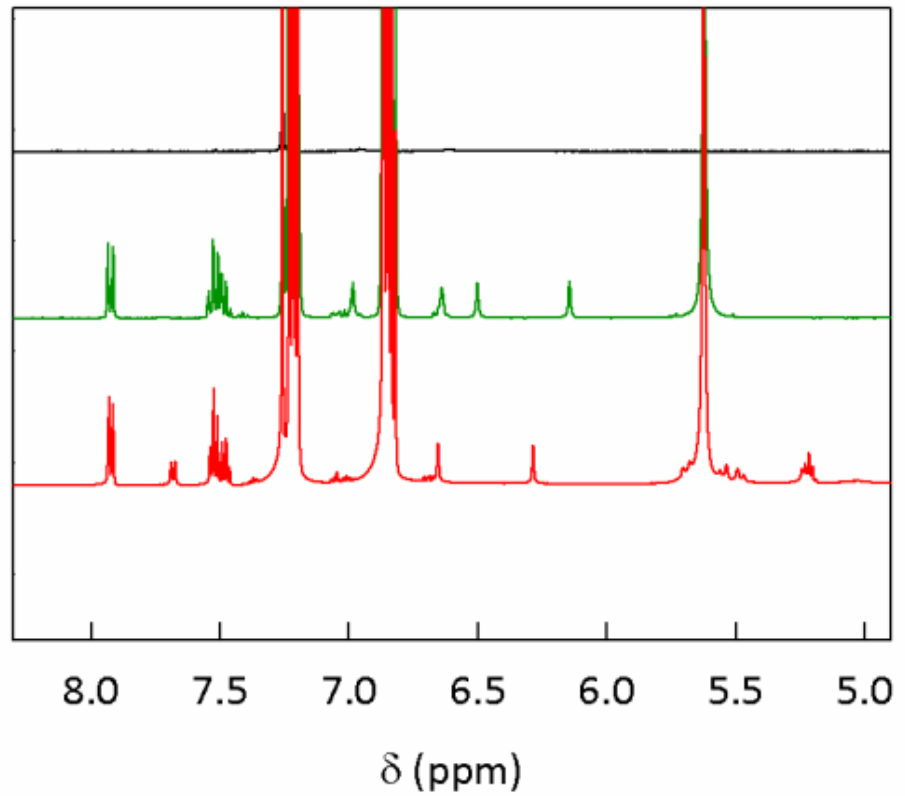

Figure 3.44 b. *Partial 500 MHz ^{1}H NMR spectrum of peptide-reference 2- before and after quenching with 10 equivalents of PH, fullerene-peptide 2- after quenching with 10 equivalents of PH, in $CDCl_3$, r.t., 2 mM. NH resonances region.*

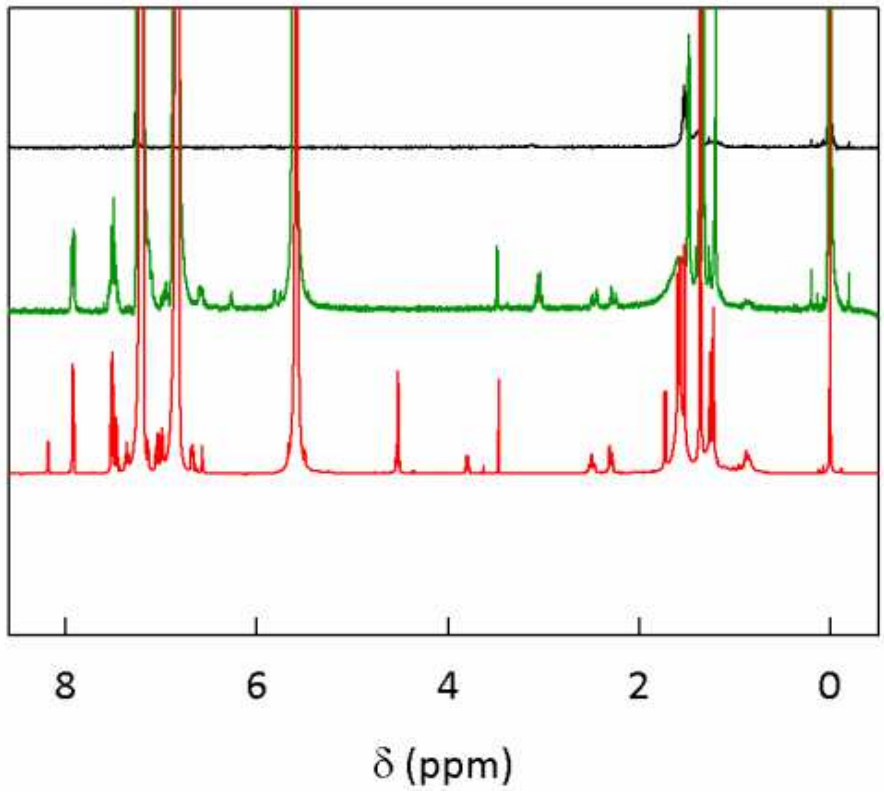

Figure 3.45 a. *500 MHz ^{1}H NMR spectrum of peptide-reference 2+ before and after quenching with 50 equivalents of PH, fullerene-peptide 2+ after quenching with 50 equivalents of PH, in $CDCl_3$, r.t., 2 mM.*

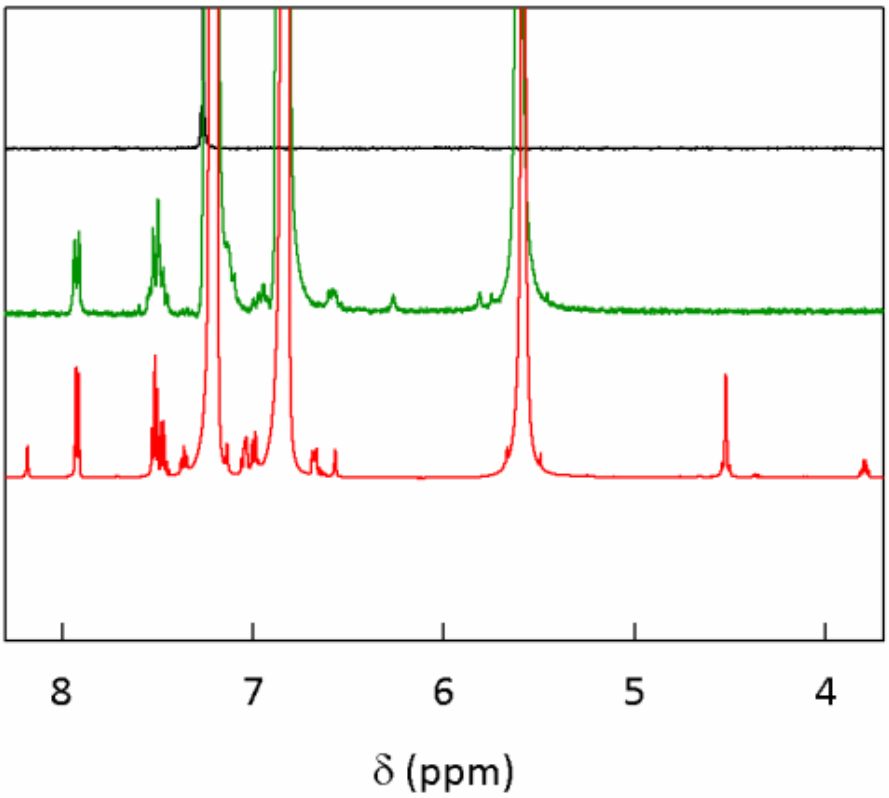

Figure 3.45 b. *Partial 500 MHz ^{1}H NMR spectrum of peptide-reference 2+ before and after quenching with 50 equivalents of PH, fullerene-peptide 2+ after quenching with 50 equivalents of PH, in $CDCl_3$, r.t., 2 mM. NH resonances region.*

3.3.5 Uv-vis characterization of fullerene-peptides

The fullerene-peptides show superimposable UV-vis absorption spectra (Figure 3.46) with very similar ε values The spectra show a strong absorption at 310 nm and a sharp peak at 430 nm, latter being typical of monomeric fulleropyrrolidine derivatives [18a,41,102,108]. The former corresponds to the C_{60} electronic transition with high oscillator strength from the ground state to the 3^1T_{1u}, already observed at 328.4 nm in *n*-hexane solutions [18a]. It is noteworthy to stress that chloroform prevents the observation of the bands at about 254 nm, also peculiar for fulleropyrrolidine derivatives[103].

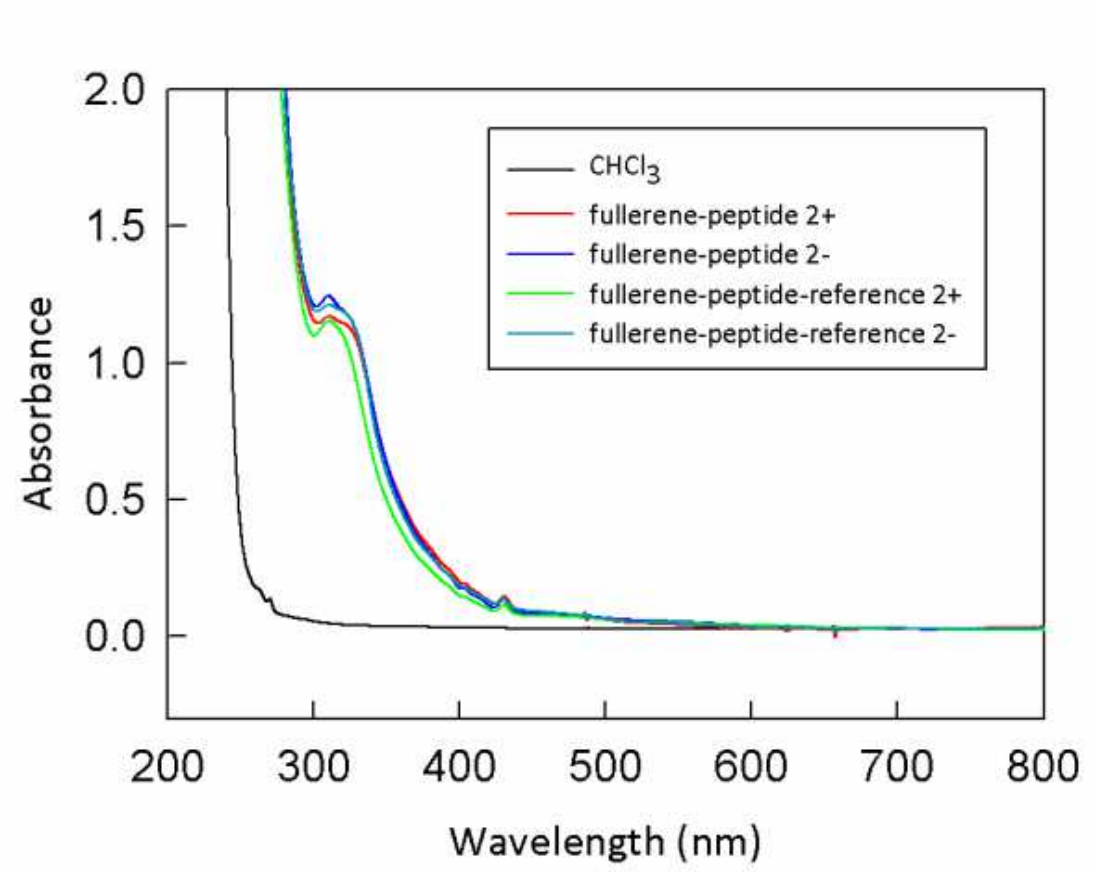

Figure 3.46. *UV-vis spectra of 0.01 mM fullerene-peptides in $CHCl_3$ at r.t .*

3.3.6 Electrochemical investigation of systems 2+ and 2-

The electrochemical investigation of compounds of interest was carried out in 1,2-dichloroethane (DCE) at 25°C with TBAH (tetrabutylammonium hexafluorophosphate) 0.1 M as supporting electrolyte and using ferrocene (Fc) as internal redox standard. In order to perform the measurements with a less volatile solvent, DCE (b.p. 84°C) was employed to dissolve the fullerene-peptides instead of $CHCl_3$ (b.p. 61°C). Both cyclic voltammetry (CV) and differential pulse voltammetry (DPV) were carried out. Due to the limited amount of products available, the measurements were carried out in a microcell that allowed to work with a limited volume of electrolytic solution, usually 1 mL. Glassy carbon was used as the working electrode material.

The voltammetric behavior of the two fullerene-peptides-reference 2+ and 2-, that bear as the only redox active group the fullerene moiety, is characterized by the presence of four reduction peaks in the potential window available in DCE (Figure 3.47).

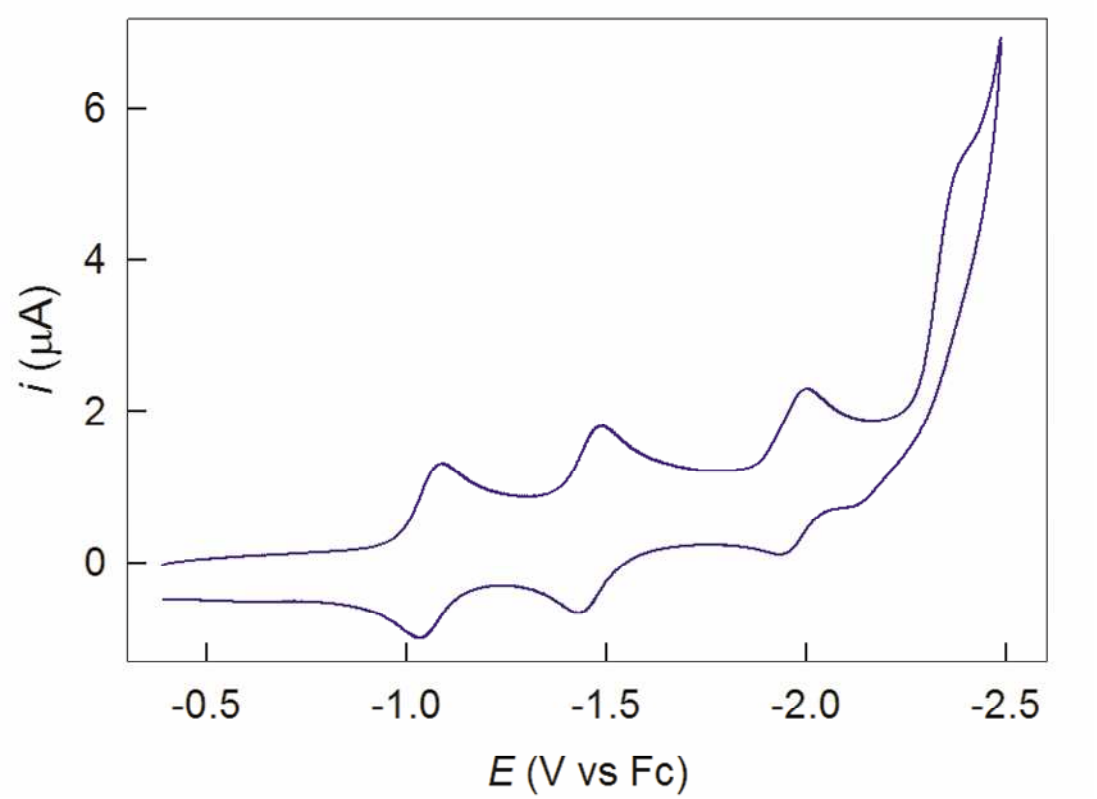

Figure 3.47. *Background-subtracted CV curves of 0.81 mM fullerene-peptide-reference 2+ in 0.1 M TBAH / DCE at a scan rate of 0.1 V/s.*

Such peaks corresponds to successive electron injection events into the fullerene. All the peaks are reversible apart for the most negative one, relative to the formation of C_{60} tetra-anion, that shows a typical catalytic behavior, that is, irreversibility and an increase of the cathodic current with respect to the other peaks. This is most probably due to the reduction of the solvent by the C_{60} tetra-anion. In the following, we will then consider only the first three reduction peaks.

From the background subtracted CV of fullerene-peptides-reference 2-, shown in figure 3.48, it is possible to appreciate the chemical and electrochemical reversibility of the three electron transfer reactions.

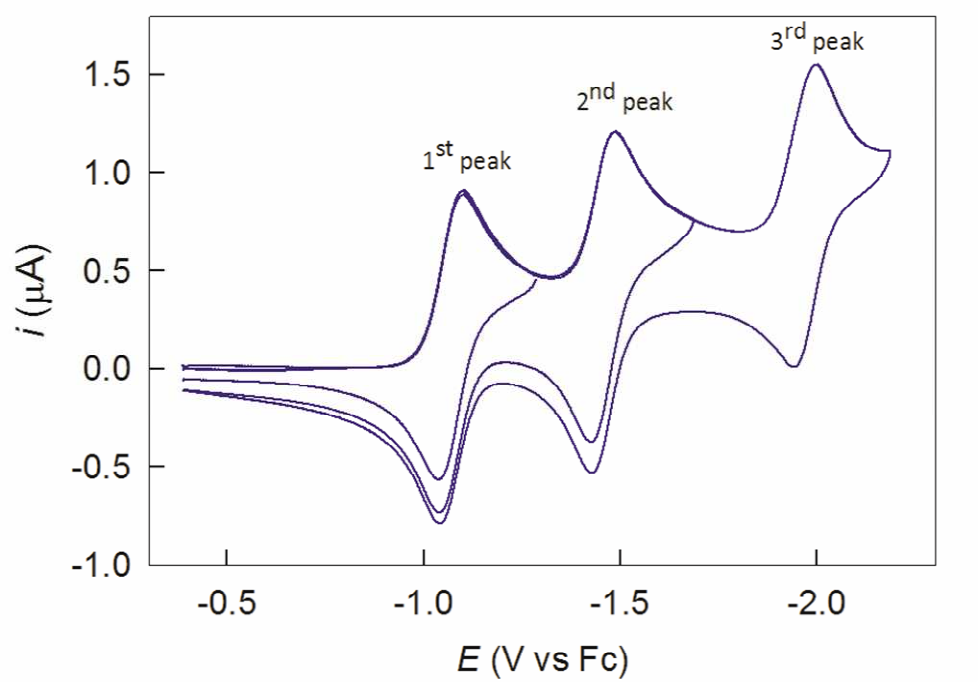

Figure 3.48. *Background-subtracted CV curves of 0.77 mM fullerene-peptide-reference 2- in 0.1 M TBAH / DCE at a scan rate of 0.1 V/s.*

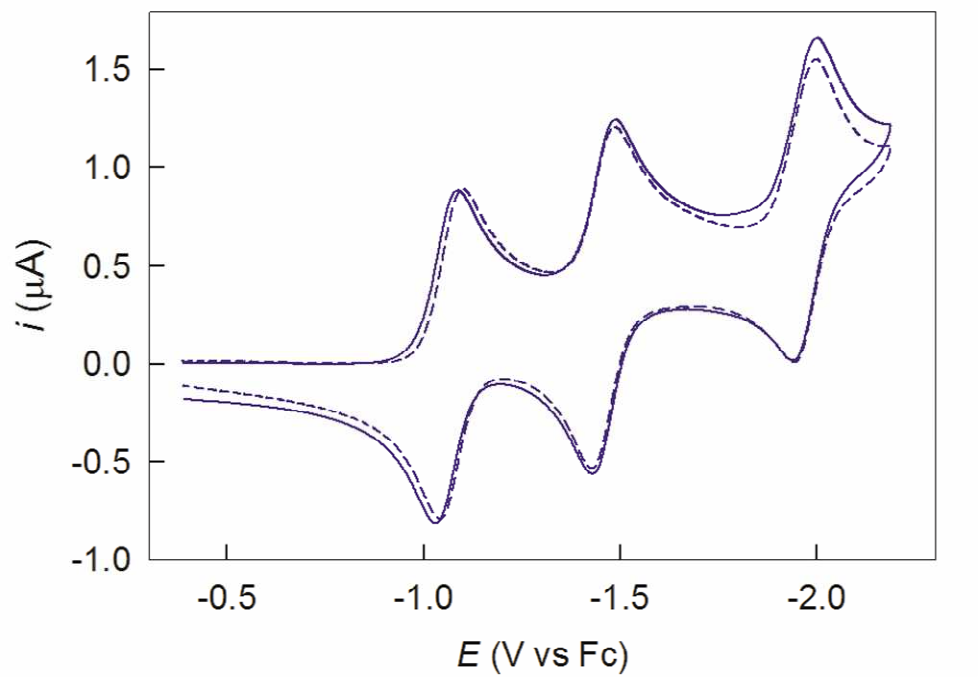

Figure 3.49. *Background-subtracted CV curves of 1 mM fullerene-peptide-reference 2- (dashed line) and fullerene-peptide-reference 2+ (continue line) in 0.1 M TBAH / DCE at a scan rate of 0.1 V/s.*

The separation between the cathodic and the anodic peak, once a good feedback correction of the ohmic drop was carried out, are in all cases about 60 mV. By comparing the E° values of the two species (Chart 3.57), calculated as the average of cathodic and anodic peak potential, it is possible to observe that the first reduction of fullerene-peptide-reference 2- is shifted negatively (14 mV) with respect to fullerene-peptide-reference 2+ (Figure 3.49). Apart from the difference in the direction of the macrodipole, the only other distinction between the 2+ series and the 2- series is on the bond that links the fullerene to the peptide. In the fullerene-peptide 2- (with or without TOAC), the peptide is attached to the C_{60} via amide bond (Figure 3.50) while in the fullerene-peptide 2+ (with or without TOAC), a tertiary amino group links the peptide to the fullerene (Figure 3.51). As a consequence, one could expect that the reduction of the C_{60} in the fullerene-peptide 2- was anticipated in respect to the fullerene-peptide 2+ being the carbonyl group of the amido bond an electro-withdrawing group. Indeed this shift was already observed by comparing the first reduction potential of N-acyl-fulleropyrrolidine with N-methyl-fulleropyrrolidine. The E° were found to be -1.00 V and -1.05 V respectively[24]. What we observe experimentally instead, goes in the opposite direction, namely, the first reduction of fullerene-peptide 2+ is anticipated in respect to the first reduction of fullerene-peptide 2- and this potential shift is consistent with the expected effect brought about by the peptide macrodipole. In fact in the 2- series, the *minus* sign of the peptide macrodipole is on the fullerene (Figure 3.50).

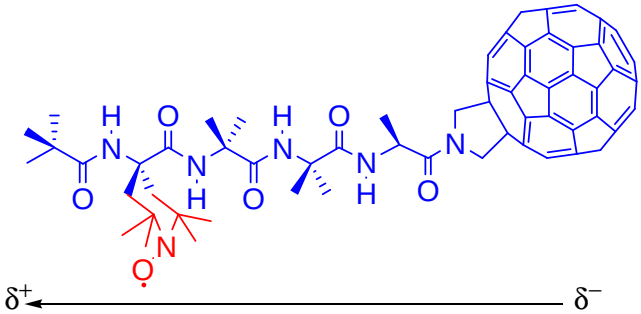

Figure 3.50 . *Molecular structure of fullerene-peptide-reference 2-. The peptide macrodipole is represented. In the fullerene-peptide-reference 2- the TOAC residue (in red) is an Aib residue.*

In the 2+ series we have the *plus* sign located on the C_{60} moiety instead (Figure 3.51).

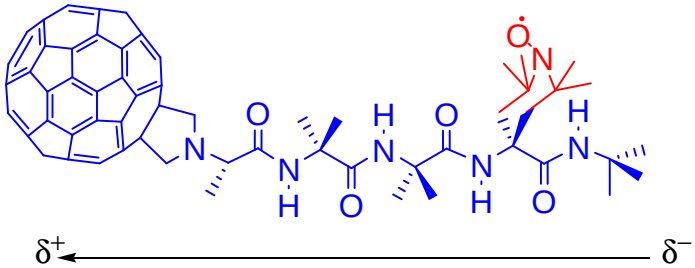

Figure 3.51 . *Molecular structure of fullerene-peptide-reference 2+-. The peptide macrodipole is represented. In the fullerene-peptide-reference 2+ the TOAC residue (in red) is an Aib residue.*

In the 2- series, the negative charge density on fullerene, produced by the peptide macrodipole, can produce an effect similar to the one introduced by an electro-donating substitutent covalently attached on fullerene which tends to raise the LUMO's energy[121] (lowest unoccupied molecular orbital) of the fullerene moiety. An increase of the LUMO energy makes the reduction more difficult because addition of an electron to the fullerene's LUMO requires more energy and thus shifts the cathodic potential to more negative values. In the 2+ series, the effect is reversed, being the positive charge density brought by the macrodipole on C_{60}. Here, the macrodipole behaves like an electro-withdrawing substituent which tends to give rising to a decrease in LUMO energy[121] and thus causes the reduction to occur at less negative potentials. This effect was already observed for C_{60} derivatives functionalized with electro-withdrawing groups such as cyanos[23] or carbonyls[24] groups. In these derivatives the first reduction peak of C_{60} is anticipated with respect to the pristine fullerene. Regarding the E° of second and third reduction peaks, no shift is observed between the fullerene-peptide-reference 2+ and 2- (Figure 3.49) suggesting that the dipole moment effect fades away in the second and third reduction.

The voltammetric analysis of fullerene-peptides 2+ and 2- allowed us to verify that the reduction potentials in both series are coincident (Figure 3.52).

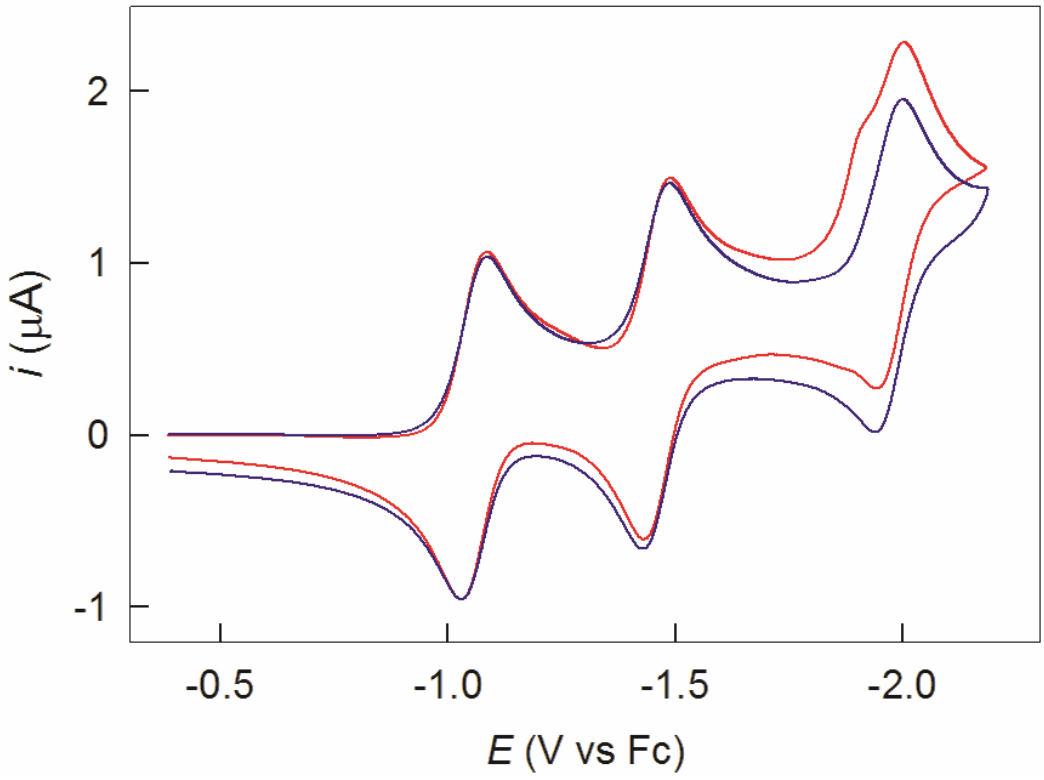

Figure 3.52. *Background-subtracted CV curves of fullerene-peptide-reference 2+ and fullerene-peptide 2+ in 0.1 M TBAH / DCE at a scan rate of 0.1 V/s.*

In the CVs of both fullerene-peptides 2+ and 2- CVs the only relevant difference with the CVs of their corresponding fullerene-peptides-reference is the presence of a shoulder before the third reversible reduction peak of C_{60}. This is attributed to the

reduction of the nitroxide radical function (Figure 3.52). The reduction of N-O• is known to be irreversible and to give rise to a peak that reflects the occurrence of a rather complex reaction.

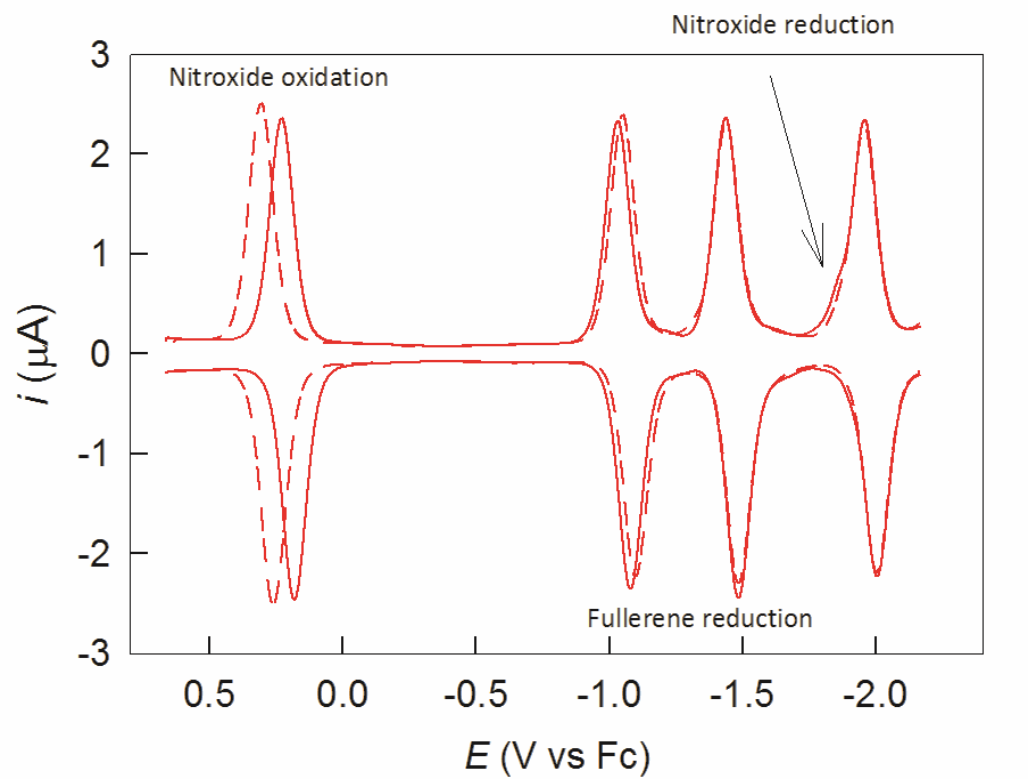

Figure 3.53. *DPVs of fullerene-peptide 2- (dashed line) and fullerene-peptide 2+ (continue line) in 0.1 M TBAH / DCE.*

On the oxidation side, by scanning the potential positively a single reversible peak is observed. This is due to the oxidation of the TOAC nitroxide radical to the oxoammonium cation (Figure 3.53). This oxidation process is electrochemically quasi-reversible, as the CVs are characterized by a peak separation of about 70 mV (Figure 3.54). The difference on the position of this peak when one goes from the fullerene-peptides 2+ to the corresponding system 2- is clearly evident.

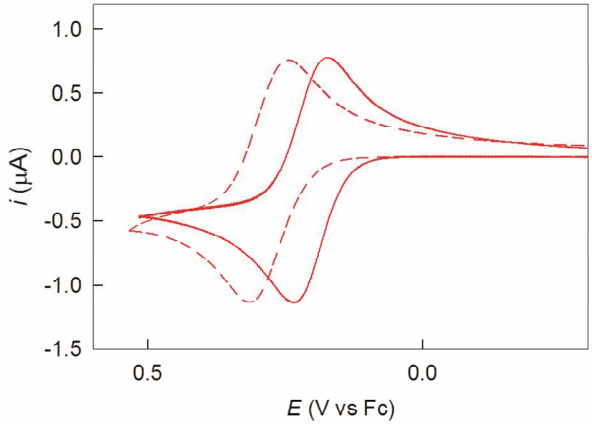

Figure 3.54. *Background-subtracted CV curves of fullerene-peptide 2- (dashed line) and fullerene-peptide 2+ (continue line) in 0.1 M TBAH / DCE at a scan rate of 0.1 V/s. The potential window was restricted to where the nitroxide oxidation takes place.*

Nitroxide oxidation in fullerene-peptide 2+ is considerably easier than that of fullerene-peptide 2- by 80 mV, and once again, this shift is on the direction expected for a dipole moment effect. Indeed in the 2+ series, the negative part of the dipole is on the TOAC side. Again, the dipole effect can be compared to the one brought about by an electro-donating group which tends to raise the energy of the SOMO[121] (singularly occupied molecular orbital). High-energy SOMOs are more willing to give up an electron than to accept an electron[121] , thus favouring the oxidation. In the 2- series, the positive side of the dipole is on TOAC. Again, the dipole effect can be compared to the one brought about by an electro-withdrawing group which tends to decrease the energy of the SOMO[121]. Low-energy SOMOs are more willing to accept an electron than to give up an electron[121] thus shifting the oxidation to more positive values.

To verify that the potential shifts are independent by the presence of the fullerene moiety and due only to the peptide macrodipole orientation, peptides-reference 2+ and 2- were studied. These two compounds only lacks of the C_{60} moiety but retains the same number of NH groups. The oxidation potentials of the TOAC nitroxide in the two compounds (Chart 3.57) differs by as much as 90 mV and are, respectively, 8 and 17 mV more positive respect to fullerene-peptides 2+ and 2-. This result confirms the relevant effect of the helix dipole moment on the energy of the TOAC's SOMO.

It is worth mentioning that addition of ferrocene, our internal redox standard for the potential values, does not induce any shift in the peak positions (Figure 3.55) allowing us to state that ferrocene is not interacting with the substrate.

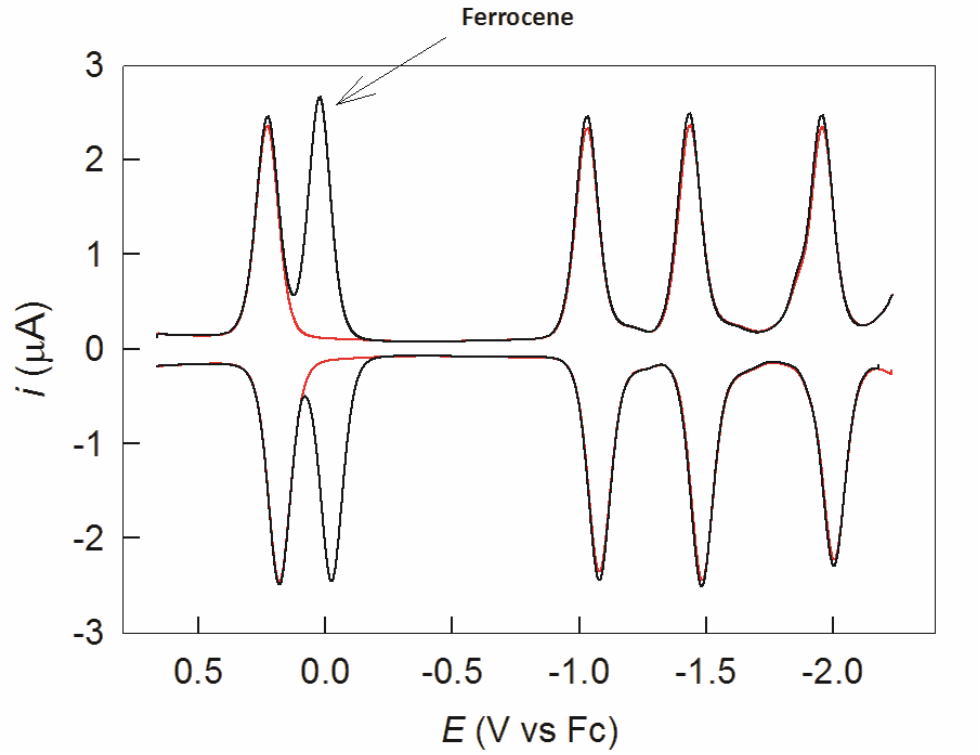

Figure 3.55. *DPVs of fullerene-peptide 2+ (red line) and fullerene-peptide 2+ (black line) in the presence of Fc, in in 0.1 M TBAH / DCE.*

At this point it is interesting to compare the oxidation potential of a TOAC derivative (Boc-TOAC-NH*t*Bu) with the potentials obtained for our systems bearing the nitroxide. Boc-TOAC-NH*t*Bu (Figure 3.56) is protected at the amino function with a urethane (Boc) and the carboxylic function of the aminoacid is transformed into a secondary amide (*tert*-butyl amide). This derivative is not a peptide and thus it can not posses an oriented dipole moment such as the one that characterizes our systems.

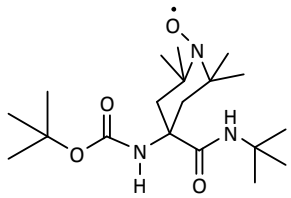

Figure 3.56 *Molecular structure of Boc-TOAC-NHtBu.*

In the absence of any oriented dipole moment, the oxidation potential of Boc-TOAC-NH*t*Bu falls at 0.262 V, thus lying roroughly in the middle of the values found for the nitroxide oxidation in the *plus* and *minus* series (Chart 3.57). This outcome points out the important role played by helix dipole on the variation of the potentials which reflect a different modulation, induced by the charge distribution of the helix dipole, on the energy of fullerene's LUMO and TOAC's SOMO.

	Reduction	**Fulleropyrrolidine**		**Oxidation Nitroxide**
	$E°_1$ (V) vs Fc	$E°_2$ (V) vs Fc	$E°_3$ (V) vs Fc	E° (V) vs Fc
Fullerene-peptide 2+	-1.056	-1.458	-1.973	+0.202
Fullerene-peptide-reference 2+	-1.056	-1.458	-1.972	
Peptide-reference 2+				+0.210
Fullerene-peptide 2-	-1.073	-1.460	-1.974	+0.283
Fullerene-peptide-reference 2-	-1.070	-1.457	-1.972	
Peptide-reference 2-				+0.300
Boc-TOAC-NH*t*Bu				+0.262

Chart 3.57. *Standard potentials of investigated systems.*

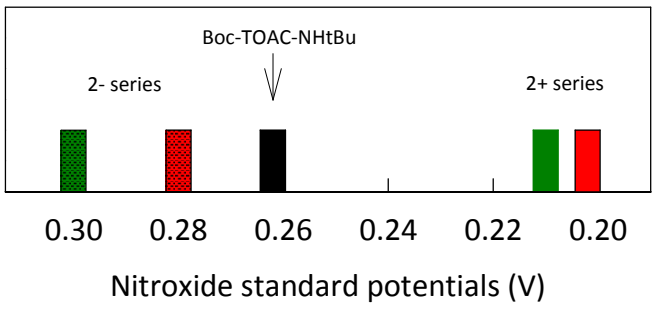

4. Conclusion

This Thesis concerns the synthesis, characterization and investigation of a series of compounds in which fullerenes, peptides, and radicals are coupled. In particular, two series of compounds were synthesized which are characterized by the presence of a fullerene moiety and / or of a nitroxide function covalently linked at the extremity of a rigid peptide. The peptide, mainly built of Aib residues, presents two intramolecular hydrogen bonds and tends to assume very likely a 3_{10}-helix secondary structure. The structured peptide sustains a strong oriented dipole moment located along the main axes of the molecule. The direction of the dipole is opposite in the two series, named 2+ and 2-, and this was expected to cause opposite effects, for example, on the redox properties of the moieties located at its extremity.

The syntheses required a considerable amount of experimental work, also because of the extremely low yields of some of the steps, which forced us to abandon some strategies that, in principle, could have been possible. In this Thesis are also described for the first time some new nitroxide and fullerene derivatives (only similar examples were described in literature). The method chosen to functionalize the fullerene was the Maggini-Prato reaction because it allowed us to work with readily accessible materials and to obtain the fullerene-peptides 2+ and 2- only by modifying the substituent at the nitrogen atom of the dipolarophile precursor. The method also does not require strong conditions and any particular functional groups to stabilize the intermediate responsible for the cycloaddition, which could interfere with the electrochemical analysis. Eventually, we could synthesize the following compounds: the fullerene-peptides 2+ and 2-, the fullerene-peptides-reference 2+ and 2- and the peptides-reference 2+ and 2-.

Characterization in solution (Mass Spectrometry, FT-IR absorption spectroscopy, ^{1}H NMR spectroscopy) proves the identity of compounds under investigation. It also provides evidence of the presence of structured peptides in both series 2- and 2+. FT-IR absorption spectra of systems 2+ and 2- reveal the presence of bonded amide protons (involved in intramolecular hydrogen bonds) and free amide protons. ^{1}H NMR and ^{13}C NMR spectra are fully compatible with the structures of the fullerene-peptide-references 2+ and 2-. 2D ROESY spectra provided evidence of highly folded conformation of both fullerene-peptide-references. ^{1}H NMR titrations revealed two different classes of NH protons: shielded (involved in intramolecular hydrogen bonds) and not shielded (free solvated NH protons). ^{1}H NMR spectra of fullerene-peptides 2+ and 2-, after quenching with diphenylhydrazine are in good agreement with the spectra of the corresponding fullerene-peptides-reference. Peaks related to the TOAC moiety are also visible. UV-vis absorptions of fullerene-peptides are typical of monomeric fulleropyrrolidine derivatives. Nitroxide quenching with diphenylhydrazine is four times slower for the 2+ system compared with the 2- system, which suggests that the rate difference is not due to the presence of the fullerene but, most likely, to the difference of the direction of the macrodipole.

Cyclic voltammetries clearly show that the first reduction peak of fullerene is anticipated in the 2+ series with respect to the 2- series. This experimental outcome is in full agreement with the effect caused by the peptide macrodipole. An even more accentuated deviation is found on the oxidation side (TOAC oxidation) where the potential shifts are once again on the direction expected for an effect of the helix dipole moment, namely, easier reduction and easier oxidation for the 2+ series while more difficult reduction and more difficult oxidation for the 2- series. It is thus possible to state that the helix dipole moment plays an important role on the tuning of the potentials of the active redox groups.

It is worthwhile to note that Aib homopeptides posses an high tendency to give raise to structured peptides which is already evident from very short oligomers[62,64,65]. The unique rigidity of short Aib homopeptides, provided by the peculiar backbone stiffness, qualify them as a successfully spacers in spectroscopic investigations. Thank to this unique feature, it can be assumed that the nitroxide-C_{60} distance in the fullerene-peptides, obtained from molecular modeling, is a good approximation to the true value. An accurate estimation of the distance is crucial for several investigations where the interactions between the fullerene (or the hydrogen molecule encapsulated inside its cage) and the nitroxide are distance-dependent. The fullerene-peptide 2+ and 2- were thus studied by TR EPR (Time-Resolved Electron Paramagnetic Resonance) by Dr. Marco Ruzzi. The technique allowed us to investigate the coupling, that is distance-dependent, between the doublet ground state of the nitroxide and the triplet state of the fullerene generated after photo-excitation. Furthermore, the H_2@fullerene-peptide 2+ and 2- were analyzed by ^{1}H NMR spectroscopy by Dr. Yongjun Li in the Turro Group and the nuclear spin relaxations and the *ortho / para* conversion rates of the encapsulated hydrogen were obtained. The research regarding the *ortho /para* hydrogen and the H_2@C_{60} has been studying in the Turro Group since many years by now and papers about this topic can be found in the references. The Turro group, by varying the spacers of a series of H_2@fullerene-nitroxide derivatives, obtained a clear distance-dependence of the nuclear spin relaxation and of the *ortho / para* conversion rate of the encapsulated hydrogen. The values obtained by studying the H_2@fullerene-peptides could provide a further evidence of this distance-dependence thank to the accuracy with which the distance is estimated.

5. References

[1] Brettreich, M.; Hirsch, A. In *Fullerenes Chemistry and Reaction*; Wiley: New York, 2005.

[2] Kratschmer, W.; Lamb, L. D.; Fostiropoulos, K.; Huffman, D. R. *Nature* **1990**, 347, 354-358.

[3] (a) Hebard, A. F.; Rosseinski, M. J.; Haddon, R. C.; Murphy, D. W.; Glarum, S. H.; Palstra, T. M.; Ramirez, A. P.; Kortan, A. R. *Nature* **1991,** *350*, 600-601. (b) Holczer, K.; Klein, O.; Huang, S.-M.; Kaner, R. B.; Fu, K.-J.; Whetten, R. L.; Diederich, F. *Science* **1991**, 252, 1154-1157. (c) Rosseinsky, M. J. *J Mater. Chem.* **1995**, 5, 1497-1513. (d) Schon, H.; Kloc, Ch.; Haddon, R.; Batlogg, B. *Science 2***000**, 288, 656-658.

[4] Khemani, K. C.; Koch, A.; Wudl, F.; Holczer, K.; Donovan, S.; Gruner, G.; Thompson, J. D. Allemand, P. M. *Science* **1991**, 253, 301-303.

[5] (a) Tutt, L. W.; Kost, A. *Nature* **1992**, 356, 225-226. (b) Kajzar F.; Taliani, C.; Danieli, R.; Rossini, S.; Zamboni, R. *Chem. Phys. Lett.* **1994**, 217, 418.

[6] (a) Prato, M. *J. Mat. Chem.* **1997**, *7*, 1097-1109. (b) Da Ros, T.; Prato, M. *Chem.Comm.* **1999**, 663-669.

[7] (a) Yannoni, C. S.; Bernier, P. P., Bethune, D. S.; Meijer, G.; Salem, J. R. *J. Am. Chem. Soc.* **1991**, 113, 3190-3192. (b) Dresselhaus, M. S.; Dresselhaus, G.; Eklund, P. C.; In Science *of Fullerenes and Carbon Nanotubes*; Academic Press: San Diego, 1996.

[8] (a) Hirsch, A. *Top. Curr. Chem.* **1999**, 199, 1-65. (b) Buhl, M.; Hirsch, A. *Chem. Rev.* **2001**, 101, 1153.

[9] (a) Reed, C. A.; Bolskar, R. D.; *Chem. Rev.* **2000**, 100, 1075-1120. (b) Haymet, A. D.; *Chem. Phys. Lett.* **1985**, 122, 421-424. (c) Haddon, R. C.; Brus, L. E.; Raghavachari, K. *Chem. Phys. Lett.* **1986**, 125, 459-464. (d) Satpathy, S. *Chem.Phys. Lett.* **1986**, 130, 545-550. (e) Hale, P. D. *J. Am. Chem. Soc.* **1986**, 108, 6087-6088.

[10] Hirsch, A.; Chen, Z.; Jiao, H. *Angew. Chem. Int. Ed. Engl.* **2000**, 39, 3915.

[11] Ajie, H.; Whetten, R.; Alvarez, M.; Anz, S.; Beck, R.; Diederich, F.; Fostiropoulos, K.; Huffman, D.; Kratschmer, W.; Rubin, Y.; Schriver, K.; Sensharma, D. *J. Phys.Chem.* **1990,** *94*, 8630-8633.

[12] Guldi, D. K.; Prato, M.; *Acc. Chem. Res.* **2000**, 695-703.

[13] Guldi, D. M.; Kamat, P. V. *Fullerenes: Chemistry, Physics and Technology* **2000**, 225-281.

[14] Corvaja, C.; Conti, F.; Franco, L.; Maggini, M. *C. R. Chimie* **2006**, 9, 909-915.

[15] Arbogast, J. W.; Darmanyan, A. P.; Foote, C. S.; Rubin, Y.; Diederich, N.; Alvarez, M.; Anz, R.; Whetter, R. *J. Phys. Chem.* **1991**, 95, 11.

[16] (a) Blaettler, C.; Jent, F.; Paul, H. *Chem. Phys. Lett.* **1990**, 166, 375. (b) Kawai, A.; Okutsu, K.; Obi, J. *J. Phys. Chem.* **1991**, 101, 434.

[17] (a) Imahori, H.; Sakata, Y. *Adv. Mater.* **1997,** *9*, 537-546. (b) Sakata, Y.; Himahori, H. *Eur. J. Org. Chem.* **1999**, 2445-2457. (c) Guldi, D. M.; *Chem. Soc. Rev.* **2002**, 31, 22-36.

[18] (a) Maggini, M.; Prato, M. *Acc. Chem. Res.* **1998**, 31, 519-526. (b) Gasyna, Z.; Schatz, P. N.; Hare, J. P.; Dennis, T. J.; Kroto, H. W.; Taylor, R.; Walton, D. R. M. *Chem. Phys. Lett.* **1991,** *83*, 283-291.
[19] Echegoyen, L.; Echegoyen, L. *Acc. Chem. Res.* **1998,** *31*, 593-601.
[20] (a) Wilson, J.; Chibante, F., Dubois, D., Kadish, M.; Flanagan, S.; Haufler, R.; *J. Am. Chem. Soc.* **1991**, 113, 4364. (b) Echegoyen, L.; Arias, F.; Xie, Q. *J. Am. Chem. Soc.* **1993**, 115, 9818-9819.
[21] Xie, Q.; Cordero, E.; Echegoyen, L. *J. Am. Chem. Soc.* **1992**, 114, 3978-3980.
[22] Stinchcombe, J.; Penicaud, A.; Bhyrappa, P.; Boyd, P. D. W.; Reed, C. A. *J. Am. Chem.Soc.* **1993,** *115*, 5212-5217.
[23] Keshavarz, M.; Knight, B.; Srdanov, G.; Wudl, F. *J. Am. Chem. Soc.* **1995,** *117*, 11371-11372.
[24] Maggini, M.; Prato, M.; Giacometti, C.; Scorrano, G.; Sandonà, G.; Farnia, G. *Tetrahedron* **1996**, 52, 5221-5234.
[25] Maggini, M.; Karlsson, A.; Scorrano, G.; Sandona`, G.; Farnia, G.; Prato, M. *J. Chem. Soc., Chem. Commun.* 1994, 589-590.
[26] Guldi, D. M.; Maggini, M.; Scorrano, G.; Prato, M. *J. Am. Chem. Soc.* **1997**, 119, 974.
[27] Wudl, F. *Acc. Chem. Res.* **1992**, 25, 157-161.
[28] Negri, F.; Orlandi, G.; Zerbetto, F. *J. Am. Chem. Soc.* **1992**, 114, 2909-2913.
[29] Morokuma, K.; Koga, N. *Chem. Phys. Lett.* **1992**, 196, 191-196.
[30] Arena, F.; Bullo, F.; Conti, F.; Corvaja, C.; Maggini, M.; Prato, M.; Scorrano, G. *J. Am. Chem. Soc.* **1997**, 789-795.
[31] Corvaja, C.; Maggini, M.; Scorrano, G.; Prato, M.; Vanzin, M. *J. Am. Chem. Soc.***1995**, 117, 8857-8858.
[32] Mazzoni, M.; Conti, F.; Corvaja, C. *Appl. Magn. Res.* **2000**, 351-361.
[33] Conti, F.; Corvaja, C.; Toffoletti, A.; Mizuochi, N.; Ohba, Y.; Yamauchi, S.; Maggini, M. *J Phys. Chem.* **2000**, 104, 4962-4967.
[34] Conti, F.; Corvaja, C.; Maggini, M.; Piu, F.; Scorrano, G.; Toffoletti, A. *Appl. Magn. Reson.* **1997**, 13, 337-346.
[35] Haddon, R. C. *Science* **1993**, *261*, 1544-1550.
[36] *Schmalz, T. G.; Seitz, D. J.; Klein, D. J.; Hite, G. E. Chem. Phys. Lett.* **1986**, 130, 203-207.
[37] Kroto, H. W. *Nature* **1987**, 329, 529-531.
[38] Schmalz, T. G.; Klein, D. J. *Buckimsterfullerenes* **1993**, 93.
[39] Haddon, R. *Acc. Chem. Res.* **1992,** *25*, 127-133.
[40] Wudl, F.; Hirsch, A.; Khemani, K.; Suzuki, T.; Allemand, P.; Koch, A.; Eckert, H.; Srdanov, G.; Webb, H. *ACS Symp. Ser.* **1992,** *481*, 161-175.
[41] Scorrano, G.; Maggini, M.; Prato, M. *J. Am. Chem. Soc.* **1993,** *115*, 9798-9799.
[42] Turro, N. J.; Murata, Y.; Chan, J. C.; Sartori, E.; Ruzzi, M.; Marti, A.; Lawler, R.; Jockush, S.; Lopez-Gejo, J.; Komatsu, K. *Acc. Chem. Res.* **2010**, 335-345.
[43] Murata, M.; Komatsu, K.; Murata, Y. *Science* **2005**, 307, 238-240.
[44] Murata, Y.; Murata, M.; Komatsu, K. *J. Am. Chem. Soc.* **2003**, 125, 7152-7153.
[45] Sartori, E.; Ruzzi, M.; Turro, N. J.; Decatur, J. D.; Doetschman, D. C.; Lawler, R. G.; Buchachenko, A. L.; Murata, Y.; Komatsu, K. *J. Am. Chem. Soc.* **2006**, 14752-14753.

[46] Spin-rotation is related to collisions changing the speed and/or the orientation of the rotation of the molecule. As the temperature is increased the molecule rotates faster and faster and the frequency of effective collisions in liquid decreases. Interaction and at low temperature the intramolecular dipole-dipole interaction between the nuclear spins: Sartori, E.; Ruzzi, M.; Turro, N. J.; Decatur, J. D.; Doetschman, D. C.; Lawler, R. G.; Buchachenko, A. L.; Murata, Y.; Komatsu, K. *J. Am. Chem. Soc.* **2006**, 14752-14753.

[47] Sartori, E.; Ruzzi, M.; Turro, N. J.; Martì, A. A.; Jockusch, S.; Doetschman, D. C. Lawler, R. G.; Chuang, Shih-Ching; Murata, Y.; Komatsu, K. *J. Am. Chem. Soc.***2008**, 10506-10507.

[48] Li, Y.; Lei, X.; Lawler, R. G.; Murata, Y.; Komatsu, K.; Turro, N. J. *J. Phys. Chem. Lett.* **2011**, 741-744.

[49] (a) Rieger, P. H. In *Electron Spin Resonance;* RCS Publishing: Cambridge, 2007. (b) ETH lecture notes, *Physical Chemistry IV: Magnetic Resonance* 2010, ETH Zurich. (c) Bolton, J. R.; Weil, J. A. In *EPR elementary theory and practicalapplication;* Wiley : New Jersey, 2007.

[50] Kuck, J.; Hammond, G. *Fullerenes: Synthesis, Properties and Chemistry of LargeCarbon Clusters*; ACS Symp. Ser., 481, American Chemical Society, Washington, DC, 1992.

[51] Toniolo, C.; Crisma, M.; Formaggio, F. *Biopolym.* **1998**, 47, 153-158.

[52] Rassat, A.; Rey, P. *Bull. Soc. Chim. Fr.* **1967**, 815-817.

[53] Toniolo, C.; Valente, E.; Formaggio, F.; Crisma, M.; Pilloni, G.; Corvaja, C.; Toffoletti, A.; Martinez, G.; Hanson, P.; Millhauser, L.; George, C.; Flippen-Anderson, L. *J. Pept. Sci.* **1995,** *1*, 45-47.

[54] Wright, K.; Sarciaux, M.; Castries, A. D.; Wakselman, M.; Mazaleyrat, J.-P.; Toffoletti, A.; Corvaja, C.; Crisma, M.; Peggion, C.; Formaggio, F.; Toniolo, C. *Eur. J. Org. Chem.* **2007,** 19, 3133-3144.

[55] Karle, I.; Balaram, P. *Biochem.* **1990,** *29*, 6747-6756.

[56] Toniolo, C.; Crisma, M.; Formaggio, F.; Peggion, C. *Biopolymers (Pept. Sci.)* **2001,** *60*, 396-419.

[57] Toniolo, C.; Benedetti, E. *Trends Biochem. Sci.* **1991,** *16*, 350-353.

[58] Goodman, M.; Toniolo, C.; Pallai, P.; Castro, B.; Martinez, J. In *Forum Peptides*, Dhor, Nancy, France, **1985**; pp 146-174.

[59] Kennedy, F.; Crisma, M.; Toniolo, C.; Chapman, D. *Biochem.* **1991,** *30*, 6541-6548.

[60] Toniolo, C.; Bonora, C.; Barone, G.; Bavoso, A.; Benedetti, E.; Blasio, B.; Grimaldi, P.; Lelj, F.; Pavone, V.; Pedone, C. *Macromol.* **1985,** *18*, 895-902.

[61] Hanson, P.; Millhauser, F.; Formaggio, F.; Crisma, M.; Toniolo, C. *J. Am. Chem. Soc.* **1996,** *118*, 7618-7625.

[62] Hanson, P.; Martinez, G.; Millhauser, G.; Formaggio, F.; Crisma, M.; Toniolo, C.; Vita, C. *Mol. Phys.* **1998,** *95*, 957-966.

[63] Shin, Y.; Newton, M.; Isied, S. *J. Am. Chem. Soc.* **2003,** *125*, 3722-3732.

[64] Hirsch, A.; Chen, Z.; Jiao, H. *Angew. Chem. Int. Ed. Engl.* **2000**, 39, 3915-3917.

[65] Antonello, S.; Formaggio, F.; Moretto, A.; Toniolo, C.; Maran, F. *J. Am. Chem. Soc.* **2003,** *125*, 2874-2875.

[66] Polo, F.; Antonello, S.; Formaggio, F.; Toniolo, C.; Maran, F. *J. Am. Chem. Soc.* **2005,** *127*, 492-493.
[67] Improta, R.; Barone, V.; Kudin, K. N.; Scuseria, G. E. *J. Am. Chem. Soc.* **2001,** *123*, 3311-3322.
[68] Wieczorek, R.; Dannenberg, J. J. *J. Am. Chem. Soc.* **2004,** *126*, 14198-14205.
[69] Toniolo, C.; Crisma, M.; Formaggio, F.; Peggion, C.; Broxterman, Q. B.; Kaptein, B. *Biopolymers (Pept. Sci.)* **2004**, 76, 162-176.
[70] Improta, R.; Antonello, S.; Formaggio, F.; Maran, F.; Rega, N.; Barone, V. J. *J. Phys. Chem. B* **2005,** *109*, 1023-1033.
[71] Improta, R.; Barone, V.; Newton, M. D. *Chemphyschem* **2006,** *7*, 1211-1214.
[72] Ozinskas, A.; Bobst, A. M. *Helv. Chim. Acta* **1980**, 63, 1407-1411.
[73] Tsuge, O.; Kanemasa, S.; Ohe, M.; Takenaka, S. *Bull. Chem. Soc. Jpn.* **1987**, 60, 4079-4089.
[74] Wudl, F.; Hirsch, A.; Li, Q. *Ang. Chem. Int. Ed.* **1991**, 1309-1310.
[75] Polese, A.; Mondini, S.; Bianco, A.; Toniolo, C.; Scorrano, G.; Guldi, D., M.; Maggini, M. *J. Am. Chem. Soc.* **1999**, 121, 3446-3452.
[76] Marchetto, R.; Schreier, S.; Nakaie, C. R. *J. Am. Chem. Soc.* **1993**, 115, 11042-11043.
[77] Kordatos, K.; Da Ros, T.; Prato, M., Bosi, S.; Vazquez, E.; Bergamin, M.; Cusan, C.; Pellarini, F.; Tomberli, V.; Baiti, B.; Pantarotto, D.; Georgakilas, G.; Spallato, G. *J. Org. Chem.* **2001**, 66, 4915.
[78] Ioutsi, V. A.; Zadorin A. A.; Khavrel, P. A.; Belov, N. M.; Ovchinnikova, N. S.; Goryunkov, A. A.; Kharybin, O. N.; Nikolaev, N. N.; Yurovskaya M. A.; Sidorov, N. L. *Tetrahedron* **2010**, 66, 3037-3043.
[79] Milic, D.; Prato, M. *Eur. J. Org. Chem.* **2010**, 476-483.
[80] Kordatos, K.; Da Ros, T.; Bosi, S.; Va´zquez, E.; Bergamin, M.; Cusan, C.; Pellarini, F.; Tomberli, V.; Baiti, B.; Pantarotto, D.; Georgakilas, V.; Spalluto, G.; Prato, M. *J. Org. Chem.* **2001**, 66, 4915-4920.
[81] Fabris, L. In monostrati peptidici su nanoparticelle e superfici d'oro. Tesi di dottorato di ricerca, Università di Padova, 2005.
[82] (a) Weinkam, R. J.; Jongersen, E. J. *J. Am. Chem. Soc.* **1971**, 7028-7033. (b) Brook, A. G.; Anderson, D. G.; Duff, J., M.; Jones, P. F.; MacRae, D. M. *J. Am. Chem.Soc.* **1968**, 90, 1078.
[83] Carpino, L. A. *J. Am. Chem. Soc.* **1993**, 4397.
[84] Carpino, L. A.; Beyermann, M.; Wenschuh, H.; Bienert, M. *Acc. Chem. Res.* **1996**, 6, 268-274.
[85] Dal Pozzo, A.; Ni, M.; Muzi, L.; Caporale, A.; De Castiglione, R.; Kaptein, B.; Broxterman, Q. B.; Formaggio, F. *J Org. Chem.* **2002**, 67, 6372-6375.
[86] Tsuge, O.; Kanemasa, S.; Ohe, M.; Takenaka, S. *Bull. Chem. Soc. Jpn.* **1989**, 62, 1960-1968.
[87] (a) Naim, A.; Shevlin, P. B. *Tetrahedron Lett.* **1992***,* 33, 7097-7100. (b) Takeuchi, A.; Li, J.; Ozawa, M.; Li, X.; Saigo, K.; Kitazawa, K. *J. Chem. Soc, Chem. Commun.* **1993**, 1784-1785.
[88] Javahery, G.; Petrie, S.; Wincel, H.; Wang, J.; Bohme, D. K. *J. Am. Chem. Soc.* **1993**, 115, 5716-5722.
[89] D'Angeli, F.; Cavicchioni, G.; Catelani, G.; Marchetti, P.; Maran, F. *Gazz. Chim. Ital.* ***1989***, 119, 471-474.

[90] D'Angeli, F.; Marchetti, M.; Cavicchioni, G.; Maran, F. *Tetr. Asym.* **1991**, 2, 1111-1121.
[91] D'Angeli, F.; Marchetti, P.; Bertolasi, V.; *J. Org. Chem.* **1995**, 60, 4013-4016.
[92] Sidani, A. R.; Toye, J.; Ghosez, K.; Rens, M.; Dekoker, A.; Haveaux, B. *Org. Synth.* **1979**, 59, 26-30.
[93] Tada, T.; Ispida, Y.; Saigo K. *J. Org. Chem.* **2006**, 71, 1633-1639.
[94] Tada, T.; Ishida, Y.; Saigo K. *Org. Lett.* **2005**, 7, 5897-5900.
[95] Bianco, A.; Lucchini, V.; Maggini, M.; Prato, M.; Scorrano, G.; Toniolo, C. *J. Pept. Sci.* **1998**, 4, 364-368.
[96] Bianco, A.; Maggini, M.; Scorrano, G.; Toniolo, C.; Marconi, G.; Villani, C.; Prato, M. *J. Am. Chem. Soc.* **1996**, 118, 4072-4080.
[97] Bonora, G. M.; Mapelli, C.; Toniolo, C.; Wilkening, R. R.; Stevens, E. S. *Int. J. Biol. Macromol.* **1984**, 6, 179-188.
[98] Kennedy, D. F.; Crisma, M.; Toniolo, C.; Chapman, D. *Biochemistry* **1991**, 30, 6541-6548.
[99] Fabris, L.; Antonello, S.; Armelao, L.; Donkers, R., L.; Polo, F.; Toniolo, C.; Maran, F. *J. Am. Chem. Soc.* **2006**, 128, 326-336.
[100] Lee, T., D.; Keana; J. W. *J. Org. Chem.* **1975**, *40*, 3145-3147.
[101] Malievskii, A. D.; Koroteev, S. V.; Kasparov, V. V. *Russian Chemical Bulletin* **1993**, *42*, 1027-1031.
[102] Angelini, G.; De Maria, P.; Fontana, A.; Pierini, M. *Langmuir* **2001**, 17, 6404-6407.
[103] Maggini, M.; Angelini, G.; Cusan, C.; DeMaria, P.; Fontana, A.; Pierini, M.; Prato, M.; Schergna, S.; Villani, C. *Eur. J. Org. Chem.* **2005**, 106, 1884-1891.
[104] Wutrich, K. In *NMR of Proteins and Nucleic Acids;* Wiley: New York, 1986.
[105] Bianco, A.; Maggini, M.; Scorrano, G.; Toniolo, C.; Prato, M.; Wudl, F. *J. Org. Chem.* **1993**, 58, 5578-5580.
[106] Kurosawa, W.; Kan, Toshiyuki, K.; Fukuyama, T. *Org. Synth.* **2002**, 79, 186-195.
[107] Miller, G. P. *C. R. Chimie* **2006**, 9, 952-959.
[108] Guldi, D. M. *J. Phys. Chem. A* **1997**, 101, 3895-3900.
[109] Bagno, A.; Claeson, S.; Maggini, M.; Martini, M., L.; Prato, M.; Scorrano, G. *Chem. Eur. J.* **2002**, 8, 1016-1023.
[110] (a) Miick, S. M.; Martinez, G. V.; Fiori, R. W.; Todd, A. P.; Millhauser, G. L. *Nature* **1992**, 359, 653-655. (b) Millhauser, G. L. *TIBS* **1992***,* 17, 448-452.
[111] Rozantsev, E. G.; Golubev, V. A.; *Izv. Akad. Nauk SSSR, Ser. Chim.* **1966**, 852.
[112] Brickmann, J.; Kothe, G. J. *Chem. Phys.* **1973**, 59, 2807-2814.
[113] Miller, J. S.; Epstein, A. J. *Angew. Chem. Int. Ed. Engl.* **1994**, 33, 385.
[114] Franco, L.; Mazzoni, M.; Corvaja, C.; Gubskya, V. P.; Berezhnaya, L. Nuretdinov, A. *Mol. Phys.* **2011**, 104, 1543-1550.
[115] Li, Y.; Lei, X.; Lawler, R.; Murata, Y.; Komatsu, K.; Turro, N. J. *J. Phys. Chem. Lett.* **2010**, 1, 2135-2138.
[116] (a) Solomon, I. *Phys. Rev.* **1955**, 99, 559-565. (b) Bloembergen, N.; Morgan, L. O. *J. Chem. Phys.* **1961**, 34, 842-850.
[117] Wigner, E. Z. *Phys. Chem.* **1933**, B23, 28-32.
[118] Atkins, P. W.; Clugston, M. J. *Mol. Phys.* **1974**, 27, 1619-1631.

[119] (a) Borah, B.; Bryant, R. G.; *J. Chem. Phys.* **1981**, 75, 3297-3300. (b) Bates, R. D. Drozdoski, W. S. *J. Chem. Phys.* **1977**, 67, 4038-4044.
[120] Ceccato, M.; Di Noto, V.; Zangoni, E.; Maran, F. Work in progress.
[121] Clayden, J.; Greeves, N.; Warren, S.; Whoters, P. In *Organic Chemistry*; Oxford University Press: Oxford, 2005.